

Electric Vehicle Fleet and Charging Infrastructure Planning

Sushil Mahavir Varma

H.Milton School of Industrial and Systems Engineering, Georgia Institute of Technology, sushil@gatech.edu

Francisco Castro

Anderson School of Management, University of California, Los Angeles, francisco.castro@anderson.ucla.edu

Siva Theja Maguluri

H.Milton School of Industrial and Systems Engineering, Georgia Institute of Technology, siva.theja@gatech.edu

We analyze an optimal electric vehicle (EV) fleet and charging infrastructure capacity planning problem in a spatial setting. As customer requests arrive at rate λ , the system operator must determine the minimum number of vehicles and chargers for a given service level along with a matching and charging policy that maximizes the service level. We provide a sharp characterization of the fleet size and the charging infrastructure requirements as the demand grows. While a system in which charging times are negligible needs extra $\Theta(\lambda^{2/3})$ vehicles on top of the nominal capacity, we show that an EV system has a fundamentally different scaling. Due to charging times, the nominal capacity of the system is increased, but this increased capacity allows for an optimal EV dispatching policy to result in an extra fleet requirement of only $\Theta(\lambda^\nu)$ for $\nu \in (1/2, 2/3]$, depending on the number of charging stations and the size of the EV battery packs. We propose the Power-of- d dispatching policy, which achieves this performance by selecting the d closest vehicles to a trip request and choosing the one with the highest battery level. We conduct detailed simulations that verify our scaling results. Lastly, we discuss how to extend our results to accommodate time-varying cyclic demand patterns.

1. Introduction

The transportation industry is undergoing a transition from Internal Combustion Engine (ICE) cars to Electric Vehicles (EVs) due to advances in technology, growing awareness of the negative impact of climate change, and widespread government support for this technology. In 2022, the United States federal government enacted the Inflation Reduction Act, which provides tax incentives for the acquisition of electric vehicles. This legislation serves as a catalyst for the widespread adoption of EVs in the US, as it encourages individuals and businesses to transition towards this technology. Additionally, the state of California has implemented an executive order mandating

that, by 2035, all new vehicle sales within the state must be zero-emission vehicles, further solidifying the shift towards EVs in the transportation industry (Padilla 2020). Major automakers such as Ford and General Motors have committed substantial resources to the manufacturing of electric vehicles. Ford plans to have between 40% to 50% of its total production to be EVs by 2030 (Ford Media Center 2021) while General Motors has said that it will sell only zero-emission vehicles by 2035 (Boudette and Davenport 2021). Several other automakers are on the same track as consumer preferences shift. In fact, the electric vehicle global market share quadrupled from 2019 to 2021 reaching nearly 10% in 2021 (Bibra et al. 2022).

This transformation is also manifesting in the on-demand transportation industry, where several ride-hailing firms have commenced offering electric vehicle services and have put forward plans to eventually transition to an entirely EV-based fleet. For example, Alto, a premium ride-hailing company operating in major US cities such as Los Angeles and San Francisco, plans to have a full EV fleet by the end of 2023 (Alto 2023). Additionally, Uber announced in 2020 its commitment to providing zero-emission rides and plans to have hundreds of thousands of electric vehicles as part of its fleet by 2025 (Uber 2020). In 2021, Revel launched an all-EV ride-sharing service in New York City and has plans to continue growing its fleet and charging infrastructure (Bellan 2021).

As the on-demand transportation industry shifts towards zero-emission vehicles, the availability (Anderson et al. 2022), cost of charging stations, and longer refueling times may present challenges. While traditional gasoline cars can refuel in minutes, electric vehicles can take significantly longer to charge (LaMonaca and Ryan 2022). Level 1 chargers, available through standard household outlets, can provide 100km of driving range after 6-8 hours of charging. Level 2 chargers, which require specialized equipment and a dedicated electrical circuit, can charge the same distance in 1-2 hours but can cost between \$2,500-\$4,900 (Nelder and Rogers 2019) for commercial installation. DC fast chargers, the quickest option, can charge 100km in as little as 10 minutes but can be quite costly, with estimates ranging from \$20,000-\$100,000 depending on the specific charging rate.

In turn, it becomes essential for an EV-based on-demand transportation system to have a comprehensive understanding of the infrastructure required to deliver a proper quality of service. A

central question then revolves around determining the minimum number of vehicles and charging stations needed to provide a given service level. Interestingly, the system dynamics and how a system operator chooses to manage the system’s infrastructure play a crucial role in answering this question. Vehicles must not only spend some of their time picking up a customer before they can start service, but they will also have to drive to a charging station and spend a non-negligible amount of time charging. For every trip request, the platform will trade off short pickup times and vehicles’ state of charge (SoC). Dispatching the closest vehicle is desirable because it minimizes the workload in the system, however, it may not be compatible with sustaining a high enough system-wide SoC. In contrast, dispatching vehicles with a high SoC gives other vehicles enough time to recharge but it could signify long pickup times. Hence, compared to a traditional setting, a platform that operates with EVs will require not only more assets in the form of both vehicles and charging infrastructure but also a more careful control mechanism to balance the intricate dynamics associated with charging. In turn, it is key to understand what is the interplay between the number of vehicles and the charging infrastructure, and what is the optimal way of dispatching in an EV on-demand transportation.

We investigate the operations of an on-demand transportation system that utilizes a fleet of electric vehicles in a spatial setting. The platform dispatches vehicles to pick up customers and take them to their destinations, but as vehicles move throughout the system, their SoC decreases. To maintain an adequate SoC for all vehicles, the platform must effectively manage the availability of charging stations and the routing of vehicles to these stations. A typical vehicle in our system will pick up a customer, transport them to their destination, and then, after multiple trips, the vehicle’s battery level will be low. The platform will then decide to send the vehicle to a charging station to recharge. After charging, or during charging, the platform can decide to dispatch the vehicle to serve another trip request. In this setting, our objective is to establish guidelines for determining the minimum number of vehicles and charging stations needed to achieve a desired level of service as demand for rides grows. Additionally, we aim to shed light on the optimal dispatch policy that appropriately balances system workload and system-wide battery levels.

1.1. Main Contributions

Model. One of the main challenges of analyzing an EV transportation system stems from the simultaneous consideration of the dynamic nature of vehicles' battery levels and the spatial aspect of the operations. Keeping track of the position and SoC of each EV in a system with hundreds of vehicles can be complex and intractable. To address this, we develop a general deterministic model that captures the aggregate system evolution under any policy used to manage the fleet. Our model includes several factors such as pickup times, trip times, time to reach a charger, and the evolution of vehicles' SoC. The generality of our framework allows us to prove a universal, policy-independent, lower bound on the number of vehicles and chargers needed to provide a given service level as trip requests increase. We also establish an almost matching upper bound by analyzing a class of policies that we coin *power-of-d vehicle dispatch*, which balance system workload and state of charge. The flexibility of our framework enables us to analyze the system's evolution under this class of policies via an appropriate state-space description and a set of ordinary differential equations that capture the changes over time in the number of vehicles with enough battery to complete a given number of trip requests. Our model achieves a balance of capturing the essential elements of the problem and enabling a tractable analysis.

General bounds. We provide a policy-independent bound on the minimum number of vehicles and chargers needed to sustain a service level of $\alpha \in (0, 1)$ that depends on the arrival rate of requests λ , the average trip times T_R , and the ratio of charge and discharge rate r . More precisely, the minimum number of vehicles and chargers has to be at least $(1 + r)T_R\alpha\lambda + \Omega(\lambda^{1-\gamma})$ and $rT_R\alpha\lambda + \Omega(\lambda^{2\gamma})$, respectively, for some $\gamma \in [1/3, 1/2]$. Here, rT_R represents the time an EV needs to spend charging due to the battery lost while completing a trip request. Thus, we need at least as many vehicles as the ones that are serving customers and recharging. Also, the number of chargers must be sufficient to accommodate all EVs that need to charge due to the energy consumed while fulfilling trip requests. Additionally, the system requires an extra $\Omega(\lambda^{1-\gamma})$ vehicles and $\Omega(\lambda^{2\gamma})$ chargers. The system requires more chargers when there are fewer vehicles. A higher density of chargers implies

a shorter drive time to a charger, which reduces the number of EVs needed. Similarly, a system with a larger fleet size can accommodate a longer drive to a charger, which reduces the number of chargers required. Furthermore, there is a limit to the benefits of adding chargers to decrease the fleet size or adding vehicles to decrease the number of chargers. In particular, the system cannot operate with less than $\Theta(\lambda^{1/2})$ extra vehicles or less than $\Theta(\lambda^{2/3})$ extra chargers. We depict the unachievable mix of fleet size and charging infrastructure in Figure 1.

Matching bounds. Under a stability assumption, we derive almost matching bounds for the fleet size and charging infrastructure: the system operator can achieve any service level $\alpha \in (0, 1)$ by setting the number of vehicles and chargers equal to $(1+r)T_R\alpha\lambda + \Theta(\lambda^{1-\gamma})$ and $rT_R\alpha\lambda + \Theta(\lambda^{2\gamma})$, respectively, for any $\gamma \in [1/3, 1/(2 + 1/N_T))$ where N_T equals the number of trips a vehicle can serve with a full battery. As N_T increases, our bounds become closer to the general bounds derived for any policy. We depict this in Figure 1. We establish this result by analyzing the system under the power-of- d dispatch policy. For every trip request, this policy chooses the d closest vehicles (including those charging) and dispatches the one with the highest SoC. By selecting an appropriate value for d , we can ensure that vehicles do not spend excessive time driving to pick up customers. At the same time, having d EVs to choose from prevents the system operator from dispatching the ones with low battery levels. Overall, this policy optimizes the trade-off between pickup times and maintaining an optimal system-wide state of charge. Our results imply that increasing the value of γ increases the number of chargers but decreases the fleet size requirement which, in turn, leads to a higher proportion of EVs with low SoC. We counteract this by choosing a higher d for the policy to identify an EV with an adequate battery level. We also establish that as EVs become more efficient and are able to serve more trips on a single charge, the battery level constraint becomes less restrictive, allowing the policy to consider a smaller pool of vehicles.

Electric vs ICE capacity planning insights. In a spatial setting without EVs (the charging time is negligible), Besbes et al. (2022) establish that the number of vehicles required to satisfy a given service level $\alpha \in (0, 1)$ scales approximately as $T_R\alpha\lambda + \Theta(\lambda^{2/3})$. The second order term, $\lambda^{2/3}$, reflects

the extra capacity needed (compared to a service system without spatial frictions) due to pickup times. We establish a related but different result. In an EV system, the first-order term is higher because $\Theta(\lambda)$ vehicles are charging on average. By appropriately managing these additional vehicles, it is possible to have a second-order term that can be (almost) as low as $\Theta(\lambda^{1/2})$. Thus, the first-order term is higher, but the second-order term can be lower depending on the matching policy and the number of chargers. In fact, we show that the closest dispatch policy from Besbes et al. (2022) fails in an EV system—it implies a second-order term that is $\Omega(\lambda)$. However, our power-of- d dispatch policy makes appropriate use of the “extra” vehicles that are charging so that the system operator can sustain a smaller fleet size as long as there are enough chargers ($\gamma \approx 1/2$). In this case, vehicles don’t have to drive too far to find a charging station, and trip requests matched to vehicles at charging stations have short pickup times. When the number of charging stations is limited (e.g., $\gamma = 1/3$), the second-order term is the same as in a system without EVs, $\Theta(\lambda^{2/3})$, because there aren’t enough charging stations to leverage their spatial density. This highlights the different nature of an EV system in which the fleet size scaling depends on the charging infrastructure. In addition, a matching policy that carefully manages both the spatial and the SoC dimensions is needed.

Simulation. We corroborate our theoretical finding using a simulator that explicitly accounts for the spatial dimension of the system and the inherent stochasticity associated with trip requests and the evolution of SoC. Our simulation results confirm our stability assumption, theoretical scaling, and the trade-off that emerges between fleet size, number of chargers, and battery pack size. Additionally, we empirically verify that power-of- d has better performance than other matching policies that select the closest vehicle or the closest vehicles with enough SoC to complete a trip.

Varying Demand Patterns. We discuss how to extend our findings to varying arrival rates and examine their impact on our capacity and infrastructure planning insights. We show that three different cases arise depending on the inhomogeneity in the demand pattern. For low and moderate variability in the demand pattern, we show that the fleet continues to behave like an EV fleet and

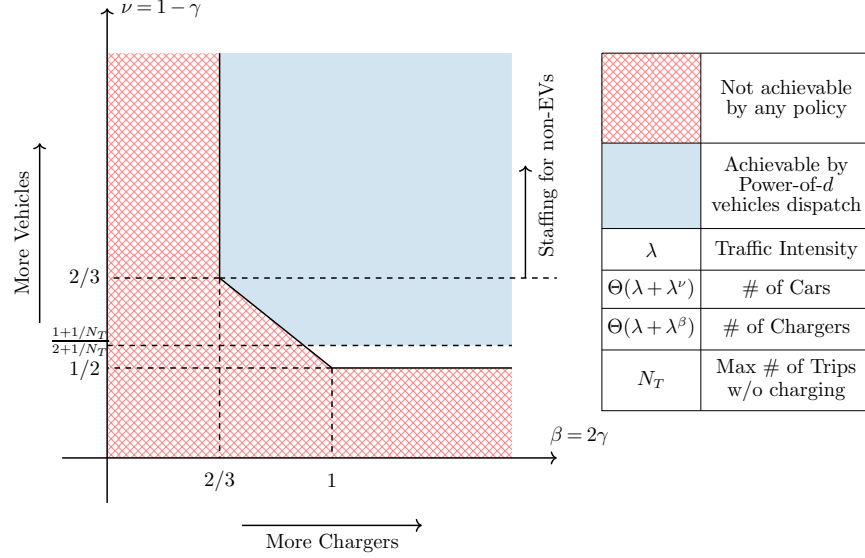


Figure 1 Illustration of the number of Vehicles and Chargers required to sustain a given service level.

so, the insights obtained from the constant arrival rate case continue to hold. On the other hand, for high variability, the fleet starts to behave like a non-EV fleet. In this case, all the charging can be executed during demand valleys so fully charged vehicles can operate like non-EV vehicles during the demand peaks. We quantify this phase transition from EV-like behavior to non-EV-like behavior and show that, along with the demand inhomogeneity, it depends on the target service level, the charge rate, and the battery pack size.

2. Literature Review

Our work lies in the intersection of studies about electric vehicles, capacity and infrastructure planning in service systems and load balancing.

2.1. Electric Vehicles

Several papers have investigated the challenges posed by electric vehicle charging, considering the potential strain on electric grids and longer refueling times. Various studies propose different solutions, such as decentralized algorithms (Gan et al. 2012, Ma et al. 2011) for load distribution during nighttime, cost and emission-based delayed charging strategies (Wu et al. 2022), and management of large-scale charging stations (Wang et al. 2016, Mukherjee and Gupta 2014). Other related research explores the optimal deployment of charging stations (Paganini et al. 2022) and

the impact and implementation of battery swapping technology (Qi et al. 2023, Avci et al. 2015). Notably, Mak et al. (2013) develop a robust optimization model for cost-effective infrastructure deployment of EVs with battery swapping, and He et al. (2021) propose a methodology for optimizing the location, size, and repositioning of charging stations in an electric vehicle-sharing system like car2go. Additionally, Abouee-Mehrizi et al. (2021) investigate the viability and environmental impact of EVs in the vehicle-sharing market, highlighting the importance of charging speed and the number of charging stations. While these studies primarily focus on charging and repositioning aspects of EV-based systems, our work centers around infrastructure planning, specifically the analysis of charging station infrastructure and fleet size in a ride-hailing system where vehicles need to pick up customers before providing service. Other related applications include optimal repositioning and recharging policies for electric bike/scooter sharing (Akturk et al. 2022, Osorio et al. 2021, Greening and Erera 2021), vehicle-to-grid electricity selling (Zhang et al. 2021), and the integration of solar power generation with battery storage (Kaps et al. 2022, Kaps and Netessine 2022).

2.2. Capacity Planning

The seminal work of Halfin and Whitt (1981) on heavy traffic limits for G/M/n queues implies that a system operator should staff $\lambda + \sqrt{\lambda}$ servers, where λ is the offered load. We refer the reader to Reed (2009) for the more general case of G/G/n queue and the survey papers Gans et al. (2003), Aksin et al. (2007) for further reading. The capacity planning implications of this stream of work do not translate directly to models with a spatial aspect as shown in Besbes et al. (2022). In particular, the authors consider a stylized spatial model of an on-demand transportation platform by approximating the pickup time by the expected distance of the closest available vehicle and show that a higher staffing of $\lambda + \lambda^{2/3}$ is needed. In their work, the system operator should maintain a higher density of available vehicles to ensure short pickup times. We consider a related but considerably more complex system as, in addition to the spatial dimension of the problem, we need to keep track of the SoC of each car which results in a much larger state space. Moreover, EVs further introduce the challenge of balancing the SoC across the fleet. Our analysis carefully optimizes

the tradeoff between SoC and pickup times as opposed to optimizing just for pickup times as in Besbes et al. (2022). Our results and scalings are also different due to charging and the possibility of utilizing “partially” charged vehicles to serve incoming customers. For additional works in the space of spatial matching, we refer the interested reader to Kanoria (2022), Akbarpour et al. (2021), Benjaafar et al. (2022), and to Daganzo and Smilowitz (2004), Lim et al. (2017) for spatial analysis in the context of supply chain and transportation.

In closely related work, Deng et al. (2022) propose a closed queueing network model to analyze infrastructure planning decisions for electric vehicle-sharing systems. They show that increasing the number of chargers improves vehicle availability and suggest that two slow chargers may be more effective than one fast charger when there is significant variability in charging times. Our main result not only provides a precise characterization of the trade-off between the number of chargers and fleet size but it also sheds light on the forces behind that trade-off. Another difference is that Deng et al. (2022) do not explicitly model the pickup and drive to the charger time and, in addition, they optimize fleet sizing and charger allocation in a sequential manner as opposed to solving a joint optimization problem.

Finally, while we use an analytical methodology to study infrastructure planning questions, a simulation-based approach has also been considered in the literature see e.g., Levin et al. (2017), Bauer et al. (2018), Loeb and Kockelman (2019), Vosooghi et al. (2019b,a), Yang et al. (2023). These papers analyze several interesting questions such as charging infrastructure planning (Bauer et al. 2018); effectiveness of shared autonomous vehicles versus personal vehicles (Levin et al. 2017); profitability of gasoline versus electric vehicles (Loeb and Kockelman 2019), and fleet sizing and charging infrastructure considering congestion effects (Yang et al. 2023).

2.3. Load Balancing

To optimize the trade-off between pickup times and balancing the SoC across the fleet, we propose the power-of- d vehicles dispatch policy that closely relates to the power-of- d choices in the load balancing literature (Vvedenskaya et al. 1996, Mitzenmacher 1996, 2001). For load balancing,

power-of- d samples d queues uniformly at random and routes the incoming arrival to the shortest one among them. In our case, power-of- d matches the incoming customer to the EV with the highest SoC among the d closest to its origin. Because of how the exogenous arrival rate scales with the number of cars in our system, it relates closely to the sub-Halfin Whitt regime (Liu and Ying 2020, Liu et al. 2022b,a, Varma et al. 2022) analyzed extensively for power-of- d choices and join the shortest queue (JSQ) policies. These papers show that the performance of the queueing systems improves with d as the load is balanced more effectively across the queues. However, in our system, we observe a trade-off between pickup times and load balancing. In particular, even though a higher value of d balances the SoC more effectively, the pickup times can also be higher. Thus, in contrast to the queueing literature, we must pick d carefully to optimize this trade-off.

3. Model

We study a deterministic electric vehicle (EV) ride-hailing system. Customers arrive to the system at an exogenous rate λ requesting trips with a uniformly distributed origin and destination over a bounded 2-dimensional region. The system consists of n electric vehicles to serve trip requests. Each EV has a battery pack size of p^* [kWh] that determines the maximum drive time before it needs to charge. We let r_d denote the discharge rate of the vehicles while driving in [kW]. Hence, an EV can drive for p^*/r_d hours before running out of charge. There is a total of m chargers in the system uniformly distributed in space which charge EVs at a rate of r_c [kW]. We assume that $r_c > r_d$, that is, the charge rate is larger than the discharge rate, and we let $r = r_d/r_c$ denote the fraction of time a vehicle must spend at a charging station for every driven unit of time.¹ EVs have a dynamic state of charge (SoC) denoted by $s_i(t) \in [0, 1]$ with $i \in [n]$. It represents the current battery level of a given vehicle at time t .

A vehicle can be in one of five states at any given time. Depending on its state, they are available to serve a rider or not. Available vehicles are in one of three states: idle, driving to a charger,

¹ This rate depends on the type of charger and vehicle. For example, the charge rate is 10-20 [kW] for level II chargers and more than 50 [kW] for the fast chargers. In this paper, we consider constant charge and discharge rates that correspond to average values.

and charging. We use $c_I(t)$, $c_{DC}(t)$, and $c_C(t)$ to denote the number of vehicles in these states, respectively. Note that we allow for the possibility of interrupting the process of charging or driving to a charger for a vehicle that is needed to serve a ride request. An EV that is picking up or driving with a customer is not available to serve new requests. We use $c_P(t)$ and $c_R(t)$ to denote these vehicles, respectively. Hence, the total number of EVs in the system satisfies

$$n = c_P(t) + c_R(t) + c_{DC}(t) + c_I(t) + c_C(t), \quad \forall t. \quad (1)$$

3.1. System Operator's Policy

Before we describe the system's dynamics, we explain the controls the system operator has to influence such dynamics. The system operator can exercise complete control over the vehicles and chargers. First, upon the arrival of a customer, the system operator decides which EVs will be available for picking up the customer (if any). For example, if all the EVs not already serving a customer have a low SoC, the system operator may decide to drop the trip request. In turn, the second lever is admission control. Third, the system operator determines what an EV does after a trip. A vehicle can be routed to the nearest available charger or remain idle until the next matching opportunity. Once an EV starts charging, the system operator decides the charging time too. In sum, a system operator's policy consists of selecting available EVs for pickup, customer admission control, routing of vehicles to chargers, admission control of EVs at chargers, and the length of a charging session. We use π to denote a policy and Π to denote the set of admissible policies. We sometimes use the superscript π to stress the dependence of a given quantity on a policy.

3.2. Dynamics

We consider a loss system, that is, an incoming customer leaves the system if not matched immediately. We use $\lambda_{\text{eff}}^\pi(t)$ to denote the effective arrival rate of customers to the system at time t . Note that, the effective arrival rate is at most the exogenous arrival rate, i.e., $\lambda_{\text{eff}}^\pi(t) \leq \lambda$. The system dynamics, influenced by the system operator's policy, determine the effective arrival rate. For every match, the assigned vehicle picks up the customer and then drives to the customer's destination. Let $q(t)$ denote the total number of customers in the system at time t . We then have

$$q(t) = c_P(t) + c_R(t), \quad \forall t. \quad (2)$$

That is, the number of customers in the system equals the total number of vehicles picking up or driving with a customer. We use T_R to denote the average trip time. For a given policy π , let the average pickup time be $T_P^\pi(t)$ at time t —the pickup time an average customer would experience at time t . Throughout the paper, we make the following assumption. There exists a constant $\tau_1 > 0$ such that

$$T_P^\pi(t) \geq \frac{\tau_1}{\sqrt{n - q(t)}}, \quad \forall t, \quad \forall \pi \in \Pi. \quad (\text{A1})$$

The right-hand side above approximates the average closest-dispatch pickup time when the number of available vehicles is $n - q(t)$.² The assumption captures that for an arbitrary policy π and a given system state, the system operator may decide to (or be limited to) use a limited fraction of EVs to serve an arriving customer thereby leading to a larger than the shortest possible average pickup time.

For a given policy π , we let $T_{DC}^\pi(t)$ denote the system average time that it would take a vehicle to reach a charger at time t . Throughout the paper, we assume that there exists a constant $\tau_2 > 0$ such that

$$T_{DC}^\pi(t) \geq \frac{\tau_2}{\sqrt{m - c_C(t)}}, \quad \forall t, \quad \forall \pi \in \Pi. \quad (\text{A2})$$

Note that $m - c_C(t)$ corresponds to the total number of free chargers at time t . Hence, the right-hand side above approximates the fastest possible closest-dispatch travel time to a charger. An arbitrary policy would have a higher travel time to a charger as it may route vehicles to chargers that are not necessarily the closest. Once an EV finishes charging, it leaves the corresponding charger and becomes idle.

² We refer the reader to Besbes et al. (2022) and Wang et al. (2022) for similar modeling approaches. The average shortest distance to k uniformly distributed points in a 2-dimensional region scales as $1/\sqrt{k}$ for k large, see Lemma 2 for a more general and formal statement.

3.3. Objective

The system operator's goal is to design a control policy $\pi \in \Pi$ so as to attain a desired long-run service level while at the same time minimizing the number of vehicles and chargers. Formally, we define a lower bound for the service level by

$$\underline{\alpha}_{\text{eff}}^{\pi} \triangleq \frac{1}{\lambda} \liminf_{T \rightarrow \infty} \frac{1}{T} \int_0^T \lambda_{\text{eff}}^{\pi}(t) dt.$$

Given a target service level $\alpha \in (0, 1)$, we seek a policy $\pi \in \Pi$ under which $\underline{\alpha}_{\text{eff}}^{\pi} \geq \alpha$ and the system operates with the minimum possible number of vehicles and chargers. We accomplish this by first characterizing the minimum number of EVs and chargers required to ensure that $\bar{\alpha}_{\text{eff}}^{\pi} \geq \alpha$, where $\bar{\alpha}_{\text{eff}}^{\pi}$ is the limsup analog of $\underline{\alpha}_{\text{eff}}^{\pi}$. Then, we propose a charging and matching policy such that $\bar{\alpha}_{\text{eff}}^{\pi} \geq \alpha$ with the minimum possible number of EVs and chargers. Such characterizations, in turn, allow us to provide various insights into capacity planning for an EV on-demand transportation system.

4. Minimum Requirement of EVs and Chargers

We derive universal, policy-independent, lower bounds on the number of EVs and chargers in terms of a desired service level $\alpha \in [0, 1]$ and the exogenous arrival rate λ for policies π such that $\bar{\alpha}_{\text{eff}}^{\pi} \geq \alpha$.

The following proposition establishes first-order lower bounds on the number of vehicles and chargers required to sustain a service level of $\bar{\alpha}_{\text{eff}}^{\pi}$ ignoring spatial frictions.

PROPOSITION 1 (First Order Lower Bounds). *For any policy π , we have that $n \geq (1+r)T_R \cdot \bar{\alpha}_{\text{eff}}^{\pi} \lambda$ and $m \geq rT_R \bar{\alpha}_{\text{eff}}^{\pi} \lambda$.*

If we disregard the pickup time, each customer spends a total of T_R amount of time in the system. Thus, at least $T_R \bar{\alpha}_{\text{eff}}^{\pi} \lambda$ number of EVs are driving. Moreover, ignoring the time to reach a charger, in order to recover the SoC expended while driving, EVs need to charge for rT_R amount of time at a charger. Therefore, at least $rT_R \bar{\alpha}_{\text{eff}}^{\pi} \lambda$ number of EVs are charging. This implies a lower bound of $rT_R \bar{\alpha}_{\text{eff}}^{\pi} \lambda$ for the number of chargers and $T_R \bar{\alpha}_{\text{eff}}^{\pi} \lambda + rT_R \bar{\alpha}_{\text{eff}}^{\pi} \lambda$ for the number of vehicles. The importance of this result is that it showcases a fundamental difference between a system with and

without EVs. The EV system has an additional requirement of $\Theta(\lambda)$ vehicles which is imposed by the need of charging the vehicles. While this increased capacity requirement makes this type of system asset-heavy, it also presents an opportunity to leverage the additional $\Theta(\lambda)$ vehicles at chargers to reduce the workload stemming from spatial frictions.

The presence of spatial frictions further increases the fleet size and the number of chargers required to attain a given service level. The pickup time decreases the service rate of customers, thereby we need more EVs to sustain the same service level. Similarly, increasing the number of chargers implies a greater spatial density of chargers which, in turn, reduces the drive time to a charger. This gives rise to a natural trade-off between the number of EVs and chargers. As we increase the number of chargers and the time to reach them decreases, the workload in the system goes down thereby allowing the system to function with fewer vehicles. The following theorem captures the impact that spatial frictions have on the fleet capacity and charging infrastructure requirements.

THEOREM 1 (Universal Lower Bounds). *Fix an $\alpha \in [\delta, 1]$ for some $\delta > 0$ and let π be such that $1 \geq \bar{\alpha}_{\text{eff}}^\pi \geq \alpha$. Then, for all $\lambda > 0$, there exists $\gamma \in [1/3, 1/2]$ such that*

$$n \geq (1+r)T_R\alpha\lambda + \Omega(\lambda^{1-\gamma}) \quad \text{and} \quad m \geq rT_R\alpha\lambda + \Omega(\lambda^{2\gamma}). \quad (3)$$

We defer the details of the proof to Section A.2 in the Appendix. Theorem 1 establishes that for any policy that achieves a service level of $\alpha \in (0, 1)$, the minimum number of vehicles and chargers should follow (3) for $\gamma \in [1/3, 1/2]$. In other words, if the number of vehicles and chargers do not scale as in (3), the system would fail to attain a service level of α (see Figure 1 for an illustration of this result).

The theorem also provides various insights related to fleet and infrastructure planning decisions. First, both more vehicles and more chargers are required compared to the first-order bounds in Proposition 1. The additional capacity requirements emerge due to spatial frictions. In particular, the second order term $\Omega(\lambda^{1-\gamma})$ for EVs corresponds to the vehicles that will be driving to both

pick up a customer and reach a charger. The second order term $\Omega(\lambda^{2\gamma})$ in the lower bound for the chargers corresponds to the charging infrastructure needed to have enough spatial density so that vehicles do not spend too much time reaching a charger. Second, the parameter γ captures a natural trade-off between n and m . As γ increases from $1/3$ to $1/2$, the fleet size requirement reduces at the expense of installing more chargers. Intuitively, more chargers reduce the drive time to a charger which translates into a lower fleet size requirement.

Third, Theorem 1 suggests a capacity planning prescription for EVs different from the one in the context of ICE vehicles which has been analyzed in Besbes et al. (2022). Their results imply that, due to the presence of spatial frictions, the number of vehicles required to sustain a service level of α should be at least $T_R\alpha\lambda + \Omega(\lambda^{2/3})$ while our bound in (3) implies a minimum requirement of $(1+r)T_R\alpha\lambda + \Omega(\lambda^{1-\gamma})$ where γ ranges from $1/3$ to $1/2$ depending on the number of chargers. Since $r > 0$, the first-order term is higher for the EV system. In particular, the finite charging rate introduces a downtime for EVs, due to which $rT_R\alpha\lambda$ more EVs are required compared to ICE cars. However, the second order term for the EV system is of lower order with $1-\gamma \in [1/2, 2/3]$ while in the ICE case, the required order is $2/3$. The increase of the first-order term and potential reduction of the second-order term are an inherent byproduct of the physics of an EV system. As we mentioned before, the system requires $\Theta(\lambda)$ vehicles charging. In turn, if the average SoC of the fleet is sufficiently high, the charging vehicles may also be available to serve arrivals thus increasing the vehicles available for pickups from $\Theta(\lambda^{2/3})$ in an ICE system to $\Theta(\lambda)$ in an EV system. This increased capacity dramatically increases the density of available EVs, resulting in shorter pickup times which translates into fewer vehicles doing pickups. However, the benefits crucially depend on charger density. If the charging network is not dense enough, the partially charged cars would spend most of their time driving to the chargers. To see this, note that a simple back-of-envelope calculation yields that the average time that vehicles spend driving to serve a customer is at least

$$T_R + \frac{\tau_1}{\sqrt{n - q(t)}} + \frac{\tau_2}{\sqrt{m - C_C(t)}} \approx T_R + \frac{\tau_1}{\sqrt{\lambda}} + \frac{\tau_2}{\sqrt{\lambda^{2\gamma}}},$$

where we have used that the vehicles available to pick up customers are $\Theta(\lambda)$ and we have parametrized the additional charging infrastructure, $m - C_C(t)$, by $\lambda^{2\gamma}$. Multiplying the above expression by $(1+r)\alpha\lambda$ yields a minimum requirement of EVs of

$$(1+r)T_R\alpha\lambda + \Omega(\lambda^{1/2}) + \Omega(\lambda^{1-\gamma}). \quad (4)$$

Now, note that 2γ must be greater than or equal to $2/3$ otherwise, as in Besbes et al. (2022), the system's vehicles would spend too much time driving to a charger and, in turn, we won't be able to attain the desired service level. Therefore, as we increase γ starting from $1/3$, we also increase the charging infrastructure which translates into shorter drive times to a charger and, consequently, into fewer vehicles. Such benefits, however, have a limit because the second term in (4) stays the same at $\lambda^{1/2}$ as we increase the number of chargers. In other words, the benefits extracted from a more dense charger network eventually saturate. Thus, to scale the system up, one should manufacture more vehicles and deploy more chargers simultaneously.

In sum, in an EV system, more vehicles are required compared to an ICE system; however, it is possible to exploit the benefit of partially charged vehicles to reduce the second-order term from $\lambda^{2/3}$ to as small as $\lambda^{1/2}$. We note that Theorem 1 is a best-case performance result, it only provides lower bounds for the number of vehicles and chargers but it does not guarantee that a system whose assets scale as in these bounds would deliver the desired service level. In the next section, we prove that these bounds are near achievable.

4.1. Proof Main Ideas

We prove Theorem 1 by analyzing a subset of state variables and describing their evolution through a set of differential equations that are valid under any policy.

We start by introducing some notations. Let $p_{dc}^\pi(t) \in [0, 1]$ be the portion of EVs that are driving to a charger and that reach the charger at time t . Also, let $T_C^\pi(t)$ be the average time an EV spends charging at time t . Now, the evolution of the number of customers ($q(t)$), the number of EVs charging ($c_c(t)$), and the aggregate SoC ($s(t)$) is as follows:

$$\dot{q}(t) = \lambda_{\text{eff}}^\pi(t) - \frac{q(t)}{T_R + T_P^\pi(t)}, \quad q(0) = q_0, \quad (5a)$$

$$\dot{c}_C(t) = p_{dc}^\pi(t) \cdot \frac{c_{DC}(t)}{T_{DC}^\pi(t)} - \frac{c_C(t)}{T_C^\pi(t)}, \quad c_C(0) = c_{C0}, \quad (5b)$$

$$\dot{s}(t) = c_C(t) \cdot r_c - (n - c_C(t) - c_I(t)) \cdot r_d, \quad s(0) = s_0, \quad (5c)$$

for some initial condition (q_0, c_{C0}, s_0) . In particular, note that customers leave the system at a rate of $1/(T_R + T_P^\pi(t))$. Thus, (5a) follows as $q(t)$ decreases at a rate of $q(t)/(T_R + T_P^\pi(t))$ and increases at a rate of $\lambda_{\text{eff}}^\pi(t)$. Next, EVs finish charging at a rate of $1/T_C^\pi(t)$. Thus, $c_C(t)$ decreases at a rate of $c_C(t)/T_C^\pi(t)$. In addition, EVs driving to a charger reach a charger at a rate of $p_{dc}^\pi(t)/T_{DC}^\pi(t)$. Thus, $c_C(t)$ increases at a rate of $p_{dc}^\pi(t)c_{DC}(t)/T_{DC}^\pi(t)$. Lastly, we consider the evolution of the aggregate SoC in (5c). As there are $c_C(t)$ vehicles charging at rate r_c , the aggregate SoC increases at rate $c_C(t) \cdot r_c$. Similarly, as the number of vehicles driving at time t is $n - c_C(t) - c_I(t)$, the aggregate SoC decreases at rate $(n - c_C(t) - c_I(t)) \cdot r_d$. Finally, because the battery pack size is finite, we have

$$T_C^\pi(t) \leq \frac{p^*}{r_c}, \quad \forall t, \quad (6)$$

where p^*/r_c is the time it takes to fully charge a vehicle.

The set of equations (5a) to (5c) partially characterizes the system evolution for an arbitrary policy π as given by the number of customers, vehicles charging, and the aggregate SoC. We would need an explicit policy to obtain a more detailed description of the system evolution, for example, the number of EVs with a certain battery level. In fact, in Section 5, we specialize our model to the power- d dispatch policy and determine via an augmented set of differential equations the evolution of the number of vehicles with a given SoC at any time. In the current section, however, our focus is on universal bounds on the service level. It turns out that equations (5a) to (5c) provide enough information to accomplish this task.

First, we analyze the equilibrium points of the differential equations given by (5) to obtain a relation between $\bar{\alpha}_{\text{eff}}^\pi$, n , and m .

PROPOSITION 2. *For any policy π , there exists $(\bar{q}, \bar{c}_C, \bar{c}_I, \bar{c}_{DC})$ such that*

$$\bar{\alpha}_{\text{eff}}^\pi \lambda \left(\frac{\tau_1}{\sqrt{n - \bar{q}}} + T_R \right) \leq \bar{q}, \quad (7a)$$

$$\frac{\bar{c}_C}{\sqrt{m - \bar{c}_C}} \cdot \frac{r_c}{p^*} \leq \frac{\bar{c}_{DC}}{\tau_2}, \quad (7b)$$

$$\bar{c}_C r_c = (n - \bar{c}_C - \bar{c}_I) r_d. \quad (7c)$$

We establish this result by analyzing the long-run average behavior of Equations (5a) to (5c) and exploiting the convexity of the lower bounds for $T_P^\pi(t)$ and $T_{DC}^\pi(t)$ in (A1) and (A2), respectively. Equation (7a) is analogous to Little's law; the number of customers in the system is equal to the product of effective arrival rate and the amount of time each customer spends in the system (pickup time plus trip time). Next, Equation (7b) says that the minimum rate of EVs departing from a charger has to be less than the maximum rate at which they arrive at a charger. In particular, (7b) is obtained by substituting a lower bound for $1/T_C^\pi(t)$ and an upper bound for $p_{dc}^\pi(t)/T_{DC}^\pi(t)$. Lastly, Equation (7c) balances the aggregate charge and discharge rates. We note that Proposition 2 does not yield a complete characterization of the equilibrium points of the differential equations in (5a) to (5c), instead, any equilibrium point satisfies (7).

As $n \approx (1+r)T_R\bar{\alpha}_{\text{eff}}^\pi\lambda$ by Proposition 1 and $q(t) \approx T_R\bar{\alpha}_{\text{eff}}^\pi\lambda$ by Equation (7a), the pickup time is approximately

$$\frac{1}{\sqrt{n-q(t)}} \approx \Theta(\lambda^{-1/2}).$$

Thus, we have

$$n = \bar{c}_R + \bar{c}_C + \bar{c}_P + \bar{c}_{DC} \approx T_R\bar{\alpha}_{\text{eff}}^\pi\lambda + rT_R\bar{\alpha}_{\text{eff}}^\pi\lambda + \lambda^{1/2} + \bar{c}_{DC}, \quad (8)$$

where we have used that the number of EVs driving with a customer is equal to the number of customers on-trip ($T_R\bar{\alpha}_{\text{eff}}^\pi\lambda$); the number of EVs charging is at least r times \bar{c}_R ; and the number of EVs picking up customers is $\lambda^{-1/2} \times \lambda = \lambda^{1/2}$. Now, from (7b), we get

$$m \geq \bar{c}_C + \left(\frac{r_c\tau_2}{p^*}\right)^2 \cdot \left(\frac{\bar{c}_C}{\bar{c}_{DC}}\right)^2 \approx rT_R\bar{\alpha}_{\text{eff}}^\pi\lambda + r\bar{c}_{DC} + \left(\frac{\lambda}{\bar{c}_{DC}}\right)^2, \quad (9)$$

where the approximation follows as the number of cars charging is equal to r times the number of cars driving. Now, by parameterizing \bar{c}_{DC} as $\lambda^{1-\gamma}$, and noting that $\bar{\alpha}_{\text{eff}}^\pi \geq \alpha$, we get

$$n \geq (1+r)T_R\alpha\lambda + \lambda^{\max\{\frac{1}{2}, 1-\gamma\}} \quad m \geq rT_R\alpha\lambda + \lambda^{\max\{2\gamma, 1-\gamma\}}.$$

The case of $\gamma > 1/2$ is erroneous as we get a tighter lower bound for m given the same lower bound for n . Similarly, $\gamma < 1/3$ is also erroneous. Restricting $\gamma \in [1/3, 1/2]$ yields the result.

5. Achieving Optimal Performance

In this section, we analyze the system under a specific policy and show that it nearly achieves the lower bound on n and m from Theorem 1. We first introduce the policy which we coin *power-of- d vehicles dispatch*, and then present the main theorem of this section and discuss its implications. In the second part of this section, we show how to model and analyze the system's performance under the power-of- d vehicles dispatch policy. The main challenge here is to find a rich but simple enough state space with a corresponding dynamical system that enables us to capture the complexities associated with the evolution of the vehicles' SoC but that it is also amenable to analysis.

The power-of- d vehicle dispatch policy effectively achieves two primary objectives: minimizing pickup times and ensuring a healthy and balanced SoC throughout the fleet. When $d = 1$, the policy simplifies to closest-dispatch, where the nearest available vehicle is assigned. On the other hand, for $d > 1$, the policy selects the d closest vehicles and assigns the request to the vehicle with the highest SoC among them. A more detailed description of this policy is presented in Algorithm 1. By considering the d closest vehicles, the policy strikes a balance between minimizing pickup distance and selecting a vehicle with a higher SoC. Indeed, for large d , the policy may opt for a vehicle with a high SoC, but this could lead to longer pickup times and potentially destabilize the overall system SoC. Conversely, when d is small, pickup times are controlled, but the policy may select vehicles with low SoC, which might be incapable of serving customers. In fact, as demonstrated in Proposition 5 (Appendix C.1), the closest dispatch fails to deliver the required service level. By carefully selecting an appropriate value for d , it becomes feasible to maintain manageable pickup times while also choosing vehicles with higher SoC compared to the closest dispatch policy.

In our second main result, we show that the power-of- d vehicles dispatch policy can achieve any given service level for almost all combinations of the number of vehicles and chargers in the lower bounds of Theorem 1. To state the theorem, we define N_T as the number of trips an EV can complete with a 100% SoC.

ALGORITHM 1: Power-of- d Vehicles Dispatch

Input : Fix $d \geq 1$
for Every Arrival **do**
 if All vehicles are busy **then**
 | The arrival is dropped;
 end
 Choose the d closest vehicles that are not driving;
 if None of the d vehicles have enough SoC for the trip **then**
 | The arrival is dropped;
 end
 Match the arrival to the vehicle with the highest SoC among the d closest;
 Once the trip ends, send the vehicle to the closest available charger;
 The vehicle becomes available for matching after it has reached a charger;
end

THEOREM 2 (Near-Matching Upper Bound). *Assume that the associated dynamical system exhibits global stability.³ Fix an $\alpha \in [\delta, 1)$ for some $\delta > 0$ and $\gamma \in \left[\frac{1}{3}, \frac{1}{2+1/N_T}\right)$ with $N_T \geq 2$. Then, there exists $\lambda_0(\alpha)$ and m, n with*

$$n = (1+r)T_R\alpha\lambda + \Theta(\lambda^{1-\gamma}), \quad \text{and}, \quad m = rT_R\alpha\lambda + \Theta(\lambda^{2\gamma}),$$

such that, under the power-of- d vehicles dispatch policy with $d = \tilde{\Theta}(\lambda^{\gamma/N_T})$, we have $\bar{\alpha}_{\text{eff}}^\pi \geq \underline{\alpha}_{\text{eff}}^\pi \geq \alpha$, $\forall \lambda \geq \lambda_0(\alpha)$,

We defer the proof of the theorem and a discussion about the stability assumption to Section 5.3. The result in Theorem 2 nearly achieves the lower bound in Theorem 1. The only discrepancy is the range of admissible values of γ : γ is restricted to be less than $\frac{1}{2+1/N_T}$ in Theorem 2 as opposed to the upper bound of $1/2$ in Theorem 1. However, as the battery pack size increases and vehicles can perform more trips with a full charge, $\frac{1}{2+1/N_T}$ can be arbitrarily close to $1/2$. This also means that the minimum required fleet size should not experience large changes for large values of N_T or, equivalently, large values of p^* . Additionally, the theorem uncovers the forces that determine the choice of d . For a fixed arrival rate, as γ increases, the number of vehicles decreases due to the increased spatial density of chargers. However, having a smaller fleet for the same arrival rate

³ We present the dynamical system that describes the evolution of the system under power-of- d vehicles dispatch in Section 5.1.

results in a larger proportion of vehicles having a lower SoC. Consequently, the value of d should be larger to ensure that the policy can locate a vehicle with a sufficiently high SoC. As N_T increases, SoC becomes less of a limiting factor, reducing the need to reach too far to find a vehicle with a sufficient SoC.

5.1. Power of d Vehicles Dispatch: Modeling

We define the detailed model that describes the system evolution under the power-of- d vehicle dispatch policy. First, we specify the pickup time, drive to the charger time, and, in turn, obtain the total time vehicles are busy. Second, we propose a tractable method to describe the evolution of the SoC of the fleet. This enables us to derive a set of differential equations that fully capture the dynamics of the system. Third, we examine the equilibrium point of the differential equations, leading to the derivation of Theorem 2.

5.1.1. Vehicles' Busy Times In the power-of- d vehicles dispatch algorithm, an EV is dispatched to a charger right after finishing a trip. Hence, for each customer served, the corresponding EV is busy for the length of the pickup time, travel time, and the drive to the charger time. In turn, we approximate $T_{DC}(t)$ by

$$T_{DC}(t) = \frac{\tau_2}{\sqrt{m - c_C(t)}}. \quad (10)$$

Since there are m chargers and a total of $c_C(t)$ vehicles charging, $m - c_C(t)$ chargers are available. Thus, the expression above represents the average distance to the closest charger, assuming that the empty chargers are distributed uniformly in space.

For the pickup time, $T_P(t)$, note that for a sequence of k two-dimensional points, the d^{th} closest point to a given point scales as $\Theta\left(\sqrt{\frac{d}{k}}\right)$ as k increases (c.f., Lemma 2 in the appendix). We then use the following approximation

$$T_P(t) = \tau_1 \sqrt{\frac{d}{n - (q(t) + c_{DC}(t))}}. \quad (11)$$

Recall that n is the total number of vehicles in the system and $q(t) + c_{DC}(t)$ vehicles are busy at time t , i.e., driving with a customer or driving to a charger. Hence, $n - (q(t) + c_{DC}(t))$ vehicles are

available to serve incoming customers. Note that $T_P(t)$ is consistent with (A1) as $d \geq 1$. The rate $\mu(t)$ at which vehicles complete serving a customer and driving to a charger is then given by

$$\frac{1}{\mu(t)} = \tau_1 \sqrt{\frac{d}{n - (q(t) + c_{DC}(t))}} + T_R + \frac{\tau_2}{\sqrt{m - c_C(t)}}. \quad (12)$$

5.1.2. State Space For every trip request, our policy must be able to identify the d closest vehicles and, crucially, select the one with the highest SoC. In turn, a description of the state of the system must include a detailed record of the fleet's SoC. However, tracking the continuous SoC's changes of each vehicle leads to an intractable model and, therefore, we use a different state description that keeps track of the number of vehicles that can fulfill a certain number of trip requests at any given time. We accomplish this in three steps. We first introduce admission control to obtain an upper bound on the time a vehicle spends driving per customer, i.e., we upper bound $1/\mu(t)$. In turn, we obtain an upper bound on SoC spent per customer served, i.e., $r_d/\mu(t)$. Then, we introduce a modified system in which the SoC spent per trip is given by this upper bound. This enables us to discretize the SoC of each EV as the SoC spent per trip is constant. Finally, our state space representation relies on this discretization to count the number of vehicles idling, charging, or busy that can fulfill a given number of trip requests.

The admission control policy is defined as follows.

DEFINITION 1 (ADMISSION CONTROL).

- Only a fraction of trips are admitted so that the arrival rate is $\tilde{\lambda} = \alpha\lambda + \Theta(\lambda^{1-\gamma})$.
- A trip request is not admitted if the number of busy cars, $q(t) + c_{DC}(t)$, exceeds $T_R\tilde{\lambda}$.
- A maximum of $A \triangleq m - \tilde{\lambda}^{2\gamma}$ vehicles are allowed to charge at a time. Vehicles with lower SoC are given precedence to charge.

Admission control then implies the following bound for the time an EV spends serving a request

$$\frac{1}{\mu(t)} \leq \tau_1 \sqrt{\frac{d}{n - T_R\tilde{\lambda}}} + T_R + \frac{\tau_2}{\sqrt{m - A}} \triangleq T_B.$$

This allows us to maintain a supply of enough available vehicles to ensure that the pickup times are small. Similarly, we are maintaining enough available chargers to ensure that the drive to the

charger times are small. Note that we will carefully choose the parameters that characterize the admission control policy so that the time a vehicle is busy matches the intuition we obtained from the lower bound analysis c.f., Equation (4).

For the remainder of the paper, we consider a modified system in which each vehicle spends $\Delta \triangleq T_B r_d$ [kWh] of battery for each trip request (pickup and trip, followed by driving to a charger). Since the modified system spend more SoC serving a trip request, any admissible decisions in the modified system are also admissible in the original system and, therefore, the bounds we derive in the former also hold in the latter. We make this observation precise in the following lemma.

LEMMA 1. *For a given λ , there exists an admissible policy $\pi \in \Pi$ for the original system that serves the same sequence of arrival as in the modified system. Thus, the effective arrival rate is identical for both systems.*

Finally, we are ready to introduce the state space description. In the modified system, the state space can be reduced to a discrete set as the SoC of all EVs is an integer multiple of Δ . Indeed, note that since the pack size of a vehicle is p^* , a fully charged vehicle can serve a total of $N_T \triangleq \lfloor p^*/\Delta \rfloor$ trip requests. For $j \in \{0, \dots, N_T\}$, we define:

$X_j^C(t) \triangleq \#$ of vehicles idling or charging that can serve no more than j trips requests at time t ,

$X_j^B(t) \triangleq \#$ of vehicles busy that can serve no more than j trips requests at time t .

These state variables aggregate vehicles either charging/idling or busy that can serve a certain number of trips or fewer, but no more. For example, $X_j^C(t)$ is the sum of vehicles that have enough battery to serve exactly 0, 1, all the way up to j trips but no $j+1$ or more trips. We note that $X_{N_T}^C(t)$ includes all vehicles that are idling and charging. Additionally, we note that $X_{N_T}^C(t) + X_{N_T}^B(t) = n$ for all $t \in \mathbb{R}_+$.

5.1.3. Transition Probabilities The evolution of $X_j^C(t)$ and $X_j^B(t)$ depends on how the policy assigns vehicles with different SoC levels to trip requests. This assignment, in turn, depends on the SoC distribution of the fleet. For example, if vehicles that can serve only a small number of

trip requests form a larger portion of the fleet, the policy will likely choose one of them to serve a trip request. To determine this, consider that trip requests arrive at uniformly random locations. As a result, the d closest vehicles can be treated as if they were randomly selected, and their SoC can be considered uniformly random as well. In other words, when selecting the d closest vehicles, we are essentially sampling d SoCs from the vehicle pool without replacement. Mathematically, define the event

$$A_j(t) \triangleq \{\text{selecting at least one vehicle that can serve } j+1 \text{ or more trips}\}, \quad \forall j \in \{0, \dots, N_T - 1\}.$$

Then, we have

$$p_j(t) \triangleq \mathbb{P}(A_j(t)) = 1 - \frac{X_j^C(t)}{X_{N_T}^C(t)} \cdot \frac{X_j^C(t) - 1}{X_{N_T}^C(t) - 1} \cdots \frac{X_j^C(t) - (d-1)}{X_{N_T}^C(t) - (d-1)}, \quad \forall j \in \{0, \dots, N_T - 1\}. \quad (13)$$

That is, $p_j(t)$ is the complement probability of choosing d vehicles, uniformly at random without replacement, that can serve j (but no more than j) or fewer trips. Intuitively, $p_j(t)$ determines the rate at which vehicles with enough SoC for $j+1$ or more trips start serving a customer. The expression above assumes that $X_j^C(t) \geq d$. For the case of $X_j^C(t) < d$, we simply have $p_j(t) = 0$.

The expressions for the pickup time given by (12) and $p_j(t)$ given by (13) elucidate the trade-off that the power-of- d vehicle dispatch policy balances. For a given system state, as d increases, the service time in the system increases because pickup times become larger. However, the probability of choosing at least one vehicle that can serve a certain number of trips increases as d increases. That is, by varying d we can induce small pickup times but a low likelihood of matching with a vehicle with high SoC, or large pickup times but a high likelihood of matching with a vehicle with high SoC. We show that, by judiciously choosing d , it is possible to optimize this trade-off and, in turn, minimize the number of vehicles and chargers in the system.

Lastly, the following upper and lower bounds for $p_j(t)$ will be useful in the analysis of the policy's performance:

$$1 - \left(\frac{X_j^C(t)}{X_{N_T}^C(t)} \right)^d \leq p_j(t) \leq 1 - \left(\frac{X_j^C(t)}{X_{N_T}^C(t)} \right)^d \left(\frac{1 - d/X_j^C(t)}{1 - d/X_{N_T}^C(t)} \right)^d,$$

where we set the lower and upper bounds to zero whenever $X_j^C(t) < d$. The lower bound corresponds to the complement probability of choosing d vehicles, uniformly at random *with replacement*, that can serve j (but no more than j) or fewer trips.

5.2. System Dynamics as ODEs

We are now ready to introduce the differential equations that describe the system's evolution under the power of d vehicle dispatch policy. Define the admission control variables $I(t) \triangleq \mathbf{1}\{X_{N_T}^B(t) \leq T_R \tilde{\lambda}\}$ and $\tilde{X}_j^C \triangleq \min\{X_j^C, A\}$. We have:

$$\dot{X}_j^B(t) = \tilde{\lambda}(p_0(t) - p_j(t))I(t) - X_j^B(t)\mu(t), \quad 1 \leq j \leq N_T, \quad (14a)$$

$$\dot{X}_j^C(t) = -\tilde{\lambda}(p_0(t) - p_j(t))I(t) - \left(\tilde{X}_j^C(t) - \tilde{X}_{j-1}^C(t)\right) \frac{1}{rT_B} + X_{j+1}^B(t)\mu(t), \quad 1 \leq j < N_T, \quad (14b)$$

$$\dot{X}_{N_T}^C(t) = -\tilde{\lambda}p_0(t)I(t) + X_{N_T}^B(t)\mu(t), \quad (14c)$$

$$\dot{X}_0^C(t) = -\tilde{X}_0^C(t) \frac{1}{rT_B} + X_1^B(t)\mu(t), \quad (14d)$$

Three events can change the system state. Namely, picking up an incoming customer, finishing service, and gaining one unit of charge. We describe the system's transitions due to these events and their relationship to (14) next.

Pickup: For $j \in \{1, \dots, N_T\}$, X_j^C reduces by one, and X_j^B increases by one if an EV with SoC at most j picks up an incoming customer. The probability of this event is $p_0(t) - p_j(t)$. As the arrival rate of admitted customers is $\tilde{\lambda}I(t)$, X_j^C reduces and, X_j^B increases with rate $\tilde{\lambda}I(t)(p_0(t) - p_j(t))$.

Finish Service: For $j \in \{1, \dots, N_T\}$, X_j^B reduces by one, and X_{j-1}^C increases by one if an EV with SoC at most j finishes a trip request (pick-up, travel to a destination, and drive to a charger). As a total of X_j^B EVs are finishing service with rate $\mu(t)$, these transitions happen with rate $X_j^B(t)\mu(t)$.

Charge: For $j \in \{0, \dots, N_T - 1\}$, X_j^C reduces by one if an EV with SoC equal to j gains one unit of charge. Note that $r_d T_B$ corresponds to the total SoC in [KWh] that a vehicle expends during a trip. Hence, while charging, it takes $(r_d T_B)/r_c$ hours to gain the SoC required for a trip. Since there are $\tilde{X}_j^C(t) - \tilde{X}_{j-1}^C(t)$ charging vehicles that have SoC exactly j , $X_j^C(t)$ decreases at rate $(\tilde{X}_j^C(t) - \tilde{X}_{j-1}^C(t))/(rT_B)$.

We obtain (14a) by combining the pickup and service rates. Similarly, we get (14b) by combining the pickup, service, and charge rate. Equations (14c) and (14d) are similar to Equations (14a) and (14b) with the difference that fully charged vehicles do not gain more SoC, and fully discharged ones cannot serve incoming customers.

5.3. Power of d Vehicles Dispatch: Analysis

We are ready to prove Theorem 2. The proof has three parts. First, we analyze the system of differential equations in (14). We characterize its equilibrium points and show existence and uniqueness. Then, under a stability assumption and a given selection of the admission control and infrastructure parameters, we analyze the unique equilibrium of the system and obtain a lower bound on the number of busy vehicles in equilibrium. Finally, we translate this bound into a lower bound for α_{eff}^π which, in turn, delivers the achievability result in Theorem 2.

We set the fleet size, number of chargers, and the admission control parameters $\tilde{\lambda}$ and A to be

$$\tilde{\lambda} = \alpha\lambda + \kappa_3\lambda^{1-\gamma}, \quad n = (1+r)T_R\tilde{\lambda} + \kappa_1\tilde{\lambda}^{1-\gamma}, \quad m = rT_R\tilde{\lambda} + \kappa_2\tilde{\lambda}^{2\gamma}, \quad A = m - \tilde{\lambda}^{2\gamma}, \quad (15)$$

for some $\kappa_1, \kappa_2, \kappa_3 > 0$ to be determined. We later show that these choices of m and n are indeed consistent with Theorem 2. Now, we present two propositions that are key in the proof of Theorem 2.

PROPOSITION 3. *Let $\tilde{\lambda}$, n , m , and A be given by (15) with $\kappa_2 \geq 2 + 4r\tau_2$, $\kappa_1 \geq 2r\tau_2$, and $N_T \geq 2$. There exist $\tilde{\lambda}_0$ such that if*

$$d = \tilde{\lambda}^{\gamma/N_T} (\log d)^{1/N_T} \quad \text{with} \quad \gamma \in \left[\frac{1}{3}, \frac{1}{2 + 1/N_T} \right),$$

then for all $\tilde{\lambda} \geq \tilde{\lambda}_0$, the dynamical system (14) admits a unique equilibrium $(\mathbf{X}^C, \mathbf{X}^B)$ such that:

$$X_{N_T}^C \leq rT_R\tilde{\lambda} + \left(\frac{rT_RN_T}{\gamma} + 2\kappa_1 \right) \tilde{\lambda}^{1-\gamma}, \quad \text{and} \quad X_{N_T}^B \geq T_R\tilde{\lambda} - \left(\frac{rT_RN_T}{\gamma} + \kappa_1 \right) \tilde{\lambda}^{1-\gamma}.$$

The above proposition proves that (14) exhibits a unique equilibrium, and provides bounds on $X_{N_T}^C$ and $X_{N_T}^B$. To prove the proposition, we set $(\dot{\mathbf{X}}^C, \dot{\mathbf{X}}^B)$ to zero in (14) and analyze the corresponding system of non-linear equations. Using this system of equations, we obtain a non-linear equation in one variable which we show to have a unique solution, thereby implying the existence of a unique fixed point. The analysis of this solution delivers the bounds on $X_{N_T}^C$ and $X_{N_T}^B$. In particular, we show that the number of busy vehicles is at least $T_R\tilde{\lambda} - \Theta(\tilde{\lambda}^{1-\gamma})$. The choice of d corresponds to the minimum value of d such that the lower bound on $X_{N_T}^B$ holds. Now, in equilibrium, (14c) results

in $\tilde{\lambda}p_0I = X_{N_T}^B\mu$, where p_0, I, μ are the equilibrium quantities corresponding to $p_0(t), I(t), \mu(t)$, respectively. Note that, $\tilde{\lambda}p_0I$ is exactly the effective arrival rate of customers, i.e., the arriving customers that are served (c.f., Definition 1). Indeed, out of the admitted customers, a p_0 fraction is not served by the power-of- d vehicles dispatch policy due to the low SoC of the selected EVs. Thus, the effective rate of customers is proportional to the number of busy vehicles, and so, the lower bound on $X_{N_T}^B$ translates into a lower bound on α_{eff}^π . We obtain said lower bound on α_{eff}^π in the following proposition.

PROPOSITION 4. *Under the same setting as in Proposition 3, if the dynamical system (14) is globally stable, then there exists $\tilde{\lambda}_1 > 0$, such that for all $\tilde{\lambda} \geq \tilde{\lambda}_1$ and for any initial condition (X_0^C, X_0^B) , we have*

$$\lambda\bar{\alpha}_{\text{eff}}^\pi \geq \lambda\alpha_{\text{eff}}^\pi \geq \tilde{\lambda} - \kappa_4\tilde{\lambda}^{1-\gamma} \quad \text{with} \quad \kappa_4 = \left(\frac{rN_T}{\gamma} + \frac{\kappa_1 + 2\tau_2}{T_R} \right).$$

As a proof sketch of the above proposition, consider the following back of the envelope calculation:

$$\lambda\bar{\alpha}_{\text{eff}}^\pi = \tilde{\lambda}p_0I = X_{N_T}^B\mu \approx \frac{X_{N_T}^B}{T_R} \geq \tilde{\lambda} - \Theta(\tilde{\lambda}^{1-\gamma}).$$

Thus, from the above proposition, we obtain a lower bound on the effective service level. To see this, substitute $\tilde{\lambda} = \alpha\lambda + \kappa_3\lambda^{1-\gamma} \leq \lambda$ with $\kappa_3 = \kappa_4$ to get

$$\lambda\bar{\alpha}_{\text{eff}}^\pi \geq \alpha\lambda + \kappa_3 \left(\lambda^{1-\gamma} - \tilde{\lambda}^{1-\gamma} \right) \geq \alpha\lambda \implies \alpha_{\text{eff}}^\pi \geq \alpha.$$

Now, it just remains to see that the choice of n and m are consistent with Theorem 2 which can be done by replacing $\tilde{\lambda}$ in the expressions for n and m in (15). This completes the proof of Theorem 2.

Finally, note that while we have established the existence and uniqueness of an equilibrium point in the dynamical system (14), we have assumed global stability. In Section 6, we conduct hundreds of simulations with different initial conditions and observe that the system converges to a fixed point in all the instances. Furthermore, we note that the ODE for Power-of- d vehicles dispatch policy is similar to the ODE for Power-of- d choices in load balancing (c.f., Section E.2) which is known to be globally stable (Mitzenmacher 2001, 1996). However, a central difference between our setting and

load balancing is that we have two types of vehicles—busy and idle/charging. This distinction, in addition to highly non-linear ODEs, makes the stability analysis challenging. Establishing global stability is then an interesting open problem that may have broader applications for load balancing in queueing systems.

6. Simulations

We build a simulator for our EV system that enables us to verify our theoretical results and insights. We aim to demonstrate the robustness of our theoretical scalings in Theorem 2, the capacity planning implications of our results, and the assumptions on pickup time and drive to the charger time. In Appendix E.2, we also explore the performance of the system under other natural matching policies and compare their performance to our proposed power-of- d dispatch policy.

We consider a $[0, 10 \text{ mi}] \times [0, 10 \text{ mi}]$ spatial region and generate random arrivals. The starting and ending coordinates of a trip request on each axis are sampled from a Uniform distribution on $[0, 10]$. The inter-arrival time between two arrivals is exponentially distributed with rate λ . In our simulations, we consider $\lambda \in \{5, 10, 20, 40, 80, 160, 320\}$ arrivals per min. We run our simulator for 1000 minutes and calculate parameters like service level by considering only the second half of the simulation to ensure that the system is in steady-state. We run each simulation instance for five randomly generated data sets and the mean value of the output is reported.

For each EV in the system, a uniformly distributed initial location in $[0, 10 \text{ mi}] \times [0, 10 \text{ mi}]$ is sampled independent of all the other EVs. The SoC is initialized to be a uniform random variable on $[0.4, 0.6]$. Also, the initial state of the EVs is set to be Idle. We set the location of chargers uniformly at random on $[0, 10 \text{ mi}] \times [0, 10 \text{ mi}]$. Each charger has m_p number of posts, i.e., charging ports, and there are $m_l = \lfloor m/m_p \rfloor$ different locations of chargers. We consider $m_p = 8$ as there are on average 8-10 posts per charger in real-life (InsideEVs 2022).

The system’s evolution will be governed by the parameters in Table 1 unless otherwise stated (Bauer et al. 2018). For each trip request, the matching algorithm picks an EV to serve the customer. If the selected EV has sufficient battery to serve the trip and an additional buffer SoC

Table 1 Parameters for the Simulations.

Parameter	Value
Charge Rate (r_c) (kilo-Watt)	20 kW
Discharge Rate (r_d) (kilo-Watt)	5 kW
Average Velocity (v_{avg}) (miles per hour)	20 mi/hr
Battery Pack Size (p^*) (kilo-Watt-hour)	40 kWh
Target Service Level (α)	0.9
Minimum SoC after finishing a trip (s_{min})	0.2
Maximum SoC to dispatch an EV to a charger (s_{max})	0.9

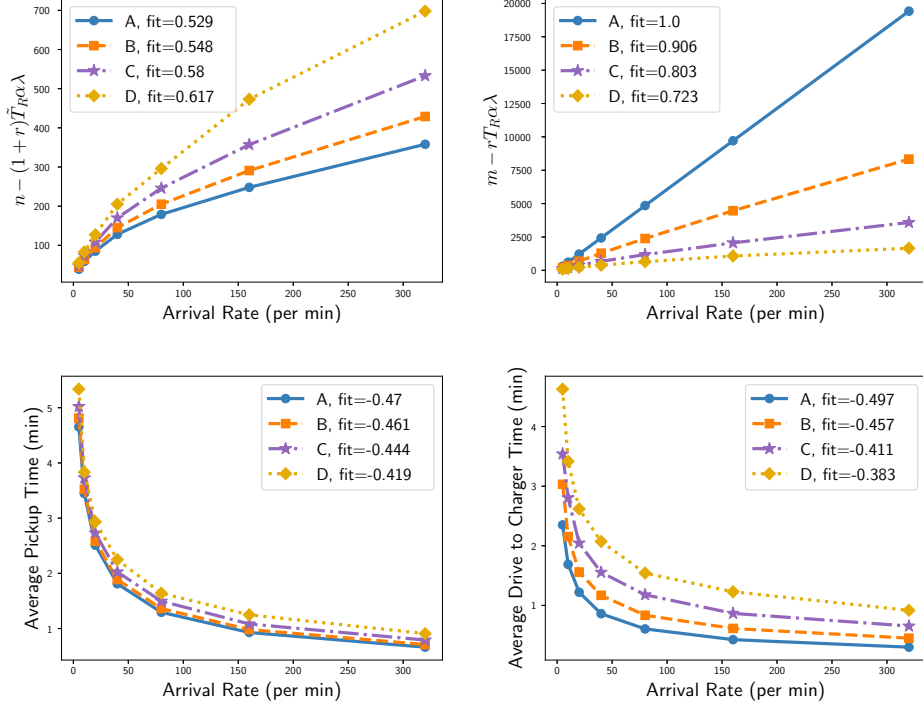
of s_{min} , then the customer is served, otherwise the customer leaves the system immediately. The buffer SoC of s_{min} allows the EV to be able to drive to a charger after finishing the trip. If the customer is served, then the EV drives from its current location to the customer's origin and then to the customer's destination. Once the trip ends, the EV's location is set to the customer's destination, and the SoC is reduced by $\Delta\text{SoC} = r_d \times (T_P + T_R) / p^*$ [kWh], where T_P and T_R are computed using v_{avg} and the corresponding euclidean distances. Next, the EV becomes idle, and if its SoC is less than s_{max} , the EV is dispatched to the closest available charger. In this case, the EV expels $r_d \times T_C / p^*$ amount of SoC to reach the charger where T_C is computed using v_{avg} and the corresponding Euclidean distance. While an EV is driving to a charger, another EV can reach the same charger and start charging earlier. Thus, it is possible that an EV reaches an unavailable charger; in which case, the EV waits at the charger until a post becomes available. If a post is available at the charger, the EV starts charging immediately. In either case, we allow to interrupt charging and dispatch an EV to pick up a customer. If the charging is not interrupted and the SoC reaches 1, the EV becomes idle. These dynamics continue for all customers and vehicles until the end of the simulation.

6.1. Simulated and Theoretical Scalings Comparison

Under the Power-of- d vehicles dispatch matching policy, we fix a sequence of number of chargers corresponding to a given β . That is, for a given β , we set $m = r\tilde{T}_R\alpha\lambda + \Theta(\lambda^\beta)$, where \tilde{T}_R is the average fulfilled trip time.⁴ Now, for a given λ and m , we simulate multiple values of fleet size and

⁴ As \tilde{T}_R is not known a priori, we first run preliminary simulations to estimate that $\tilde{T}_R \approx 15.14$ mins. In Section E.3 in the appendix, we provide more details about the simulation setup and the choice of various parameters and constants.

Figure 2 Fleet size buffer (top left), number of chargers buffer (top right), average pickup time (bottom left), and average drive to charger time (bottom right) for Po2 as a function of arrival rate. Fit corresponds to the slope of the linear regression line of log of x and y variables.



then conduct linear regression (fleet size versus service level) to infer the fleet size corresponding to 90% service level. We refer the reader to Fig. 10 in Appendix E.3 for more details. We then recover the empirical value of $1 - \gamma$ by computing the slope of a linear regression between $\log(\lambda)$ and $\log(n - (1 + r)\tilde{T}_R\alpha\lambda)$. This procedure is repeated for different values of β and the results are reported in Fig. 2 and Table 2. For the theoretical values in Table 2, we fix the value of β and

Table 2 Theoretical versus empirical β , $1 - \gamma$, average pickup time fit, and average drive to the charger time fit as a function of arrival rate.

Series	β	$1 - \gamma$			Pickup (min)			To Charger (min)		
		Fit	Theo	Error %	Fit	Theo	Error %	Fit	Theo	Error %
A	1	0.529	0.508	4.1%	-0.472	-0.492	4.1%	-0.485	-0.5	3%
B	0.906	0.548	0.547	0.2%	-0.461	-0.493	6.5%	-0.457	-0.453	0.9%
C	0.803	0.580	0.599	3.2%	-0.441	-0.494	10.7%	-0.411	-0.402	2.2%
D	0.723	0.616	0.639	3.6%	-0.419	-0.494	15.2%	-0.383	-0.362	5.8%

report the corresponding values of $1 - \gamma$, pickup time scaling, and drive to charger time scaling as

prescribed by Theorem 2. In particular,

$$\gamma = \min \left\{ \frac{1}{2 + 1/N_T}, \frac{\beta}{2} \right\} \implies 1 - \gamma = \max \left\{ 0.508, 1 - \frac{\beta}{2} \right\},^5$$

and that the pickup time and the drive to the charger time are approximately

$$T_P \approx \frac{\tau_1 \sqrt{d(1+r)}}{\sqrt{rn}} \sim n^{\gamma/(2N_T)-1/2} = n^{\gamma/64-1/2}, \quad \text{and} \quad T_C \approx \frac{\tau_2}{\sqrt{m-A}} \sim n^{-\beta/2}.$$

Observe that the error percentage for γ is consistently below 5% which provides empirical verification of Theorem 2. We conduct further simulations and expand on the trade-off observed between fleet size and number of chargers in Appendix E.1. Next, the error percentage for the exponent of the drive to the charger is also small (below 6%) which verifies the functional form of drive to charger given by (10). Lastly, note that the error percentage for pickup time is large for small values of β .⁶ However, the theory suggests that the pickup time should be insensitive to the values of β and γ for large p^* . One can indeed observe that the pickup time in Figure 2 is quite insensitive to the values of γ and β .

6.2. Performance of Power-of- d as a function of d

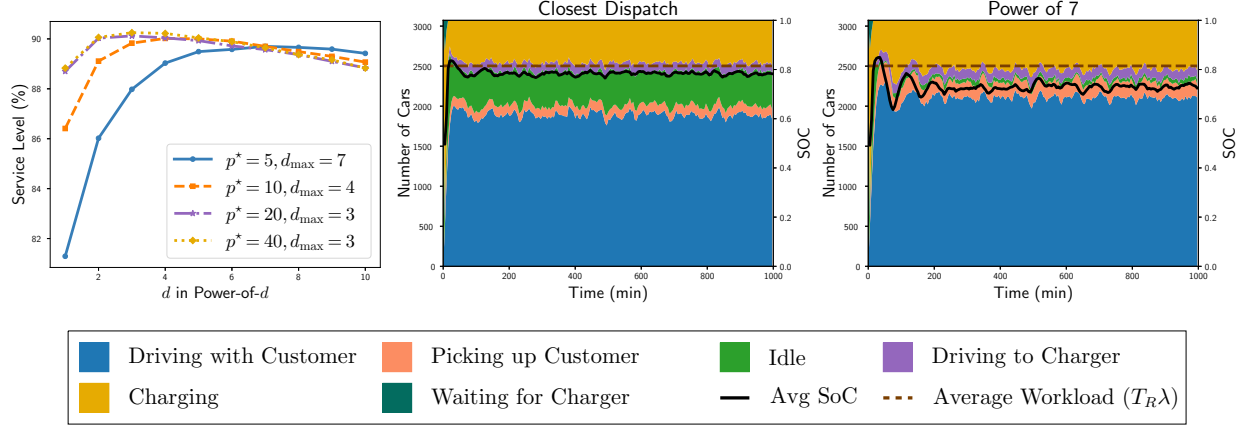
In this section, we analyze the performance of power-of- d vehicles dispatch (Pod) for various battery pack sizes $p^* \in \{5, 10, 20, 40\}$ [kWh], and $d \in \{1, \dots, 10\}$. Note that $d = 1$ corresponds to closest-dispatch (CD). The results are reported in Figure 3.

First, we observe that as the battery pack size increases, the optimal value of d reduces. This is consistent with Theorem 2 which prescribes that the optimal d satisfies $d \sim \lambda^{\gamma/N_T}$ —for larger p^* , vehicles that are closer are more likely to have a high enough SoC. Second, note that the difference in the service level between CD and Po2 is more pronounced as the battery pack size decreases. In particular, a small battery size exacerbates the effect of ineffective balancing of the fleet SoC and deteriorates the service level. Third, Figure 3 shows that for $p^* \geq 10$ [kWh] most of the service

⁵ $N_T = p^*/(r_d \times T_B) \approx p^*/(r_d \times T_R) = 32$.

⁶ The error is due to the departure from the assumption that EVs considered for a match are uniformly distributed in space. In particular, the considered EVs are mostly at a charger, and a smaller β exacerbates this effect.

Figure 3 Service Level (left) of Power-of- d for various values of d and pack size p^* . We set $\lambda = 160$, $n = 3072$, $m = 2600$ (325 locations with 8 posts at each location), and d_{\max} is the d for which maximum service level is attained. We also plot the time series for CD (center) and Po7 (right) with $p^* = 5\text{kWh}$.



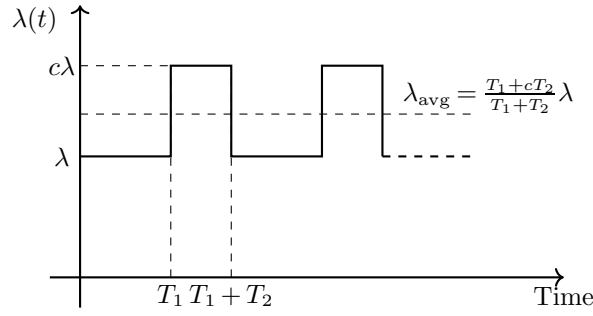
level gains are already achieved for $d = 2$. While d should be optimally selected, this suggests that Po2 can perform well in practice.

To further understand the role of d in the Pod dispatch policy, we plot the time series of CD and Po7 for $p^* = 5$ [kWh] in Figure 3. Recall that CD matches a trip request to the closest vehicle. However, if that vehicle does not have enough battery to serve the request, the request is lost. In turn, this gives some vehicles enough time to fully charge at the expense of losing customers. Indeed, in the figure, we observe a larger fraction of EVs idling (with a 100% SoC) under CD than under Po7, and a smaller fraction of EVs driving with a customer and charging under CD compared to Po7. In particular, the simulation corresponding to Figure 3 results in an 81.3% and an 89.7% service level for CD and Po7, respectively. In other words, having idle EVs while losing customers implies that CD makes inefficient matching decisions. On the other hand, Po7 ensures there are almost no idle EVs, which can be interpreted as employing the otherwise idle EVs to serve customers resulting in a higher service level. We conduct a more extensive comparison between Pod and CD in Appendix E.2. Additionally, we show the superiority of Pod compared to another matching policy called closest available dispatch (CAD) in Appendix E.2. In particular, CAD matches a customer to the closest EV with a sufficient SoC to serve the trip.

7. Varying Arrival Rate

In this section, we aim to understand how the infrastructure planning results extend to the case of time-varying arrival rate. We consider a canonical setting of perpetual peaks and valleys with customer arrival rate $\lambda(t)$ as shown in Fig. 4. In particular, the arrival rate is given by alternating valleys of duration T_1 and peaks of duration T_2 with arrival rates λ and $c\lambda$, respectively, for some $c > 1$. Let the average arrival rate be given by $\lambda_{\text{avg}} = \frac{T_1 + cT_2}{T_1 + T_2}\lambda$.

Figure 4 The arrival rate of customers as a function of time



As a first step in understanding the infrastructure planning prescription in this setting, we present a universal lower bound result analogous to Proposition 1.

THEOREM 3 (First Order Lower Bounds). Fix an $\alpha \in (0, 1)$ and let π be such that $\bar{\alpha}_{\text{eff}}^\pi \geq \alpha$. In addition, let the arrival rate be given by Figure 4 and $rT_2/T_1 < 1$. Then, the following statements are true.

I. If $\alpha \leq \frac{T_1 + T_2}{T_1 + cT_2}$, then

$$n \geq (1 + r)\alpha\lambda_{\text{avg}}T_R, \quad m \geq r\alpha\lambda_{\text{avg}}T_R.$$

II. If $\alpha \in \left(\frac{T_1 + T_2}{T_1 + cT_2}, \frac{1 + T_2/T_1}{(1 + cT_2/T_1)(1 - rT_2/T_1)} \right)$, then $\exists c_\alpha \in \left[0, \alpha - \frac{T_1 + T_2 - cT_R(1 + T_2/T_1)}{T_1 + cT_2} \right]$ such that

$$n \geq (1 + r)\alpha\lambda_{\text{avg}}T_R + \frac{T_1}{T_2} \left(\alpha - \frac{T_1 + T_2}{T_1 + cT_2} - c_\alpha \right) \lambda_{\text{avg}}T_R - \frac{cT_R^2\lambda}{T_2}, \quad m \geq r\alpha\lambda_{\text{avg}}T_R + c_\alpha\lambda_{\text{avg}}T_R.$$

III. If $\alpha \geq \frac{1 + T_2/T_1}{(1 + cT_2/T_1)(1 - rT_2/T_1)}$, then there exists $c_r \in \left[0, \frac{rT_2}{T_1} - \frac{cT_R(1 + T_2/T_1)}{T_1 + cT_2} \right]$ such that

$$n \geq (1 + r)\alpha\lambda_{\text{avg}}T_R + \frac{T_1}{T_2} \left(\alpha - \frac{T_1 + T_2}{T_1 + cT_2} - c_\alpha \right) \lambda_{\text{avg}}T_R - \frac{cT_R^2\lambda}{T_2}, \quad m \geq r\alpha\lambda_{\text{avg}}T_R + c_\alpha\lambda_{\text{avg}}T_R.$$

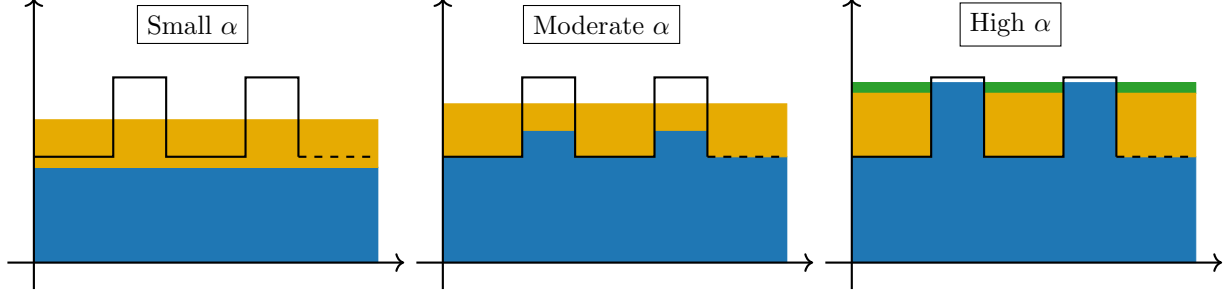


Figure 5 Illustration of the phase transition in the system dynamics as the target service level increases. The black curve represents the amount of incoming workload, the blue shaded region represents the number of EVs driving, the yellow shaded region represents the number of EVs charging, and the green region represents the idling EVs.

We assume $rT_2/T_1 < 1$ just for the ease of exposition. Under the less realistic case of $rT_2/T_1 \geq 1$, we can show that only Case I and II exist with $\alpha = \frac{T_1+T_2}{T_1+cT_2}$ bifurcating the two cases.

In Case I, as the target service level is sufficiently low, one can essentially serve a constant fraction of the incoming demand by dropping a large enough fraction of customers during the peak demand periods. This behavior is illustrated in Figure 5 (left). In this case, the infrastructure planning prescription boils down to the same as in the constant arrival rate setting (c.f., Theorem 1) so that we can augment Theorem 3 with the second order term to conclude that: there exists $\gamma \in [1/3, 1/2]$, such that

$$n \geq (1+r)\alpha T_R \lambda_{\text{avg}} + \lambda^{1-\gamma}, \quad m \geq r\alpha T_R \lambda_{\text{avg}} + \lambda^{2\gamma}.$$

In Case II, the target service level is large enough that the system operator is forced to meet a non-zero fraction of the additional demand during the peaks as illustrated in Figure 5 (center). Thus, the number of EVs driving with a customers is larger during the peaks, and so, there is an opportunity for a larger fraction of EVs to charge during the valleys. However, as the target service level is not too large, the difference between the demand met during the peaks and valleys is not pronounced enough to move all the charging during the valleys. Essentially, a fraction of charging during the peaks is swapped with a fraction of driving during the valleys. Such a swapping does not change the utilization of the EVs (no idling), and so, the fleet size requirement should remain

unaltered. However, the increase of charging during the valleys increases the overall charging station requirement.

Consistent with the above intuition, Case II of Theorem 3 with the largest value of c_α (i.e., under a sufficiently large m) shows that the lower bound $n \geq (1+r)\alpha\lambda_{\text{avg}}T_R$ is recovered. As the value of c_α reduces, the number of chargers decreases. Thus, the system is forced to flatten the charging of EVs, which results in moving some of the charging from the valleys to the peaks. Due to this, the fleet size requirement increases. Thus, there is a first-order trade-off between the fleet size and the number of chargers, characterized by the parameter c_α .

Note that, a non-zero fraction ($\Theta(\lambda)$) of EVs are charging at any point in time, and so, a non-zero fraction of partially charged EVs are available to dispatch to pick up an incoming customer. Similar to Theorem 1, one can benefit from these partially charged EVs to reduce the pickup times from $\lambda^{2/3}$ to $\sqrt{\lambda}$. This leads us to propose the following EV-based second-order scaling: there exists

$$c_\alpha \in \left[0, \alpha - \frac{T_1+T_2-cT_R(1+T_2/T_1)}{T_1+cT_2}\right] \text{ and } \gamma \in \left[\frac{1}{3}, \frac{1}{2}\right] \text{ such that}$$

$$n \geq (1+r)\alpha\lambda_{\text{avg}}T_R + \frac{T_1}{T_2} \left(\alpha - \frac{T_1+T_2}{T_1+cT_2} - c_\alpha \right) \lambda_{\text{avg}}T_R + \lambda^{1-\gamma}, \quad m \geq r\alpha\lambda_{\text{avg}}T_R + c_\alpha\lambda_{\text{avg}}T_R + \lambda^{2\gamma}. \quad (16)$$

Note that, we omitted the term $\frac{cT_R^2\lambda}{T_2}$ from the above equation. Such a term arises in the theorem due to the edge effects induced by the transitions from peaks to valleys and vice versa. In particular, the number of EVs driving at the start of the valley will gradually decrease to reach a certain steady-state value. A dispatching policy cognizant of peak-valley-peak transitions can potentially benefit from it, e.g., by admitting more customers at the end of the peak, resulting in a lower fleet size requirement for a given target service level. As our bounds are applicable for any policy π , the edge effects materialize in the form of $\frac{cT_R^2\lambda}{T_2}$. Nonetheless, we believe that any dispatching policy that does not account for the edge effects cannot do better than (16).

Finally, in Case III, the target service level is so large that the difference in the number of EVs driving during the peaks and valleys is pronounced as depicted in Figure 5 (right). Thus, all the charging can be implemented during the valleys. In fact, the service level requirement is so large,

that the bottleneck determining the fleet size is the number of EVs driving during the peaks. Consistent with this intuition, Case III of Theorem 3 with the largest c_α corresponds to a lower bound of $\alpha_2 c \lambda T_R$ on the fleet size, where α_2 is the minimum fraction of peak demand required to be met to ensure the overall target service level is achieved. Now, as no EVs are charging during the peaks, they are essentially operating like a non-EV fleet. Thus, the second order scaling proposed by Besbes et al. (2022) for non-EV fleet (which corresponds to $\gamma = 1/3$) is more suitable. However, if the value of c_α is reduced, i.e., the number of chargers is reduced, some of the charging moves from the valleys to the peaks. Thus, for $c_\alpha < \frac{rT_2}{T_1} - \frac{cT_R(1+T_2/T_1)}{T_1+cT_2}$, a non-zero fraction of EVs is charging and available for pickups at all times. In this case, we can recover the EV scaling. In turn, our infrastructure planning prescription is as follows: there exists

$$(c_\alpha, \gamma) \in \left\{ \left[0, \frac{rT_2}{T_1} - \frac{cT_R(1+T_2/T_1)}{T_1+cT_2} \right) \times \left[\frac{1}{3}, \frac{1}{2} \right] \right\} \cup \left(\frac{rT_2}{T_1} - \frac{cT_R(1+T_2/T_1)}{T_1+cT_2}, \frac{1}{3} \right)$$

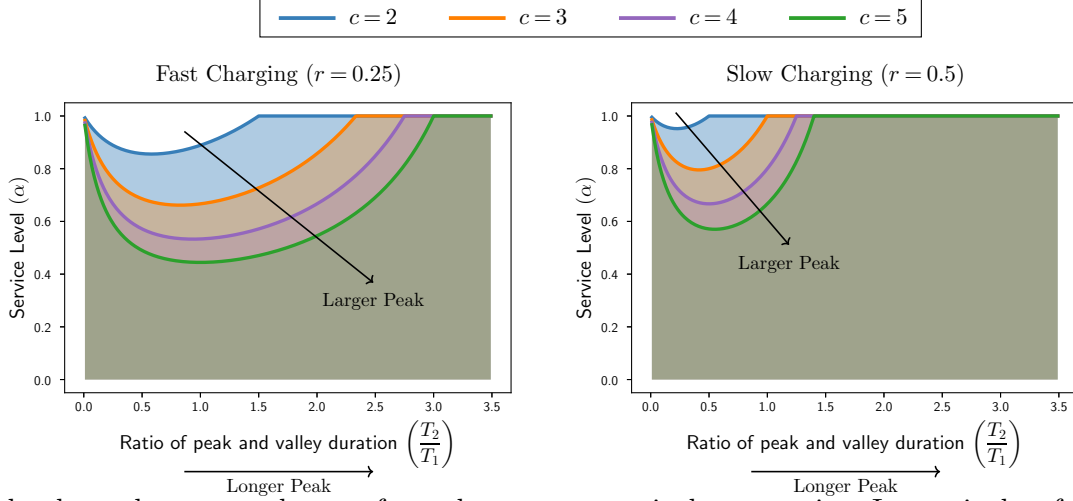
such that

$$n \geq (1+r)\alpha\lambda_{\text{avg}}T_R + \frac{T_1}{T_2} \left(\alpha - \frac{T_1+T_2}{T_1+cT_2} - c_\alpha \right) \lambda_{\text{avg}}T_R + \lambda^{1-\gamma}, \quad m \geq r\alpha\lambda_{\text{avg}}T_R + c_\alpha\lambda_{\text{avg}}T_R + \lambda^{2\gamma}.$$

Similar to Case II, we omitted the term $cT_R^2\lambda/T_2$ corresponding to the edge effects.

In summary, we observe that the EV-based scaling is applicable for Case I and II, and also for Case III when the number of charging stations is limited. On the other hand, with enough charging stations, Case III is expected to obey the non-EV scaling proposed by Besbes et al. (2022). Figure 6 illustrates the values of $(\alpha, c, r, T_2/T_1)$ for which such a transition occurs. A few observations are in order. If T_2/T_1 is too small or too large, i.e., the arrival rate is dominated by either a long peak or a long valley, then the EV-based scaling holds for a broad range of the target service level. In particular, if the peak is long, then, it is harder for the EV fleet to serve the incoming demand for a prolonged period of time without charging. On the other hand, if the peak is short, then, one can drop most of the peak demand while still being able to satisfy the target service level, and so, the system serves a near-constant arrival rate of customers. Thus, the EV-based scaling is valid for a broader range of α . Next, as c increases, the EV-based scaling holds for a restricted range of target

Figure 6 Applicability of the EV-based second-order scaling as a function of $(c, r, T_2/T_1)$. The shaded region represents the value of target service levels (α) for which the EV-based scaling applies, i.e., we fall under Case I or II of Theorem 3. The left figure is for $r = 0.25$ (fast charging) and the right figure is for $r = 0.5$ (slow charging).



service levels as the system departs from the constant arrival rate setting. In particular, for large values of c , the fleet is not charging during the peaks as in Case III of Figure 5, and so, behaves like a non-EV system. Lastly, as r increases, i.e., the charge rate decreases, a larger fraction of the fleet needs to charge to compensate for the aggregate discharge rate. Due to an increased requirement of the fraction of charging EVs, Case II of Theorem 3 as illustrated in Figure 5 is applicable for a larger range of α . In other words, the difference between the customers served during the peak and valley should be larger (i.e., larger α) to be able to translate all the charging to the valleys. Thus, slower charging implies that the EV-based scaling is more pertinent.

We end the discussion by commenting on the relation to the battery pack size p^* , or equivalently, N_T . The non-EV-based scaling is only applicable if the battery pack size is large enough to sustain the peak demand, i.e., $p^* \geq r_d \alpha_2 c \lambda T_R T_2 / n$, where α_2 is the minimum fraction of peak demand required to be met to ensure the target service level is attained. If p^* is smaller than this threshold, then, the regions corresponding to the EV-based scaling in Figure 6 will be more pronounced.

8. Conclusions

In this work, we model an electric vehicle ride-hailing system as a dynamical system and provide a universal lower bound on the number of vehicles and chargers required to achieve a given service

level. In particular, these bounds are valid for any matching and charging policy. We complement the lower bound with a near-matching upper bound under the power-of- d vehicles dispatch policy. We optimize the trade-off between short pickup times and balancing the SoC across the fleet by carefully choosing the value of d . We also check the robustness of our results and insights via simulation. Finally, we discuss how our results apply in a time-varying arrival rate setting. In sum, this work sheds light on the capacity planning decisions of electric vehicles and the unique trade-offs that emerge from the spatial and state of charge dynamics in this class of systems.

References

- Abouee-Mehrizi H, Baron O, Berman O, Chen D (2021) Adoption of electric vehicles in car sharing market. *Production and Operations Management* 30(1):190–209.
- Akbarpour M, Alimohammadi Y, Li S, Saberi A (2021) The value of excess supply in spatial matching markets.
- Aksin Z, Armony M, Mehrotra V (2007) The modern call center: A multi-disciplinary perspective on operations management research. *Production and operations management* 16(6):665–688.
- Akturk D, Candogan O, Gupta V (2022) Managing resources for shared micromobility: Approximate optimality in large-scale systems. *Available at SSRN 4155841* .
- Alto (2023) <https://ridealto.com/ev>, [Online; accessed 05-Feb-2023].
- Anderson EG, Bhargava HK, Boehm J, Parker G (2022) Electric vehicles are a platform business: What firms need to know. *California Management Review* 64(4):135–154.
- Avci B, Girotra K, Netessine S (2015) Electric vehicles with a battery switching station: Adoption and environmental impact. *Management Science* 61(4):772–794.
- Bauer GS, Greenblatt JB, Gerke BF (2018) Cost, energy, and environmental impact of automated electric taxi fleets in manhattan. *Environmental science & technology* 52(8):4920–4928.
- Bellan R (2021) Revel launches an all-electric rideshare service with a fleet of 50 Teslas. <https://bit.ly/RevelTesla>, [Online; accessed 05-Feb-2023].
- Benjaafar S, Wu S, Liu H, Gunnarsson EB (2022) Dimensioning on-demand vehicle sharing systems. *Management Science* 68(2):1218–1232.

- Besbes O, Castro F, Lobel I (2022) Spatial capacity planning. *Operations Research* 70(2):1271–1291.
- Bibra EM, Connelly E, Dhir S, Drtil M, Henriot P, Hwang I, Le Marois JB, McBain S, Paoli L, Teter J (2022) Global ev outlook 2022: Securing supplies for an electric future.
- Boudette N, Davenport C (2021) G.M. will sell only zero-emission vehicles by 2035. <https://www.nytimes.com/2021/01/28/business/gm-zero-emission-vehicles.html>, [Online; accessed 05-Feb-2023].
- Daganzo CF, Smilowitz KR (2004) Bounds and approximations for the transportation problem of linear programming and other scalable network problems. *Transportation science* 38(3):343–356.
- Deng Y, Gupta A, Shroff NB (2022) Fleet sizing and charger allocation in electric vehicle sharing systems. *IFAC Journal of Systems and Control* 22:100210.
- Ford Media Center (2021) <https://bit.ly/FordEVShift>, [Online; accessed 05-Feb-2023].
- Gan L, Topcu U, Low SH (2012) Optimal decentralized protocol for electric vehicle charging. *IEEE Transactions on Power Systems* 28(2):940–951.
- Gans N, Koole G, Mandelbaum A (2003) Telephone call centers: Tutorial, review, and research prospects. *Manufacturing & Service Operations Management* 5(2):79–141.
- Greening LM, Erera AL (2021) Effective heuristics for distributing vehicles in free-floating micromobility systems. Technical report, Working Paper.
- Halfin S, Whitt W (1981) Heavy-traffic limits for queues with many exponential servers. *Operations research* 29(3):567–588.
- He L, Ma G, Qi W, Wang X (2021) Charging an electric vehicle-sharing fleet. *Manufacturing & Service Operations Management* 23(2):471–487.
- InsideEVs (2022) Tesla supercharging network: Almost 400 stations added in q4 2022. <https://insideevs.com/news/633377/tesla-supercharging-network-2022q4/>, [Online; accessed 15-Jun-2023].
- Kanoria Y (2022) Dynamic spatial matching. *Proceedings of the 23rd ACM Conference on Economics and Computation*, 63–64.

- Kaps C, Marinesi S, Netessine S (2022) When should the off-grid sun shine at night? optimum renewable generation and energy storage investments. *Optimum Renewable Generation and Energy Storage Investments*. (January 5, 2022) .
- Kaps C, Netessine S (2022) Privately-owned battery storage-reshaping the way we do electricity. *Available at SSRN* .
- LaMonaca S, Ryan L (2022) The state of play in electric vehicle charging services—a review of infrastructure provision, players, and policies. *Renewable and sustainable energy reviews* 154:111733.
- Levin MW, Kockelman KM, Boyles SD, Li T (2017) A general framework for modeling shared autonomous vehicles with dynamic network-loading and dynamic ride-sharing application. *Computers, Environment and Urban Systems* 64:373–383.
- Lim MK, Mak HY, Shen ZJM (2017) Agility and proximity considerations in supply chain design. *Management Science* 63(4):1026–1041.
- Liu X, Gong K, Ying L (2022a) Large-system insensitivity of zero-waiting load balancing algorithms. *ACM SIGMETRICS Performance Evaluation Review* 50(1):101–102.
- Liu X, Gong K, Ying L (2022b) Steady-state analysis of load balancing with coxian-2 distributed service times. *Naval Research Logistics (NRL)* 69(1):57–75.
- Liu X, Ying L (2020) Steady-state analysis of load-balancing algorithms in the sub-halfin-whitt regime. *Journal of Applied Probability* 57(2):578–596.
- Loeb B, Kockelman KM (2019) Fleet performance and cost evaluation of a shared autonomous electric vehicle (saev) fleet: A case study for austin, texas. *Transportation Research Part A: Policy and Practice* 121:374–385.
- Ma Z, Callaway DS, Hiskens IA (2011) Decentralized charging control of large populations of plug-in electric vehicles. *IEEE Transactions on control systems technology* 21(1):67–78.
- Mak HY, Rong Y, Shen ZJM (2013) Infrastructure planning for electric vehicles with battery swapping. *Management science* 59(7):1557–1575.

-
- Mitzenmacher M (1996) Load balancing and density dependent jump markov processes. *Proceedings of 37th Conference on Foundations of Computer Science*, 213–222 (New York, NY, USA: IEEE), URL <http://dx.doi.org/10.1109/SFCS.1996.548480>.
- Mitzenmacher M (2001) The power of two choices in randomized load balancing. *IEEE Transactions on Parallel and Distributed Systems* 12(10):1094–1104.
- Mukherjee JC, Gupta A (2014) A review of charge scheduling of electric vehicles in smart grid. *IEEE Systems Journal* 9(4):1541–1553.
- Nelder C, Rogers E (2019) Reducing ev charging infrastructure costs. Rocky Mountain Institute.
- Osorio J, Lei C, Ouyang Y (2021) Optimal rebalancing and on-board charging of shared electric scooters. *Transportation Research Part B: Methodological* 147:197–219.
- Padilla A (2020) EXECUTIVE ORDER N-79-20. <https://bit.ly/ExecOrderCali>, [Online; accessed 05-Feb-2023].
- Paganini F, Espíndola E, Marvid D, Ferragut A (2022) Optimization of spatial infrastructure for ev charging. *2022 IEEE 61st Conference on Decision and Control (CDC)*, 5035–5041 (Cancun, Mexico: IEEE).
- Qi W, Zhang Y, Zhang N (2023) Scaling up electric-vehicle battery swapping services in cities: A joint location and repairable-inventory model. *Management Science* .
- Reed J (2009) The $g/gi/n$ queue in the halfin–whitt regime. *The Annals of Applied Probability* 19(6):2211 – 2269.
- Srinivasa S, Haenggi M (2009) Distance distributions in finite uniformly random networks: Theory and applications. *IEEE Transactions on Vehicular Technology* 59(2):940–949.
- Uber (2020) Millions of trips a day, zero emissions and a shift to sustainable packaging. <https://bit.ly/UberSustainability>, [Online; accessed 05-Feb-2023].
- Varma SM, Castro F, Maguluri ST (2022) Power-of- d choices load balancing in the sub-halfin whitt regime.
- Vosooghi R, Kamel J, Puchinger J, Leblond V, Jankovic M (2019a) Robo-taxi service fleet sizing: assessing the impact of user trust and willingness-to-use. *Transportation* 46:1997–2015.
- Vosooghi R, Puchinger J, Jankovic M, Vouillon A (2019b) Shared autonomous vehicle simulation and service design. *Transportation Research Part C: Emerging Technologies* 107:15–33.

-
- Vvedenskaya ND, Dobrushin RL, Karpelevich FI (1996) Queueing system with selection of the shortest of two queues: An asymptotic approach. *Problemy Peredachi Informatsii* 32(1):20–34.
- Wang G, Zhang H, Zhang J (2022) On-demand ride-matching in a spatial model with abandonment and cancellation. *Operations Research* 0.
- Wang Q, Liu X, Du J, Kong F (2016) Smart charging for electric vehicles: A survey from the algorithmic perspective. *IEEE Communications Surveys & Tutorials* 18(2):1500–1517.
- Wu OQ, Yücel Ş, Zhou Y (2022) Smart charging of electric vehicles: An innovative business model for utility firms. *Manufacturing & Service Operations Management* 24(5):2481–2499.
- Yang J, Levin MW, Hu L, Li H, Jiang Y (2023) Fleet sizing and charging infrastructure design for electric autonomous mobility-on-demand systems with endogenous congestion and limited link space. *Transportation Research Part C: Emerging Technologies* 152:104172.
- Zhang Y, Lu M, Shen S (2021) On the values of vehicle-to-grid electricity selling in electric vehicle sharing. *Manufacturing & Service Operations Management* 23(2):488–507.

Appendix A: Universal Lower Bounds

A.1. Analyzing the ODE

Proof of Proposition 2 First, we note that $(q(t), c_C(t), c_I(t), c_{DC}(t))$ are all bounded in $[0, n]$. Hence, if we denote any of these quantities by $y(t)$ we have that $\frac{1}{T} \int_0^T y(t) dt$ is a bounded sequence in a compact set. Therefore, it has a subsequence that converges. We can therefore create a subsequence for which all of the integrals $\frac{1}{T} \int_0^T y(t) dt$ with $y(t) \in \{q(t), c_C(t), c_I(t), c_{DC}(t)\}$ converge. Note that here we are abusing notation and using T instead of explicitly writing the subsequence. We note that this does not affect what we want to prove. Let us use $(\bar{q}, \bar{c}_C, \bar{c}_I, \bar{c}_{DC})$ to denote the limit of each of these integrals (of the subsequences).

We first show eq. (7a). Recall that from eq. (5a) we have that

$$\dot{q}(t) = \lambda_{\text{eff}}^\pi(t) - \frac{q(t)}{T_R + T_P^\pi(t)}.$$

Integrating the equation above from 0 to T and dividing by T yields

$$\begin{aligned} \frac{q(T) - q_0}{T} &= \frac{1}{T} \int_0^T \lambda_{\text{eff}}^\pi(t) dt - \frac{1}{T} \int_0^T \frac{q(t)}{T_R + T_P^\pi(t)} dt \\ &\stackrel{(A1)}{\geq} \frac{1}{T} \int_0^T \lambda_{\text{eff}}^\pi(t) dt - \frac{1}{T} \int_0^T \frac{q(t)}{T_R + \frac{\tau_1}{\sqrt{n-q(t)}}} dt \\ &\geq \frac{1}{T} \int_0^T \lambda_{\text{eff}}^\pi(t) dt - \frac{\frac{1}{T} \int_0^T q(t) dt}{T_R + \frac{\tau_1}{\sqrt{n - \frac{1}{T} \int_0^T q(t) dt}}} \end{aligned}$$

where the last inequality follows from the concavity of $h(x) = x/(T_R + \tau_1/\sqrt{n-x})$ (we provide a proof of this at the end of the current proof) and Jensen's inequality. Taking the limit when $T \uparrow \infty$ we have

$$\bar{q} \geq \bar{\alpha}_{\text{eff}}^\pi \lambda \cdot \left(T_R + \frac{\tau_1}{\sqrt{n - \bar{q}}} \right),$$

where we have used the definition of $\bar{\alpha}_{\text{eff}}^\pi$. Now we prove eq. (7b). From eq. (5b) we have

$$\begin{aligned} \dot{c}_c(t) &= p_{dc}^\pi(t) \cdot \frac{c_{DC}(t)}{T_{DC}^\pi(t)} - \frac{c_C(t)}{T_C^\pi(t)} \\ &\stackrel{(a)}{\leq} \frac{c_{DC}(t)}{T_{DC}^\pi(t)} - c_C(t) \cdot \frac{r_c}{p^*} \\ &\stackrel{(A2)}{\leq} \frac{c_{DC}(t) \cdot \sqrt{m - c_C(t)}}{\tau_2} - c_C(t) \cdot \frac{r_c}{p^*} \end{aligned}$$

where in (a) we have used that $p_{dc}^\pi(t) \leq 1$ and that $T_C^\pi(t) \leq p^*/r_c$. Dividing both sides above by $\sqrt{m - c_C(t)}$ and integrating yields

$$\begin{aligned} \frac{1}{T} (-2\sqrt{m - c_C(T)} + 2\sqrt{m - c_C(0)}) &\leq \frac{1}{T} \int_0^T \frac{c_{DC}(t)}{\tau_2} dt - \frac{1}{T} \int_0^T \frac{c_C(t)}{\sqrt{m - c_C(t)}} \cdot \frac{r_c}{p^*} dt \\ &\leq \frac{1}{T} \int_0^T \frac{c_{DC}(t)}{\tau_2} dt - \frac{\frac{1}{T} \int_0^T c_C(t) dt}{\sqrt{m - \frac{1}{T} \int_0^T c_C(t) dt}} \cdot \frac{r_c}{p^*} \end{aligned} \tag{17}$$

where we have used that

$$\int_0^T \frac{\dot{c}_c(t)}{\sqrt{m - c_C(t)}} dt = -2\sqrt{m - c_C(T)} + 2\sqrt{m - c_C(0)},$$

and the convexity of $x/\sqrt{m-x}$ together with Jensen's inequality. Taking the limit as $T \uparrow \infty$ in eq. (17) yields

$$\frac{\bar{c}_C}{\sqrt{m - \bar{c}_C}} \cdot \frac{r_c}{p^*} \leq \frac{\bar{c}_{DC}}{\tau_2}.$$

Finally, from (5c) we have

$$\dot{s}(t) = c_C(t) \cdot r_c - (n - c_C(t) - c_I(t)) \cdot r_d.$$

As before we integrate from 0 to T , divide by T and take the limit. By doing so, because $s(t)$ is bounded, we obtain that

$$\bar{c}_C \cdot r_c = (n - \bar{c}_C - \bar{c}_I) \cdot r_d.$$

To conclude the proof we show that $h(x) = x/(T_R + \tau_1/\sqrt{n-x})$ is concave. We have

$$\frac{d^2}{dx^2} h(x) = \frac{\tau_1 (x (T_R \sqrt{n-x} + 3\tau_1) - 4n (T_R \sqrt{n-x} + \tau_1))}{4(n-x)^{3/2} (T_R \sqrt{n-x} + \tau_1)^3},$$

the denominator is positive, while the numerator is non-positive because

$$x (T_R \sqrt{n-x} + 3\tau_1) \leq n (T_R \sqrt{n-x} + 3\tau_1) \leq 4n (T_R \sqrt{n-x} + \tau_1).$$

Proof of Proposition 1 By eq. (7c) we have

$$\bar{c}_C = (n - \bar{c}_C - \bar{c}_I)r \iff \bar{c}_C = (n - \bar{c}_I) \frac{r}{1+r}.$$

Therefore,

$$n = \bar{q} + \bar{c}_C + \bar{c}_I + \bar{c}_{DC} \geq \bar{q} + \bar{c}_C + \bar{c}_I = \bar{q} + n \frac{r}{1+r} + \frac{\bar{c}_I}{1+r} \geq \bar{q} + n \frac{r}{1+r}.$$

Now, from eq. (7a) we have that $\bar{q} \geq T_R \bar{\alpha}_{\text{eff}}^\pi \lambda$. Hence, we have

$$\frac{n}{1+r} = n - n \frac{r}{1+r} \geq \bar{q} \geq T_R \bar{\alpha}_{\text{eff}}^\pi \lambda \implies n \geq (1+r) T_R \bar{\alpha}_{\text{eff}}^\pi \lambda.$$

Now, by (7b), we get

$$m \geq \bar{c}_C + \left(\frac{r_c \tau_2 \bar{c}_C}{p^* \bar{c}_{DC}} \right)^2 \geq \bar{c}_C \stackrel{(7c)}{=} (n - \bar{c}_C - \bar{c}_I)r \stackrel{(1)}{=} (\bar{q} + \bar{c}_{DC})r \geq r\bar{q} \stackrel{(7a)}{\geq} r T_R \bar{\alpha}_{\text{eff}}^\pi \lambda.$$

This completes the proof.

A.2. Proof of Theorem 1

Proof of Theorem 1 We prove the contrapositive. In particular, we show that if for all $\gamma \in [1/3, 1/2]$ and $\kappa_1, \kappa_2 > 0$, we have

$$n \leq (1+r)T_R\alpha\lambda + \kappa_1\lambda^{1-\gamma} \quad \text{OR} \quad m \leq rT_R\alpha\lambda + \kappa_2\lambda^{2\gamma},$$

then, $\bar{\alpha}_{\text{eff}}^\pi < \alpha$. We consider three cases.

Case I: $n \leq (1+r)T_R\alpha\lambda + \kappa_1\lambda^{1-\gamma}$ holds for all $\gamma \in [1/3, 1/2]$ and $\kappa > 0$. By using (7a), we get

$$\begin{aligned} \lambda \bar{\alpha}_{\text{eff}}^\pi &\leq \frac{\bar{q}}{\frac{\tau_1}{\sqrt{n-q}} + T_R} \\ &\stackrel{(a)}{\leq} \frac{n/(1+r)}{\frac{\tau_1}{\sqrt{n}} + T_R} - \frac{\bar{c}_{DC}}{T_R + \tau_1} \\ &= \frac{n}{(1+r)T_R} \left(1 + \frac{\tau_1}{T_R\sqrt{n}}\right)^{-1} - \frac{\bar{c}_{DC}}{T_R + \tau_1} \\ &\stackrel{(b)}{\leq} \frac{n}{(1+r)T_R} \left(1 - \frac{\tau_1}{\tau_1 + T_R} \frac{1}{\sqrt{n}}\right) - \frac{\bar{c}_{DC}}{T_R + \tau_1} \\ &= \frac{n}{(1+r)T_R} - \frac{\tau_1}{T_R(1+r)(\tau_1 + T_R)}\sqrt{n} - \frac{\bar{c}_{DC}}{T_R + \tau_1} \\ &\leq \alpha\lambda + \kappa_1\lambda^{1-\gamma} - \frac{\tau_1}{T_R(1+r)(\tau_1 + T_R)}\sqrt{n} - \frac{\bar{c}_{DC}}{T_R + \tau_1} \\ &\stackrel{(c)}{<} \alpha\lambda \end{aligned} \tag{18}$$

where (a) follows by upper bounding \bar{q} as follows:

$$\begin{aligned} \bar{q} &= n - \bar{c}_C - \bar{c}_I - \bar{c}_{DC} \\ &\leq n - \bar{c}_C - \bar{c}_I \\ &\leq n - \bar{c}_C - \bar{c}_I \frac{r_d}{r_c + r_d} \end{aligned} \tag{19}$$

$$\stackrel{(7c)}{=} \frac{nr_c}{r_c + r_d} = \frac{n}{1+r}. \tag{20}$$

Next, (b) follows as

$$\frac{1}{1 + \frac{C}{\sqrt{n}}} \leq 1 - \frac{C}{C+1} \frac{1}{\sqrt{n}} \quad \forall n \geq 1.$$

Lastly, (c) follows by picking $\gamma = 1/2$ and $\kappa_1 = \frac{\tau_1}{2T_R(1+r)(\tau_1 + T_R)}$. This completes the Case I as the last inequality implies $\bar{\alpha}_{\text{eff}}^\pi < \alpha$.

Case II: $m \leq rT_R\alpha\lambda + \kappa_2\lambda^{2\gamma}$ holds for all $\gamma \in [1/3, 1/2]$ and $\kappa_2 > 0$. By using (7b), we get

$$m \geq \bar{c}_C + \left(\frac{r_c\tau_2}{p^*}\right)^2 \left(\frac{\bar{c}_C}{\bar{c}_{DC}}\right)^2$$

$$\begin{aligned}
&\stackrel{(a)}{=} r\bar{q} + r\bar{c}_{DC} + \left(\frac{r_c\tau_2}{p^*}\right)^2 \left(\frac{r\bar{q}}{\bar{c}_{DC}}\right)^2 \\
&\stackrel{(b)}{\geq} rT_R\bar{\alpha}_{\text{eff}}^\pi\lambda + r\bar{c}_{DC} + \left(\frac{r_dT_R\tau_2}{p^*}\right)^2 \left(\frac{\bar{\alpha}_{\text{eff}}^\pi\lambda}{\bar{c}_{DC}}\right)^2 \\
&\stackrel{(c)}{\geq} rT_R\bar{\alpha}_{\text{eff}}^\pi\lambda + \frac{3}{2^{1/3}}r_d^{4/3}\left(\frac{T_R\tau_2}{p^*r_c}\right)^{2/3}(\bar{\alpha}_{\text{eff}}^\pi\lambda)^{2/3}, \\
&\stackrel{(d)}{\geq} rT_R\bar{\alpha}_{\text{eff}}^\pi\lambda + \frac{3}{2^{1/3}}r_d^{4/3}\left(\frac{T_R\tau_2}{p^*r_c}\right)^{2/3}\delta^{2/3}\lambda^{2/3}
\end{aligned} \tag{21}$$

where (a) follows by (7c) and (1). Specifically, $\bar{c}_C = r(n - \bar{c}_C - \bar{c}_I) = r(\bar{q} + \bar{c}_{DC})$. Next, (b) follows by (7a) as $\bar{q} \geq \bar{\alpha}_{\text{eff}}^\pi\lambda T_R + \bar{\alpha}_{\text{eff}}^\pi\lambda \frac{\tau_1}{\sqrt{n-q}} \geq \bar{\alpha}_{\text{eff}}^\pi\lambda T_R$. Further, (c) follows by noting that $c_1x + c_2/x^2$ is minimized at $x = (c_2/(2c_1))^{1/3}$, which implies

$$c_1x + \frac{c_2}{x^2} \geq \frac{3}{2^{1/3}}c_1^{2/3}c_2^{1/3}.$$

Lastly, (d) follows as $\alpha \geq \delta$. Now, by picking $\gamma = 1/3$ and $\kappa_2 < \frac{3}{2^{1/3}}r_d^{4/3}(T_R\tau_2/(r_cp^*))^{2/3}\delta^{2/3}$, we obtain a contradiction. This shows that Case II is not possible.

Case III: There exists $\gamma_1, \gamma_2 \in [1/3, 1/2]$ such that for all $\kappa_1, \kappa_2 > 0$, we have

$$n \leq (1+r)T_R\alpha\lambda + \kappa_1\lambda^{1-\gamma_1} \quad \text{and} \quad m \leq rT_R\alpha\lambda + \kappa_2\lambda^{2\gamma_2}.$$

Consider the largest such γ_1 and the smallest such γ_2 . Note that, $\gamma_1 \geq \gamma_2$, as otherwise, if $\gamma_1 < \gamma_2$, then

$$n \leq (1+r)T_R\alpha\lambda + \kappa_1\lambda^{1-\gamma_1} \quad \forall \gamma \leq \gamma_1$$

$$m \leq rT_R\alpha\lambda + \kappa_2\lambda^{2\gamma_2} \quad \forall \gamma > \gamma_1.$$

In other words, we have $\gamma_2 \leq \gamma_1 + \epsilon$ for all $\epsilon > 0$. As ϵ is arbitrary, we get $\gamma_2 \leq \gamma_1$ which is a contradiction.

Now, we prove this case by contradiction. Let $\bar{\alpha}_{\text{eff}}^\pi \geq \alpha$, then by (18) and (21), we get

$$\bar{c}_{DC} \leq \kappa_1\lambda^{1-\gamma_1} \quad \bar{c}_{DC} \geq \frac{r_dT_R\tau_2\delta}{p^*\sqrt{\kappa_2}}\lambda^{1-\gamma_2}.$$

By picking $\kappa_1\sqrt{\kappa_2} \leq r_dT_R\tau_2\delta/(2p^*)$ and noting that $\gamma_1 \geq \gamma_2$, we get a contradiction. This completes the proof of the theorem.

Appendix B: Matching Upper Bounds

B.1. Proof of Lemma 1

Proof of Lemma 1 Consider a coupled modified and original model, i.e., they both have an identical arrival sequence and an identical initial state. Now, let π_a be such that the dispatching decisions in the original model are exactly the same as in the modified model operating under π_s , where π_s is an admissible

policy for the modified model. In particular let π_a be such that for any $i \in [n]$, EV i serves the same customer and follows it up by driving to the same charger as in the modified model under π_s . Under such a coupling, the location of all the EVs are identical under the two models. In addition, the following is true.

- EV i is picking up customer k in the original model if and only if it is picking up customer k in the modified model.
- EV i is driving with customer k in the original model if and only if it is driving with customer k in the modified model.
- EV i is driving to charger $j \in [m]$ in the original model if and only if it is driving to charger j in the modified model.
- If charger j is available in the modified model, then it is available in the original model.
- In the modified model, EV i expels at least as much SoC as in the original model by picking up and dropping the customer followed by driving to the charger.
- If EV i is charging in the modified model, then it is either charging in the original model or it is idling at the charger location with 100% SoC in the original model. On the other hand, if EV i is charging in the original model, then it is charging in the modified model.

Using the above information, we conclude that $\text{SoC}_i^a(t) \geq \text{SoC}_i^s(t)$ for all $t \in \mathbb{R}_+$, $i \in [n]$. That is, the SoC of each EV is path wise larger in the original model. Lastly, if π_s is admissible for the modified model, then we have $\text{SoC}_i^s(t) \geq 0$ for all $t \in \mathbb{R}_+$, $i \in [n]$. Thus, π_a is admissible for the original model as $\text{SoC}_i^a(t) \geq \text{SoC}_i^s(t) \geq 0$ for all $t \in \mathbb{R}_+$, $i \in [n]$. This completes the proof. \square

B.2. Fixed point for Power-of-d Vehicles Dispatch

Proof of Proposition 3 Consider the system of differential equations in (14). Any equilibrium (X^C, X^B) of this dynamical system must satisfy:

$$\tilde{\lambda}(p_0 - p_j)I = X_j^B \mu, \quad 1 \leq j \leq N_T, \quad (22a)$$

$$\tilde{\lambda}(p_0 - p_j)I + \left(\tilde{X}_j^C - \tilde{X}_{j-1}^C \right) / (rT_B) = X_{j+1}^B \mu, \quad 1 \leq j < N_T, \quad (22b)$$

$$\tilde{\lambda}p_0I = X_{N_T}^B \mu, \quad (22c)$$

$$\tilde{X}_0^C \mu / r = X_1^B \mu, \quad (22d)$$

where $I = \mathbf{1}\{X_{N_T}^B \leq n/(1+r)\}$,

$$1 - \left(\frac{X_j^C}{X_{N_T}^C} \right)^d \leq p_j \leq 1 - \left(\frac{X_j^C}{X_{N_T}^C} \right)^d \left(\frac{1 - d/X_j^C}{1 - d/X_{N_T}^C} \right)^d, \quad (23)$$

and

$$\frac{1}{\mu} = \tau_1 \sqrt{\frac{d}{n - X_{N_T}^B}} + T_R + \frac{\tau_2}{\sqrt{m - \min\{X_{N_T-1}^C, A\}}}.$$

First, we present upper and lower bounds on T_B that will be useful later in the proof. We have

$$T_B = \tau_1 \sqrt{\frac{d}{n - T_R \tilde{\lambda}}} + T_R + \frac{\tau_2}{\sqrt{m - A}} \stackrel{*}{\leq} \frac{\tau_1}{\sqrt{r T_R}} \tilde{\lambda}^{\frac{\gamma/N_T - 1}{2}} \log \tilde{\lambda} + T_R + \tau_2 \tilde{\lambda}^{-\gamma} \quad (24)$$

$$T_B = \tau_1 \sqrt{\frac{d}{n - T_R \tilde{\lambda}}} + T_R + \frac{\tau_2}{\sqrt{m - A}} \stackrel{**}{\geq} \frac{\tau_1}{\sqrt{T_R}} \tilde{\lambda}^{\frac{\gamma/N_T - 1}{2}} + T_R, \quad (25)$$

where $(*)$ follows as $n \geq (1+r)T_R \tilde{\lambda}$ and $A = m - \tilde{\lambda}^{2\gamma}$. Next, $(**)$ follows as $n = (1+r)T_R \tilde{\lambda} + \kappa_1 \tilde{\lambda} \geq 2T_R \tilde{\lambda}$ for $\tilde{\lambda} \geq \tilde{\lambda}_{00}$ for some $\tilde{\lambda}_{00} > 0$. Now, we show the following steps to prove the proposition:

- (a) $I = 1$.
- (b) $\tilde{X}_j^C = rT_B \mu X_{j+1}^B$ for $j \in \{1, \dots, N_T - 1\}$.
- (c) $\tilde{X}_j^C = X_j^C$ for all $j \in \{0, 1, \dots, N_T - 1\}$.
- (d) $X_{N_T}^C$ uniquely determines all other states.
- (e) X_j^C increases with $X_{N_T}^C$.
- (f) We argue that there exists a unique $X_{N_T}^C$ such that $X_{N_T}^C + X_{N_T}^B = n$.
- (g) We show that the solution, $\hat{X}_{N_T}^C$, to the equation

$$1 - \frac{n-x}{T_B \tilde{\lambda}} = \left(\frac{r(n-x)}{x} \right)^{d^{N_T}} \left(\frac{rT_B}{rT_R + \kappa_1 \tilde{\lambda}^{-\gamma}} \right)^{\frac{d^{N_T} - d}{d-1}},$$

is such that $\hat{X}_{N_T}^C \geq X_{N_T}^C$.

- (h) We show that $\hat{X}_{N_T}^C$ is such that

$$\hat{X}_{N_T}^C - rT_R \tilde{\lambda} = \mathcal{O}(\tilde{\lambda}^{1-\gamma}).$$

We first show (a). If $I = 0$ then $X_{N_T}^B > n/(1+r)$ and from (22c), we would get that $X_{N_T}^B = 0$, a contradiction.

Next, we establish (b). Combining (22a) and (22b), we deduce that

$$\tilde{X}_j^C - \tilde{X}_{j-1}^C = rT_B \mu (X_{j+1}^B - X_j^B) \quad \forall j \in \{1, \dots, N_T - 1\}.$$

The latter relations implies that

$$\tilde{X}_j^C - \tilde{X}_0^C = rT_B \mu (X_{j+1}^B - X_1^B) \quad \forall j \in \{1, \dots, N_T - 1\}.$$

Using (22d) we obtain that $\tilde{X}_j^C = rT_B \mu X_{j+1}^B$ for $j \in \{1, \dots, N_T - 1\}$.

Now, we establish (c) by showing that $X_{N_T-1}^C \leq A$. Assume not, then, by (b), we have

$$\begin{aligned}
X_{N_T}^B &= \frac{A}{rT_B\mu} \geq \frac{T_R}{rT_B} \left(rT_R\tilde{\lambda} + (\kappa_2 - 1)\tilde{\lambda}^{2\gamma} \right) \\
&\stackrel{(24)}{\geq} \frac{1}{1 + \frac{\tau_1}{T_R\sqrt{rT_R}}\tilde{\lambda}^{\frac{\gamma/N_T-1}{2}} \log \tilde{\lambda} + \frac{\tau_2}{T_R}\tilde{\lambda}^{-\gamma}} \left(T_R\tilde{\lambda} + \frac{\kappa_2 - 1}{r}\tilde{\lambda}^{2\gamma} \right) \\
&\geq \left(1 - \frac{\tau_1}{T_R\sqrt{rT_R}}\tilde{\lambda}^{\frac{\gamma/N_T-1}{2}} \log \tilde{\lambda} - \frac{\tau_2}{T_R}\tilde{\lambda}^{-\gamma} \right) \left(T_R\tilde{\lambda} + \frac{\kappa_2 - 1}{r}\tilde{\lambda}^{2\gamma} \right) \\
&\stackrel{**}{\geq} T_R\tilde{\lambda} + \frac{\kappa_2 - 1}{r}\tilde{\lambda}^{2\gamma} - \frac{2\tau_1}{\sqrt{rT_R}}\tilde{\lambda}^{\frac{\gamma/N_T+1}{2}} \log \tilde{\lambda} - 2\tau_2\tilde{\lambda}^{1-\gamma} \\
&\stackrel{***}{\geq} T_R\tilde{\lambda} + \frac{\kappa_2 - 1}{2r}\tilde{\lambda}^{2\gamma} - 2\tau_2\tilde{\lambda}^{1-\gamma} \\
&> T_R\tilde{\lambda},
\end{aligned}$$

where the first inequality follows as $1/\mu \geq T_R$. Next, (*) follows as $1/(1+x) \geq 1-x$ for $x \geq 0$. Further, (**) follows for $\tilde{\lambda} \geq \tilde{\lambda}_{01}$ for some $\tilde{\lambda}_{01} > 0$ as $2\gamma < 1$, implying $(\kappa_2 - 1)\tilde{\lambda}^{2\gamma}/r \leq T_R\tilde{\lambda}$. Now, (***) follows for $\tilde{\lambda} \geq \tilde{\lambda}_{02}$ for some $\tilde{\lambda}_{02} > 0$ as $(\gamma/N_T + 1)/2 \leq (\gamma/2 + 1)/2 < 2\gamma$ for all $\gamma \geq 1/3$. Finally, the last inequality follows by noting that $\kappa_2 \geq 2 + 4r\tau_2$. We now arrive at a contradiction as $X_{N_T}^B \leq T_R\tilde{\lambda}$ by the admission control policy (Definition 1). Thus, we have $X_j^C \leq X_{N_T-1}^C \leq A$ for all $j \in \{0, 1, \dots, N_T - 1\}$. We now move to showing (d), (e) and (f). Note that from (b), it is enough to solve only for X^C . Combining (b), (c), and (22), we have

$$X_{j-1}^C = rT_B\tilde{\lambda}(p_0 - p_j), \quad 1 \leq j < N_T, \quad (26a)$$

$$X_{N_T-1}^C = rT_B\tilde{\lambda}p_0, \quad (26b)$$

$$X_{N_T}^C + \frac{X_{N_T-1}^C}{r} = n. \quad (26c)$$

From (26b) and (26c), we can solve for p_0 as a function of $X_{N_T}^C$

$$p_0 = \frac{n - X_{N_T}^C}{T_B\tilde{\lambda}}, \quad (27)$$

which implies that X_0^C is uniquely determined by $X_{N_T}^C$. Additionally, from (26a) we have that for all $j \in \{1, \dots, N_T - 1\}$

$$p_j = p_0 - \frac{X_{j-1}^C}{rT_B\tilde{\lambda}}. \quad (28)$$

That is, X_0^C is uniquely determined by $X_{N_T}^C$, and all X_j^C 's for $j \in \{1, \dots, N_T - 1\}$ are iteratively determined starting from X_0^C . Hence, all X_j^C 's are uniquely determined by $X_{N_T}^C$. Now, we inductively show that X_j^C is a strictly increasing function of $X_{N_T}^C$ in the following claim:

CLAIM 1. Given (27) and (28), X_j^C is a strictly increasing function of $X_{N_T}^C$ for all $j \in \{0, 1, \dots, N_T - 1\}$.

From (26c), we can write

$$X_{N_T}^C = n - \frac{X_{N_T-1}^C(X_{N_T}^C)}{r}, \quad (29)$$

where the left-hand side (LHS) increases while the right-hand side (RHS) decreases with $X_{N_T}^C$ by Claim 1.

Hence, there must exist a unique $X_{N_T}^C$ that solves the system of equations above. This shows uniqueness.

In order to show (g), we find a lower bound on $X_{N_T-1}^C$ in terms of $X_{N_T}^C$. From (28), we have

$$X_{j-1}^C = \tilde{\lambda} T_B r (p_0 - p_j) \leq \tilde{\lambda} T_B r \left(\left(\frac{X_j^C}{X_{N_T}^C} \right)^d - \left(\frac{X_0^C}{X_{N_T}^C} \right)^d \left(\frac{1 - d/X_0^C}{1 - d/X_{N_T}^C} \right)^d \right) \quad \forall j \in \{1, \dots, N_T - 1\},$$

where the last inequality follows by using the lower bound on p_j and upper bound on p_0 given by (23). Using the above inequality, we obtain a lower bound on X_j^C as follows:

$$X_j^C \geq X_{N_T}^C \left(\frac{1}{r T_B \tilde{\lambda}} X_{j-1}^C + \left(\frac{X_0^C}{X_{N_T}^C} \right)^d \left(\frac{1 - d/X_0^C}{1 - d/X_{N_T}^C} \right)^d \right)^{1/d} \geq X_{N_T}^C \left(\frac{1}{r T_B \tilde{\lambda}} X_{j-1}^C \right)^{1/d} \quad \forall j \in \{1, \dots, N_T - 1\}$$

Starting from $N_T - 1$ and iterating over $j \in \{1, \dots, N_T - 1\}$ in the above inequality, we get

$$\begin{aligned} X_{N_T-1}^C &\geq X_{N_T}^C \left(\frac{1}{r T_B \tilde{\lambda}} X_{N_T-2}^C \right)^{1/d} \\ &\geq X_{N_T}^C \left(\frac{1}{r T_B \tilde{\lambda}} \left(X_{N_T}^C \left(\frac{1}{r T_B \tilde{\lambda}} X_{N_T-3}^C \right)^{1/d} \right) \right)^{1/d} \\ &= (X_{N_T}^C)^{1+1/d} \left(\frac{1}{r T_B \tilde{\lambda}} \right)^{1/d+1/d^2} (X_{N_T-3}^C)^{1/d^2} \\ &\vdots \\ &\geq (X_{N_T}^C)^{\sum_{j=0}^{N_T-2} \frac{1}{d^j}} \left(\frac{1}{r T_B \tilde{\lambda}} \right)^{\sum_{j=1}^{N_T-1} \frac{1}{d^j}} (X_0^C)^{1/d^{N_T-1}} \\ &= X_{N_T}^C \left(X_{N_T}^C \frac{1}{r T_B \tilde{\lambda}} \right)^{\sum_{j=1}^{N_T-1} \frac{1}{d^j}} \left(\frac{X_0^C}{X_{N_T}^C} \right)^{1/d^{N_T-1}} \\ &\stackrel{(*)}{\geq} X_{N_T}^C \left(\frac{r T_R + \kappa_1 \tilde{\lambda}^{-\gamma}}{r T_B} \right)^{\frac{d^{N_T} - d}{(d-1)d^{N_T}}} \left(\frac{X_0^C}{X_{N_T}^C} \right)^{1/d^{N_T-1}}, \\ &\stackrel{(**)}{\geq} X_{N_T}^C \left(\frac{r T_R + \kappa_1 \tilde{\lambda}^{-\gamma}}{r T_B} \right)^{\frac{d^{N_T} - d}{(d-1)d^{N_T}}} \left(1 - \frac{1}{T_B \tilde{\lambda}} (n - X_{N_T}^C) \right)^{1/d^{N_T}}, \end{aligned} \quad (30)$$

where $(*)$ follows by using $X_{N_T}^C \geq r T_R \tilde{\lambda} + \kappa_1 \tilde{\lambda}^{1-\gamma}$ which is true because $X_{N_T}^B \leq T_R \tilde{\lambda}$. Also, $(**)$ follows by noting that $1 - (X_0^C/X_{N_T}^C)^d \leq p_0 = (n - X_{N_T}^C)/(T_B \tilde{\lambda})$. Now, we define

$$\hat{X}_{N_T-1}^C = \hat{X}_{N_T}^C \left(\frac{r T_R + \kappa_1 \tilde{\lambda}^{-\gamma}}{r T_B} \right)^{\frac{d^{N_T} - d}{(d-1)d^{N_T}}} \left(1 - \frac{1}{T_B \tilde{\lambda}} (n - \hat{X}_{N_T}^C) \right)^{1/d^{N_T}},$$

where $\hat{X}_{N_T}^C + \hat{X}_{N_T-1}^C/r = n$. As the LHS of the above equation is strictly decreasing function of $\hat{X}_{N_T}^C$ and the RHS is an increasing function, it has a unique solution. By (30), we conclude that $\hat{X}_{N_T-1}^C \leq X_{N_T-1}^C$ and $\hat{X}_{N_T}^C \geq X_{N_T}^C$. This completes (g) as $\hat{X}_{N_T}^C$ is the solution of the following equation:

$$1 - \frac{n-x}{T_B \tilde{\lambda}} = \left(\frac{r(n-x)}{x} \right)^{d^{N_T}} \left(\frac{rT_B}{rT_R + \kappa_1 \tilde{\lambda}^{-\gamma}} \right)^{\frac{d^{N_T}-d}{d-1}}. \quad (31)$$

Finally, we establish (h) by contradiction. Let

$$x \geq rT_R \tilde{\lambda} + B \tilde{\lambda}^{1-\gamma} \quad \text{with } B = \frac{rT_R N_T}{\gamma} + 2\kappa_1$$

be a solution of the equation given by (g). Now, we upper bound each term in RHS. We have

$$\left(\frac{r(n-x)}{x} \right)^{d^{N_T}} \stackrel{*}{\leq} \left(\frac{rT_R \tilde{\lambda} - B \tilde{\lambda}^{1-\gamma}/2}{rT_R \tilde{\lambda} + B \tilde{\lambda}^{1-\gamma}} \right)^{d^{N_T}} \leq \left(1 - \frac{B}{2rT_R} \tilde{\lambda}^{-\gamma} \right)^{d^{N_T}} \stackrel{**}{=} \left(1 - \frac{B}{2rT_R} d^{-N_T} \log d \right)^{d^{N_T}} \leq 2d^{-\frac{B}{2rT_R}}.$$

where (*) follows as $\kappa_1 \leq B/2$, (**) follows as $\tilde{\lambda}^{-\gamma} = d^{-N_T} \log d$, and the last inequality follows for all $\tilde{\lambda} \geq \tilde{\lambda}_{03}$ for some $\tilde{\lambda}_{03} > 0$ as $d^{\frac{B}{2rT_R}} \left(1 - \frac{B}{2rT_R} d^{-N_T} \log d \right)^{d^{N_T}} \rightarrow 1$ as $\tilde{\lambda} \rightarrow \infty$. Next, we have

$$\begin{aligned} \left(\frac{rT_B}{rT_R + \kappa_1 \tilde{\lambda}^{-\gamma}} \right)^{\frac{d^{N_T}-d}{d-1}} &\stackrel{(24)}{\leq} \left(\left(1 + \frac{\tau_1}{T_R \sqrt{rT_R}} \tilde{\lambda}^{\frac{\gamma/N_T-1}{2}} \log \tilde{\lambda} + \frac{\tau_2}{T_R} \tilde{\lambda}^{-\gamma} \right) \frac{1}{1 + \kappa_1 \tilde{\lambda}^{-\gamma}/(rT_R)} \right)^{\frac{d^{N_T}-d}{d-1}} \\ &\stackrel{*}{\leq} \left(\left(1 + \frac{\tau_1}{T_R \sqrt{rT_R}} \tilde{\lambda}^{\frac{\gamma/N_T-1}{2}} \log \tilde{\lambda} + \frac{\tau_2}{T_R} \tilde{\lambda}^{-\gamma} \right) \left(1 - \frac{\kappa_1}{2rT_R} \tilde{\lambda}^{-\gamma} \right) \right)^{\frac{d^{N_T}-d}{d-1}} \\ &\stackrel{**}{\leq} \left(1 + \frac{\tau_1}{T_R \sqrt{rT_R}} \tilde{\lambda}^{\frac{\gamma/N_T-1}{2}} \log \tilde{\lambda} \right)^{\frac{d^{N_T}-d}{d-1}} \leq 2, \end{aligned}$$

where (*) follows for $\tilde{\lambda} \geq \tilde{\lambda}_{04}$ for some $\tilde{\lambda}_{04} > 0$ as $1/(1+x) \leq 1-x/2$ for $x \in (0,1)$. Next, (**) follows as $\kappa_1 \geq 2r\tau_2$. Finally, the last inequality follows for $\tilde{\lambda} \geq \tilde{\lambda}_{05}$ for some $\tilde{\lambda}_{05} > 0$ as

$$\tilde{\lambda}^{\frac{\gamma/N_T-1}{2}} \frac{d^{N_T}-d}{d-1} \log \tilde{\lambda} \leq \tilde{\lambda}^{\frac{\gamma/N_T-1}{2}} d^{N_T-0.5} \log \tilde{\lambda} \leq \tilde{\lambda}^{\gamma-1/2} (\log \tilde{\lambda})^2 \rightarrow 0 \text{ as } \tilde{\lambda} \rightarrow \infty$$

which implies

$$\left(1 + \frac{\tau_1}{T_R \sqrt{rT_R}} \tilde{\lambda}^{\frac{\gamma/N_T-1}{2}} \log \tilde{\lambda} \right)^{\frac{d^{N_T}-d}{d-1}} \rightarrow 1 \text{ as } \tilde{\lambda} \rightarrow \infty.$$

Thus, the RHS of (31) is upper bounded as follows:

$$\left(\frac{rT_B}{rT_R + \kappa_1 \tilde{\lambda}^{-\gamma}} \right)^{\frac{d^{N_T}-d}{d-1}} \left(\frac{r(n-x)}{x} \right)^{d^{N_T}} \leq 4d^{-\frac{B}{2rT_R}}.$$

Now, we provide a lower bound on LHS. We have

$$1 - \frac{n-x}{T_B \tilde{\lambda}} \geq 1 - \frac{T_R}{T_B} + \frac{(B-\kappa_1)}{T_B} \lambda^{-\gamma} \stackrel{(25)}{\geq} 1 - \frac{1}{1 + \frac{\tau_1}{T_R^{3/2}} \tilde{\lambda}^{\frac{\gamma/N_T-1}{2}}} \stackrel{*}{\geq} \frac{\tau_1}{2T_R^{3/2}} \tilde{\lambda}^{\frac{\gamma/N_T-1}{2}} > \frac{\tau_1}{2T_R^{3/2}} d^{-\frac{N_T}{2\gamma}},$$

where (*) follows for all $\tilde{\lambda} \geq \tilde{\lambda}_{06}$ for some $\tilde{\lambda}_{06} > 0$ as $1/(1+x) \leq 1-x/2$ for $x \in (0, 1)$. Next, the last inequality follows by noting that $\tilde{\lambda}^{\frac{\gamma/N_T-1}{2}} \geq d^{1/2-N_T/(2\gamma)} > d^{-N_T/(2\gamma)}$. Combining the bounds on LHS and RHS of (31), we get

$$\begin{aligned} 4d^{-\frac{B}{2rT_R}} &\geq \left(\frac{r(n-x)}{x}\right)^{d^{N_T}} \left(\frac{rT_B}{rT_R + \kappa_1 \tilde{\lambda}^{-\gamma}}\right)^{\frac{d^{N_T}-d}{d-1}} \\ &= 1 - \frac{n-x}{T_B \tilde{\lambda}} \\ &> \frac{\tau_1}{2T_R^{3/2}} d^{-\frac{N_T}{2\gamma}}. \end{aligned}$$

Now, by noting that $B > \frac{rT_R N_T}{\gamma}$, there exists $\tilde{\lambda}_{07}$ such that for all $\tilde{\lambda} \geq \tilde{\lambda}_{07}$, we have

$$\frac{\tau_1}{2T_R^{3/2}} d^{-\frac{N_T}{2\gamma}} \geq 4d^{-\frac{B}{2rT_R}}.$$

Thus, we arrive at a contradiction. This completes the proof with $\tilde{\lambda}_0 = \max_{i \in [7]} \{\tilde{\lambda}_{0i}\}$,

$$B = \frac{rT_R N_T}{\gamma} + 2\kappa_1, \quad \kappa_2 \geq 2 + 4r\tau_2, \quad \kappa_1 \geq 2r\tau_2. \quad \square$$

Proof of Claim 1 We prove this claim by Induction. The base case corresponds to X_j^C for $j = 0$. By (27), we have

$$\prod_{i=1}^{d-1} X_0^C - i = \left(1 - \frac{n - X_{N_T}^C}{T_B \tilde{\lambda}}\right) \prod_{i=1}^{d-1} X_{N_T}^C - i$$

The RHS is a strictly increasing function of $X_{N_T}^C$ as $X_{N_T}^C \geq d$. Also, the LHS is a one-to-one mapping with X_0^C as $X_0^C \geq d$. In particular, if $X_0^C \leq d$, then $p_0 = 0$ which implies $X_{N_T}^B = 0$ by (22c), which is a contradiction. Combining the two, we conclude that X_0^C is a strictly increasing function of $X_{N_T}^C$.

Now, we prove the induction step which corresponds to X_j^C , assuming that X_{j-1}^C is a strictly increasing function of $X_{N_T}^C$. By (28) and (27), we have

$$\prod_{i=1}^{d-1} X_j^C - i = \left(1 - \frac{n - X_{N_T}^C}{T_B \tilde{\lambda}} + \frac{X_{j-1}^C}{rT_B \tilde{\lambda}}\right) \prod_{i=1}^{d-1} X_{N_T}^C - i.$$

Note that the RHS is a strictly increasing function of $X_{N_T}^C$ as X_{j-1}^C is a strictly increasing function of $X_{N_T}^C$ by induction hypothesis. Thus, similar to the base case, we conclude that X_j^C is a strictly increasing function of $X_{N_T}^C$. This completes the proof of the claim. \square

B.3. Service Level for Power-of-d Vehicles Dispatch

Proof of Proposition 4 By global stability and Proposition (3), for all $\epsilon > 0$, there exists $t_0 > 0$ such that for all $t \geq t_0$, we have

$$X_{N_T}^B(t) \geq T_R \tilde{\lambda} - B \tilde{\lambda}^{1-\gamma} - \epsilon,$$

for $B = \frac{r T_R N_T}{\gamma} + \kappa_1$ and $\tilde{\lambda} \geq \tilde{\lambda}_0$. Using this and (14c), we get

$$\begin{aligned} \lambda p_0(t) I(t) &= X_{N_T}^B(t) \mu(t) - \dot{X}_{N_T}^C(t) \\ &\geq \left(T_R \tilde{\lambda} - B \tilde{\lambda}^{1-\gamma} - \epsilon \right) \mu(t) - \dot{X}_{N_T}^C(t) \\ &\stackrel{(a)}{\geq} \frac{1}{T_B} \left(T_R \tilde{\lambda} - B \tilde{\lambda}^{1-\gamma} \right) - \frac{\epsilon}{T_R} - \dot{X}_{N_T}^C(t) \\ &\stackrel{(24)}{\geq} \frac{1}{1 + \frac{\tau_1}{T_R \sqrt{r T_R}} \tilde{\lambda}^{\frac{\gamma/N_T-1}{2}} \log \tilde{\lambda} + \frac{\tau_2}{T_R} \tilde{\lambda}^{-\gamma}} \left(\tilde{\lambda} - \frac{B}{T_R} \tilde{\lambda}^{1-\gamma} \right) - \frac{\epsilon}{T_R} - \dot{X}_{N_T}^C(t) \\ &\stackrel{(b)}{\geq} \left(1 - \frac{\tau_1}{T_R \sqrt{r T_R}} \tilde{\lambda}^{\frac{\gamma/N_T-1}{2}} \log \tilde{\lambda} - \frac{\tau_2}{T_R} \tilde{\lambda}^{-\gamma} \right) \left(\tilde{\lambda} - \frac{B}{T_R} \tilde{\lambda}^{1-\gamma} \right) - \frac{\epsilon}{T_R} - \dot{X}_{N_T}^C(t) \\ &\geq \tilde{\lambda} - \frac{B + \tau_2}{T_R} \tilde{\lambda}^{1-\gamma} - \frac{\tau_1}{T_R \sqrt{r T_R}} \tilde{\lambda}^{\frac{\gamma/N_T+1}{2}} \log \tilde{\lambda} - \frac{\epsilon}{T_R} - \dot{X}_{N_T}^C(t) \\ &\stackrel{(c)}{\geq} \tilde{\lambda} - \frac{B + 2\tau_2}{T_R} \tilde{\lambda}^{1-\gamma} - \frac{\epsilon}{T_R} - \dot{X}_{N_T}^C(t) \end{aligned} \tag{32}$$

where (a) follows as $1/T_B \leq \mu(t) \leq 1/T_R$. Next, (b) follows as $1/(1+x) \geq 1-x$ for $x \geq 0$. Lastly, (c) follows by noting that $\gamma < 1/(2 + 1/N_T)$, we get $1 - \gamma > (\gamma/N_T + 1)/2$. Thus, there exists $\tilde{\lambda}_{11} > 0$ such that for all $\tilde{\lambda} \geq \tilde{\lambda}_{11}$, we have

$$\frac{\tau_2}{T_R} \tilde{\lambda}^{1-\gamma} \geq \frac{\tau_1}{T_R \sqrt{r T_R}} \tilde{\lambda}^{\frac{\gamma/N_T+1}{2}} \log \tilde{\lambda}.$$

Now, by integrating both sides of (32), we get

$$\begin{aligned} \frac{1}{T} \int_0^T \lambda_{\text{eff}}^{\pi(d)}(t) dt &= \frac{1}{T} \int_0^T \lambda p_0(t) I(t) dt \\ &\geq \frac{1}{T} \int_{t_0}^T \lambda p_0(t) I(t) dt \\ &\geq \frac{T - t_0}{T} \left(\tilde{\lambda} - \frac{B + 2\tau_2}{T_R} \tilde{\lambda}^{1-\gamma} - \frac{\epsilon}{T_R} \right) - \frac{X_{N_T}^C(T) - X_{N_T}^C(t_0)}{T} \\ &\geq \frac{T - t_0}{T} \left(\tilde{\lambda} - \frac{B + 2\tau_2}{T_R} \tilde{\lambda}^{1-\gamma} - \frac{\epsilon}{T_R} \right) - \frac{n}{T} \end{aligned}$$

Now, by taking the limit infimum as $T \rightarrow \infty$ on both sides, we get

$$\liminf_{T \rightarrow \infty} \frac{1}{T} \int_0^T \lambda_{\text{eff}}^{\pi(d)}(t) dt \geq \tilde{\lambda} - \frac{B + 2\tau_2}{T_R} \tilde{\lambda}^{1-\gamma} - \frac{\epsilon}{T_R}$$

As the above is true for all $\epsilon > 0$, we get

$$\lambda \alpha_{\text{eff}}^{\pi} \geq \tilde{\lambda} - \frac{B + 2\tau_2}{T_R} \tilde{\lambda}^{1-\gamma} = \tilde{\lambda} - \left(\frac{rN_T}{\gamma} + \frac{\kappa_1 + 2\tau_2}{T_R} \right) \tilde{\lambda}^{1-\gamma}.$$

This completes the proof with $\tilde{\lambda}_1 = \max\{\tilde{\lambda}_0, \tilde{\lambda}_{11}\}$ □

B.4. Proof of Theorem 2

Proof of Theorem 2 The workhorses for proving this theorem are Proposition 3 and Proposition 4. Now, we use the lower bound on $\bar{\alpha}_{\text{eff}}^{\pi}$ in Proposition 4 to show achievability under Power-of- d vehicles dispatch policy. In particular, consider

$$\tilde{\lambda} = \alpha\lambda + \left(\frac{rN_T}{\gamma} + \frac{\kappa_1 + 2\tau_2}{T_R} \right) \lambda^{1-\gamma},$$

with

$$\lambda \geq \lambda_{00} = \left(\left(\frac{rN_T}{\gamma} + \frac{\kappa_1 + 2\tau_2}{T_R} \right) \frac{1}{1-\alpha} \right)^{1/\gamma}$$

to ensure that $\tilde{\lambda} \leq \lambda$. Now, substituting $\tilde{\lambda}$ in terms of λ in Proposition (4), we get

$$\lambda \bar{\alpha}_{\text{eff}}^{\pi} \geq \lambda \alpha_{\text{eff}}^{\pi} \geq \tilde{\lambda} - \left(\frac{rN_T}{\gamma} + \frac{\kappa_1 + 2\tau_2}{T_R} \right) \tilde{\lambda}^{1-\gamma} = \alpha\lambda + \left(\frac{rN_T}{\gamma} + \frac{\kappa_1 + 2\tau_2}{T_R} \right) (\lambda^{1-\gamma} - \tilde{\lambda}^{1-\gamma}) \geq \alpha\lambda.$$

Thus, we have $\bar{\alpha}_{\text{eff}}^{\pi} \geq \alpha_{\text{eff}}^{\pi} \geq \alpha$. Now, note that, we have

$$\begin{aligned} n &= (1+r)T_R\tilde{\lambda} + \kappa_1\tilde{\lambda}^{1-\gamma} \geq (1+r)T_R\alpha\lambda + \kappa_1\delta^{1-\gamma}\lambda^{1-\gamma} \\ n &= (1+r)T_R\tilde{\lambda} + \kappa_1\tilde{\lambda}^{1-\gamma} \leq (1+r)T_R\alpha\lambda + \left(\frac{(1+r)rT_RN_T}{\gamma} + \kappa_1 + (1+r)(\kappa_1 + 2\tau_2) \right) \lambda^{1-\gamma}. \end{aligned}$$

The above two bounds imply that $n = (1+r)T_R\alpha\lambda + \Theta(\lambda^{1-\gamma})$. Similarly, we have

$$\begin{aligned} m &= rT_R\tilde{\lambda} + \kappa_2\tilde{\lambda}^{2\gamma} \geq rT_R\alpha\lambda + \kappa_2\delta^{2\gamma}\lambda^{2\gamma} \\ m &= rT_R\tilde{\lambda} + \kappa_2\tilde{\lambda}^{2\gamma} \leq rT_R\alpha\lambda + \left(\frac{r^2T_RN_T}{\gamma} + \kappa_2 + r(\kappa_1 + 2\tau_2) \right) \lambda^{2\gamma}, \end{aligned}$$

where the last inequality follows by noting that $2\gamma \geq 1 - \gamma$. Thus, we have $m = rT_R\alpha\lambda + \Theta(\lambda^{2\gamma})$. So, by setting

$$\lambda_0(\alpha) = \max \left\{ \lambda_{00}(\alpha), \frac{\tilde{\lambda}_0}{\delta}, \frac{\tilde{\lambda}_1}{\delta} \right\},$$

the proof is complete. □

Appendix C: Extensions and Additional Insights

C.1. Failure of Closest Dispatch

We first present the performance of Algorithm 1 when $d = 1$.

PROPOSITION 5 (Failure of Closest Dispatch). *Fix an $\alpha \in [\delta, 1]$ for some $\delta > 0$. Also, let $m = \infty$ and $1 \geq \bar{\alpha}_{\text{eff}}^\pi \geq \alpha$, where π is the power-of- d vehicle dispatch policy with $d = 1$. Then, there exists $\lambda_0, \epsilon > 0$, such that*

$$n \geq (1+r)T_R\alpha\lambda + \epsilon\lambda \quad \forall \lambda \geq \lambda_0.$$

Proposition 1 establishes that the closest dispatch algorithm requires more vehicles to satisfy the demand, even with infinitely many chargers. Under this policy, we greedily minimize the pickup distance. However, in terms of battery level, we are less likely to choose an EV with a high SoC because the closest distance essentially picks a vehicle at random regarding its battery levels. Thus, the variance of SoC across the fleet is higher, resulting in a fraction of EVs being unable to serve customers due to low SoC. To compensate for unavailable EVs, a larger fleet size is warranted, as otherwise, an incoming arrival is more likely to be rejected due to the closest vehicle having low SoC.

Proof of Proposition 5 First, we note that $(X_j^B(t), X_j^C(t))$ are all bounded in $[0, n]$. Hence, if we denote any of these quantities by $y(t)$ we have that $\frac{1}{T} \int_0^T y(t) dt$ is a bounded sequence in a compact set. Therefore, it has a subsequence that converges. We can therefore create a subsequence for which all of the integrals $\frac{1}{T} \int_0^T y(t) dt$ with $y(t) \in \{X_j^B(t), X_j^C(t)\}$ converge. Note that here we are abusing notation and using T instead of explicitly writing the subsequence. We note that this does not affect what we want to prove. Let us use $(\bar{X}_j^B(t), \bar{X}_j^C(t))$ to denote the limit of each of these integrals (of the subsequences).

We start by characterizing lower and upper bounds for $\mu(t)$. Note that, as $m = \infty$, we have

$$\mu(t) = \frac{1}{T_R + \tau_1 / \sqrt{n - q(t)}} \leq \frac{1}{T_R} \quad \forall t \in \mathbb{R}_+.$$

Now, by the admission control policy, we have $q(t) \leq n/(1+r)$ for all $t \in \mathbb{R}_+$. Using this, we get

$$\mu(t) = \frac{1}{T_R + \tau_1 / \sqrt{n - q(t)}} \geq \frac{1}{T_R + \tau_1 \sqrt{1+r}/\sqrt{r}}.$$

For the ease of notation, we define

$$\mu_l \triangleq \frac{1}{T_R + \tau_1 \sqrt{1+r}/\sqrt{r}}, \quad \mu_u \triangleq \frac{1}{T_R}.$$

Now, by adding (14a) and (14b), we get

$$\frac{\dot{X}_j^B(t) + \dot{X}_j^C(t)}{\mu(t)} = X_{j+1}^B(t) - X_j^B(t) - \frac{1}{r} (X_j^C(t) - X_{j-1}^C(t)). \quad (33)$$

By integrating the left hand side of the above equation, we get

$$-\frac{2n}{\mu_l} \leq -\frac{\dot{X}_j^B(0) + \dot{X}_j^C(0)}{\mu_l} \leq \int_{t=0}^T \frac{\dot{X}_j^B(t) + \dot{X}_j^C(t)}{\mu(t)} \leq \frac{\dot{X}_j^B(T) + \dot{X}_j^C(T)}{\mu_l} \leq \frac{2n}{\mu_l}$$

Now, by dividing by T and taking the limit supremum as $T \rightarrow \infty$, we get

$$\limsup_{T \rightarrow \infty} \frac{1}{T} \int_{t=0}^T \frac{\dot{X}_j^B(t) + \dot{X}_j^C(t)}{\mu(t)} = 0.$$

Using the above equality in (33), we get

$$\bar{X}_j^C - \bar{X}_{j-1}^C = r (\bar{X}_{j+1}^B - \bar{X}_j^B) \quad \forall j \in \{1, \dots, N_T - 1\} \quad (34)$$

Following the same steps for (14d), we get

$$\bar{X}_0^C = r \bar{X}_1^B. \quad (35)$$

By adding (34) for $1 \leq j \leq k$, we get

$$\bar{X}_k^C - \bar{X}_0^C = r (\bar{X}_{k+1}^B - \bar{X}_1^B) \quad \forall k \in \{1, \dots, N_T - 1\}.$$

In addition, by using (35), we get

$$\bar{X}_k^C = r \bar{X}_{k+1}^B \quad \forall k \in \{0, 1, \dots, N_T - 1\}.$$

Again, by summing (14a) for $j+1$ and (14b) for j , we get

$$\begin{aligned} \dot{X}_{j+1}^B(t) + \dot{X}_j^C(t) &= \lambda (p_j(t) - p_{j+1}(t)) I(t) - (X_j^C(t) - X_{j-1}^C(t)) \frac{\mu(t)}{r} \\ &= \frac{\lambda}{X_{N_T}^C} (X_{j+1}^C(t) - X_j^C(t)) I(t) - (X_j^C(t) - X_{j-1}^C(t)) \frac{\mu(t)}{r} \\ &\leq \frac{(1+r)\lambda}{nr} (X_{j+1}^C(t) - X_j^C(t)) - (X_j^C(t) - X_{j-1}^C(t)) \frac{\mu_l}{r} \end{aligned}$$

where the last inequality follows by the admission control. In particular, $X_{N_T}^B(t) \leq n/(1+r)$ which implies $X_{N_T}^C(t) \geq nr/(r+1)$ for all $t \in \mathbb{R}_+$. Now, by integrating both sides from 0 to T , dividing by T , and then taking the limit supremum, we get

$$(\bar{X}_j^C - \bar{X}_{j-1}^C) \frac{\mu_l}{r} \leq \frac{(1+r)\lambda}{rn} (\bar{X}_{j+1}^C - \bar{X}_j^C) \quad \forall j \in \{1, \dots, N_T - 1\}.$$

Using the above inequality multiple times, we get

$$\bar{X}_j^C - \bar{X}_{j-1}^C \leq \frac{(1+r)\lambda}{n\mu_l} (\bar{X}_{j+1}^C - \bar{X}_j^C) \leq \left(\frac{(1+r)\lambda}{n\mu_l} \right)^{N_T-j} (\bar{X}_{N_T}^C - \bar{X}_{N_T-1}^C) \quad \forall j \in \{1, \dots, N_T-1\}.$$

Now, by taking $j = 1$ in (14a), we get

$$\begin{aligned} \dot{X}_1^B(t) &= \frac{\lambda}{\bar{X}_{N_T}^C(t)} (X_1^C(t) - X_0^C(t)) I(t) - X_1^B(t) \mu_l \\ &\leq \frac{(1+r)\lambda}{nr} (X_1^C(t) - X_0^C(t)) I(t) - X_1^B(t) \mu_l \end{aligned}$$

Now, by integrating both sides from 0 to T , dividing by T , and then taking the limit supremum, we get

$$\bar{X}_0^C = r\bar{X}_1^B \leq \frac{(1+r)\lambda}{n\mu_l} (\bar{X}_1^C - \bar{X}_0^C) \leq \left(\frac{(1+r)\lambda}{n\mu_l} \right)^{N_T} (\bar{X}_{N_T}^C - \bar{X}_{N_T-1}^C)$$

Now, we use the upper bounds on $\bar{X}_j^C - \bar{X}_{j-1}^C$ to obtain a lower bound on $\bar{X}_{N_T}^C - \bar{X}_{N_T-1}^C$ as follows:

$$\begin{aligned} n &= \bar{X}_{N_T}^C + \bar{X}_{N_T}^B \\ &= \bar{X}_{N_T}^C + \frac{\bar{X}_{N_T-1}^C}{r} \\ &\leq \frac{r+1}{r} \bar{X}_{N_T}^C \\ &= \frac{r+1}{r} \left(\sum_{j=1}^{N_T} (\bar{X}_j^C - \bar{X}_{j-1}^C) + \bar{X}_0^C \right) \\ &\leq \frac{r+1}{r} (\bar{X}_{N_T}^C - \bar{X}_{N_T-1}^C) \sum_{j=0}^{N_T} \left(\frac{(1+r)\lambda}{n\mu_l} \right)^{N_T-j} \\ &= \frac{r+1}{r} (\bar{X}_{N_T}^C - \bar{X}_{N_T-1}^C) \left((N_T+1) \mathbb{1} \left\{ \frac{(1+r)\lambda}{n\mu_l} = 1 \right\} + \frac{1 - \left(\frac{(1+r)\lambda}{n\mu_l} \right)^{N_T+1}}{1 - \frac{(1+r)\lambda}{n\mu_l}} \mathbb{1} \left\{ \frac{(1+r)\lambda}{n\mu_l} \neq 1 \right\} \right) \end{aligned}$$

The last inequality implies the following:

$$\bar{X}_{N_T}^C - \bar{X}_{N_T-1}^C \geq \frac{nr}{1+r} \left(\frac{1}{N_T+1} \mathbb{1} \left\{ \frac{(1+r)\lambda}{n\mu_l} = 1 \right\} + \frac{1 - \frac{(1+r)\lambda}{n\mu_l}}{1 - \left(\frac{(1+r)\lambda}{n\mu_l} \right)^{N_T+1}} \mathbb{1} \left\{ \frac{(1+r)\lambda}{n\mu_l} \neq 1 \right\} \right)$$

Now, using the above inequality, we get

$$\begin{aligned} n &= \bar{X}_{N_T}^B + \bar{X}_{N_T}^C \\ &= \bar{X}_{N_T}^B + r\bar{X}_{N_T}^B + \bar{X}_{N_T}^C - \bar{X}_{N_T-1}^C \\ &\geq (r+1)\bar{X}_{N_T}^B + \frac{nr}{1+r} \left(\frac{1}{N_T+1} \mathbb{1} \left\{ \frac{(1+r)\lambda}{n\mu_l} = 1 \right\} + \frac{1 - \frac{(1+r)\lambda}{n\mu_l}}{1 - \left(\frac{(1+r)\lambda}{n\mu_l} \right)^{N_T+1}} \mathbb{1} \left\{ \frac{(1+r)\lambda}{n\mu_l} \neq 1 \right\} \right) \end{aligned}$$

This provides us with the following upper bound on $\bar{X}_{N_T}^B$:

$$\bar{X}_{N_T}^B \leq \frac{n}{1+r} - \frac{nr}{(1+r)^2} \left(\frac{1}{N_T+1} \mathbb{1} \left\{ \frac{(1+r)\lambda}{n\mu_l} = 1 \right\} + \frac{1 - \frac{(1+r)\lambda}{n\mu_l}}{1 - \left(\frac{(1+r)\lambda}{n\mu_l} \right)^{N_T+1}} \mathbb{1} \left\{ \frac{(1+r)\lambda}{n\mu_l} \neq 1 \right\} \right)$$

Note that, by (14c), we have

$$\dot{X}_{N_T}^C(t) = -\lambda p_0(t)I(t) + X_{N_T}^B(t)\mu(t) \leq -\lambda p_0(t)I(t) + X_{N_T}^B(t)\mu_u.$$

Now, by integrating both sides from 0 to T , dividing by T , and then taking the limit supremum, we get

$$\begin{aligned} \lambda\alpha &\leq \lambda\bar{\alpha}_{\text{eff}}^\pi \leq \bar{X}_{N_T}^B \mu_u \leq \frac{\bar{X}_{N_T}^B}{T_R} \\ &\leq \frac{n}{T_R(1+r)} - \frac{nr}{T_R(1+r)^2} \left(\frac{1}{N_T+1} \mathbb{1} \left\{ \frac{(1+r)\lambda}{n\mu_l} = 1 \right\} + \frac{1 - \frac{(1+r)\lambda}{n\mu_l}}{1 - \left(\frac{(1+r)\lambda}{n\mu_l} \right)^{N_T+1}} \mathbb{1} \left\{ \frac{(1+r)\lambda}{n\mu_l} \neq 1 \right\} \right) \end{aligned} \quad (36)$$

$$\begin{aligned} &\stackrel{(a)}{\leq} \frac{n}{T_R(1+r)} - \frac{nr}{T_R(1+r)^2} \min \left\{ \frac{1}{N_T+1}, \frac{1/(\delta\mu_l T_R) - 1}{1/(\delta\mu_l T_R)^N - 1} \right\} \\ &\stackrel{(b)}{=} \frac{n}{T_R(1+r)} \left(1 - \frac{\epsilon}{T_R(1+r)\delta} \right), \end{aligned} \quad (37)$$

where (a) follows as $\lambda \leq \frac{n}{T_R(1+r)\delta}$ by (36), which implies

$$\frac{1}{N_T+1} \mathbb{1} \left\{ \frac{(1+r)\lambda}{n\mu_l} = 1 \right\} + \frac{1 - \frac{(1+r)\lambda}{n\mu_l}}{1 - \left(\frac{(1+r)\lambda}{n\mu_l} \right)^{N_T+1}} \mathbb{1} \left\{ \frac{(1+r)\lambda}{n\mu_l} \neq 1 \right\} \leq \min \left\{ \frac{1}{N_T+1}, \frac{1/(\delta\mu_l T_R) - 1}{1/(\delta\mu_l T_R)^N - 1} \right\},$$

where $\mu_l = \frac{1}{T_R + \tau_1 \sqrt{1+r}/\sqrt{r}}$. Next, (b) follows by setting

$$\epsilon \triangleq T_R r \delta \min \left\{ \frac{1}{N_T+1}, \frac{1/(\delta\mu_l T_R) - 1}{1/(\delta\mu_l T_R)^N - 1} \right\}.$$

Now, using (37), we get the following lower bound on n :

$$\begin{aligned} n &\geq (1+r)T_R\alpha\lambda \left(1 - \frac{\epsilon}{T_R(1+r)\delta} \right)^{-1} \\ &\stackrel{(a)}{\geq} (1+r)T_R\alpha\lambda \left(1 + \frac{\epsilon}{T_R(1+r)\delta} \right) \\ &\stackrel{(b)}{\geq} (1+r)T_R\alpha\lambda + \epsilon\lambda, \end{aligned}$$

where (a) follows by noting that $\epsilon/(T_R(1+r)\delta) \leq 1$ and (b) follows as $\alpha \geq \delta$. This completes the proof. \square

C.2. Pack Size versus Fleet Size

By Theorem 2, to obtain a service level of α under the power-of- d vehicles dispatch algorithm, we have

$$n \asymp (1+r)T_R\lambda + \lambda^{\frac{1+1/N_T}{2+1/N_T}}, \quad (38)$$

for large enough m . Note that the right-hand side of the above equation is a decreasing function of N_T . Thus, a smaller fleet size is sufficient, given a larger battery. As evident from the discussion on ICE cars, the exponent of the second-order term is less than $2/3$ due to the double counting of partially charged cars. Now, if the pack size is large, the fraction of partially charged cars will be higher, resulting in increased benefits. Equation (38) quantifies this phenomenon. In short, a trade-off exists between the fleet and the pack size quantified by (38). It is also interesting to note that the benefits from a larger pack size exhibit the law of diminishing marginal utility. In particular, define $f(N_T) = (1+r)T_R\lambda + \lambda^{\frac{1+1/N_T}{2+1/N_T}}$ and note that $f''(N_T) \geq 0$. Thus, n is a convex function of N_T which implies that the benefit of increasing the pack size reduces for larger values of the pack size.

C.3. Battery Charging versus Battery Swapping

Battery swapping is an alternate approach to replenishing the SoC of an EV. Rather than charging the battery pack, a spare one with a higher SoC replaces it. In particular, the spare battery pack charges while the EV is driving, which later replaces the original battery pack. One can interpret fleet of EVs equipped with battery swapping technology as a fleet of ICE vehicles. In particular, the time required to replenish the charge by swapping the battery would be of the same order as refueling an ICE vehicle. Thus, by Besbes et al. (2022), we can conclude that the fleet size (n_{bs}) and battery (b_{bs}) requirements for EV with battery swapping is

$$n_{bs} = T_R\lambda + \Theta(\lambda^{2/3}), \quad b_{bs} = (1+r)T_R\lambda + \Theta(\lambda^{2/3}). \quad (39)$$

In particular, the fleet size requirement follows from Besbes et al. (2022) and for each EV, at least $(1+r)$ batteries are required to balance the aggregate discharge rate with the aggregate charge rate. On the other hand, by Theorem 1 and 2, the fleet size (n_{bc}) and battery requirements (b_{bc}) for EV with battery charging is

$$n_{bc} = b_{bc} = (1+r)T_R\lambda + \Theta(\lambda^{1-\gamma}) \quad \text{for } \gamma \in \left[\frac{1}{3}, \frac{1}{2+1/N_T}\right). \quad (40)$$

Thus, even though the fleet size requirement under battery charging is higher, the number of battery packs required is smaller compared to battery swapping, especially with a high density of chargers. In today's world, battery packs are the bottleneck in manufacturing electric vehicles. Thus, battery swapping is a viable option for ride-hailing systems only if battery manufacturing is accelerated in the future.

Appendix D: Auxiliary Results

LEMMA 2 (Eq. 12 in Srinivasa and Haenggi (2009)). Let Z_1, Z_2, \dots, Z_k be a sequence of independent uniformly distributed random points in a 2-dimensional Euclidean ball \mathcal{C} . Let $Z^{(d)}(z_0)$ be the d^{th} closest point in the sequence to a point z_0 in the interior of \mathcal{C} then

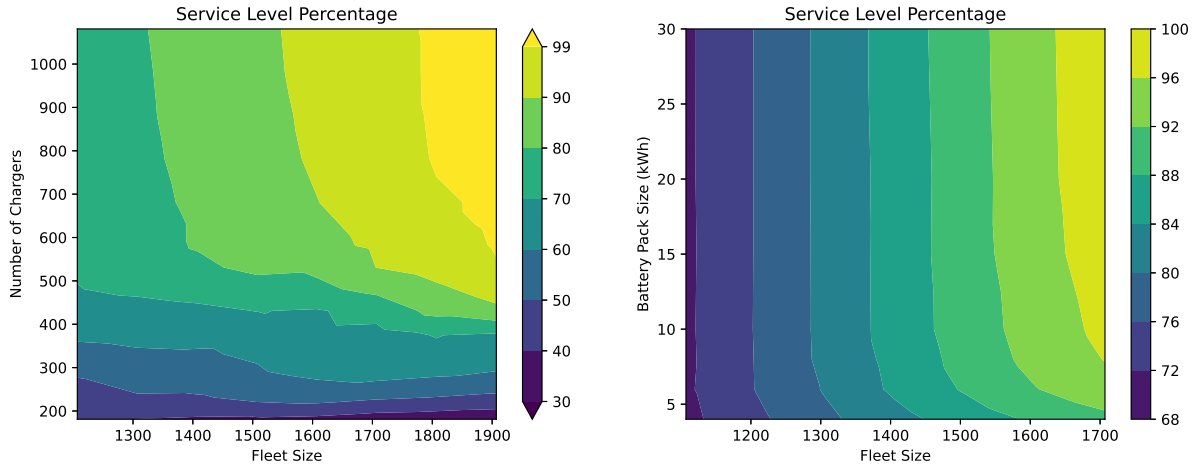
$$\mathbb{E} [\|Z^{(d)}(z_0) - z_0\|] = \Theta \left(\sqrt{\frac{d}{k}} \right), \quad \text{as } k \uparrow \infty.$$

Appendix E: Additional Simulations

E.1. Fleet Size, Number of Chargers, and Battery Pack Size Trade-off

As discussed in Theorem 1, there is a tradeoff between chargers and EVs. We showcase this tradeoff in the left panel of Figure 7. For a fixed arrival rate, the figure shows how more vehicles are needed to reach a certain service level as the number of charger decrease, and vice versa. Additionally, in agreement with Theorem 2, the right panel of the figure shows that for larger values of p^* the fleet size requirement remains largely constant.

Figure 7 Contour of service level as a function of the fleet size and the number of chargers (left), and fleet size and battery pack size (right). We set $\lambda = 80$ per min and $m_p = 1$.



E.2. Matching Algorithms Comparison

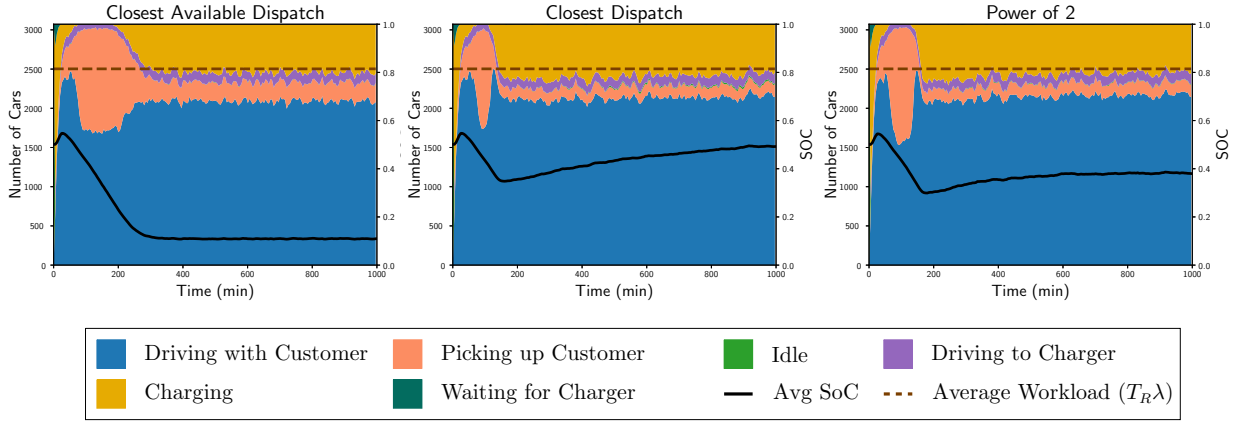
We compare the performance of three different matching algorithm: closest dispatch, power-of- d with $d = 2$, and closest available dispatch (CAD). In CAD, we match a trip request to its closest available EV, i.e., closest EV with sufficient battery to serve the trip. If no such EV exists, then the customer is dropped. That

is, CAD is a natural extension to closest dispatch which keeps searching for a vehicle with enough SoC if the closest vehicle does not have enough battery to serve a request.

These matching algorithms are inspired by the long line of literature on routing in load balancing. In particular, one can interpret our model as a load balancing model by interpreting $N_T - \text{SoC}_i(t)$ as queue lengths and dispatching an EV as routing an incoming customer, where $\text{SoC}_i(t)$ is the SoC of i^{th} EV at time t . Then, CAD corresponds to joining the idle queue, CD corresponds to random routing, and Pod corresponds to power-of- d choices routing.

We start by qualitatively comparing the three algorithms in Figure 8. As the SoC of all the EVs is initialized

Figure 8 Evolution of the state for CAD, CD, and Po2 with $n = 3072$, $m = 2600$ (325 locations with 8 posts at each location), and $\lambda = 160$ per min

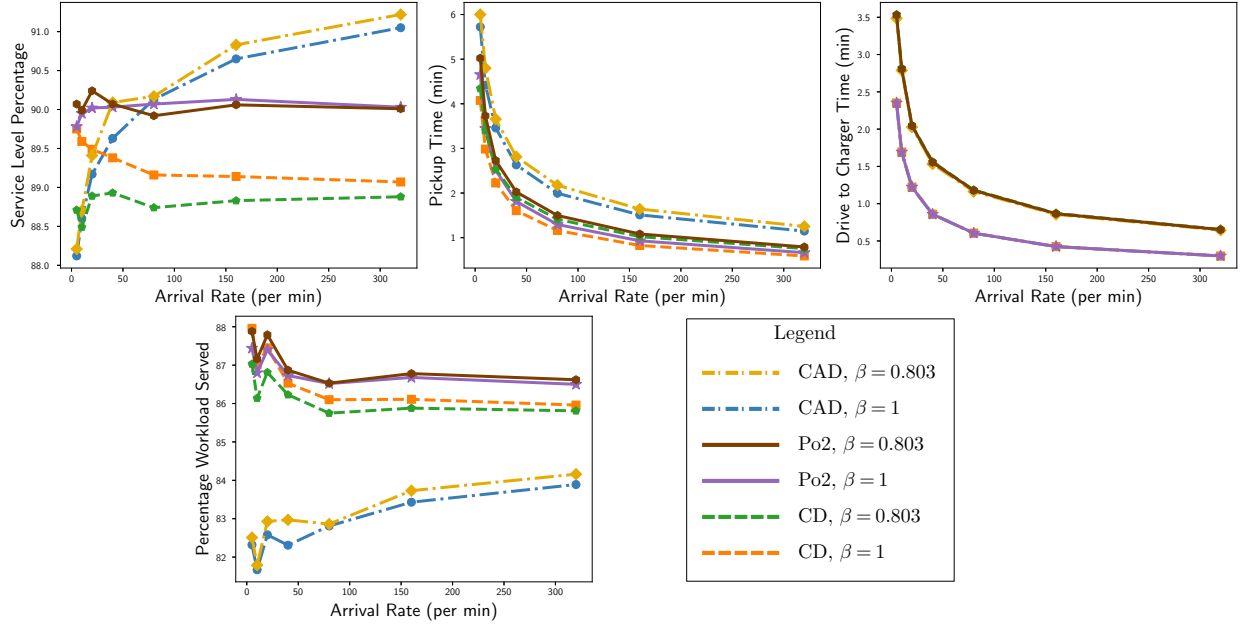


away from 0, all three algorithms initially serve all incoming customers. The SoC of the fleet decreases with time, which then results in dropping incoming customers. Under CAD, all customers are served until the SoC of all the EVs reduces to the minimum allowable SoC.⁷ As seen in Figure 8 (left), initially, the blue region (almost) fills out the average workload implying that all customers are initially served. As the fleet can only sustainably serve 90% of the demand, the fleet average SoC (black line) consistently drops during this time. Now, with a lower fleet SoC, the density of available EVs reduces which results in a larger pickup time (the orange region expands at $t \approx 100$). In turn, large pickup times negatively affect the fleet SoC, and this negative cycle continues until the fleet SoC drops to the minimum and stays there. In summary, in an attempt to serve all incoming customers, CAD experiences large pickup times in transience which, in turn,

⁷ In Figure 3, the SoC drops below s_{\min} as EVs drive to the charger after finishing a trip.

results in low fleet SoC in steady state. On the other hand, CD and Po2 have a more stable fleet SoC in steady state as these algorithms actively drop incoming customers if the nearby EVs do not have enough SoC.

Figure 9 Service level percentage (top left), pickup time (top center), drive to charger time (top right), and percentage workload served (bottom left) as a function of the arrival rate for CAD, CD, and Po2. The fleet size and number of charger corresponds to Series A and C in Fig. 2.



We simulate the three matching algorithms for different values of λ . The fleet size and number of chargers correspond to Series A and Series C in Figure 2, i.e., $\beta = 1$ and $\beta = 0.803$, respectively. The results are reported in Figure 9. First, note that as the charging algorithm is identical across simulations, the drive to the charger time is identical for CAD, CD, and Po2. Next, we observe that the pickup time is the largest for CAD as it always tries to dispatch an EV irrespective of its distance to the customer. In addition, the pickup time for CD is the smallest as it either matches the closest EV or drops the customer. Even though the pickup times for Po2 are larger, it achieves a better service level compared to CD as it balances the SoC more efficiently across the fleet. Additionally, Proposition 5 (Appendix C.1) shows that CD has a fundamentally higher fleet requirement compared to Po2. On the other hand, CAD can achieve a larger service level compared to Po2. However, observe that the percentage of workload served⁸ is much smaller

⁸ Percentage of workload served is defined as the ratio of miles actually driven with a customer and the total miles requested by customers.

for CAD compared to Po2 as well as CD. A high service level and a low workload imply that CAD is biased toward shorter trips. In particular, as the fleet SoC is consistently low (as seen in Fig. 8) for CAD, the longer the trip distance, the harder it is to find an available EV for it. Dropping long trip requests reduces the average fulfilled trip time, allowing the algorithm to serve more customers but lesser workload. In turn, Po2 (and more generally Pod) may be preferred over CD and CAD as it showcases good performance in terms of pickup times, service level, and workload and it also nearly achieves the minimum infrastructure planning requirements.

E.3. Details on Asymptotic Simulations

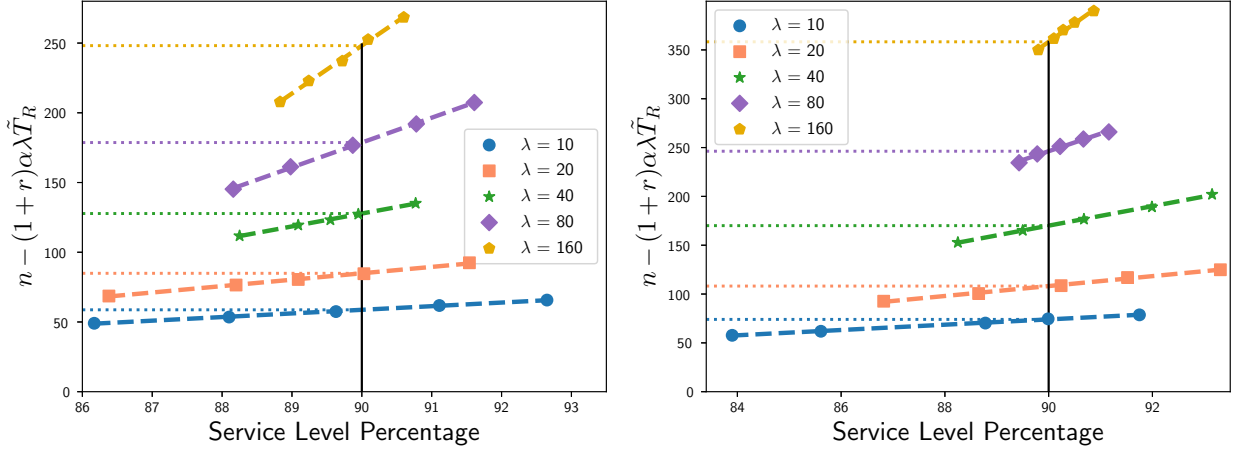
In this section, we expand on the results of Section 6.1 and the corresponding simulation setup. We devise the following procedure to verify the theoretical scalings as in Theorem 2. First, we fix a sequence of arrival rates $\lambda \in \{5, 10, 20, 40, 80, 160, 320\}$. Then, we fix a sequence of m corresponding to a given value of $\beta \in \{0.7, 0.8, 0.9, 1\}$. In particular, we set

$$m = r\tilde{T}_R\alpha\lambda + c\left(\tilde{T}_R\lambda\right)^\beta \quad (41)$$

where $\alpha = 0.9$ is the target service level, $r = 0.25$ is the ratio of discharge rate and charge rate, $c = 4$ is a constant, and \tilde{T}_R is the average fulfilled trip time. Note that \tilde{T}_R is not known a priori as it depends on $\bar{\alpha}_{\text{eff}}^\pi$, which in turn depends on system parameters like λ, n , and m . In particular, Pod is biased slightly towards shorter trips as longer trips are more likely to be rejected. Due to this bias, we get $\tilde{T}_R < T_R$. We observed empirically that $\tilde{T}_R \approx [15, 15.3]$ mins and $T_R \approx [15.6, 15.7]$ mins. Based on this empirical observation, we set $\tilde{T}_R = 15.14$ which allows us to approximate m for a given β .

We make three comments on (41). First, we use \tilde{T}_R as opposed to T_R in Theorem 2 because the customers that are rejected do not affect the dynamics of the system at all. Hence, the trip time experienced by the EVs corresponds to \tilde{T}_R . Second, we set the second order term as $c\left(\tilde{T}_R\lambda\right)^\beta$ as opposed to $c\lambda^\beta$ in Theorem 2 mainly because the former is dimensionless and has a better interpretation. In particular, $\tilde{T}_R\lambda$ corresponds to the workload, which determines the number of EVs driving with a customer, in turn determining the minimum number of EVs required to charge to sustain the fleet SoC. The number of EVs required to charge then determines the charger requirements. Lastly, we set $c = 4$ for two reasons. First, to ensure that the resultant average drive to the charger time is comparable to the average pickup time. Second, we set c to be large enough to encourage achieving the asymptotic scaling as in Theorem 2. For small values of c , we observe

Figure 10 Fleet size buffer corresponding to 90% service level. The markers correspond to simulated values and the line is a linear regression fit. The plot corresponds to $\beta = 1$ (left) and $\beta = 0.8$ (right).



that the EVs have to wait at the chargers for small values of λ . In particular, the decision of selecting the closest available charger is blind to the EVs that are already driving to a charger. Thus, an EV dispatched to an available charger may have to wait at the charger before it starts charging. This effect is exacerbated for small values of λ as the drive to the charger time is large. Due to EVs waiting at the chargers, the simulation starts departing from the theory which warrants larger values of λ to verify the theoretical scalings.

After fixing (λ, m) sequence, we run the simulation for various values of the fleet size to infer the fleet size corresponding to the 90% service level. In particular, for each tuple (λ, m) , we run the simulation for five different values of the fleet size. Each simulation is repeated five times with different seeds and the average values are considered. As shown in Fig. 10, we carry out linear regression between service level and fleet size buffer $(n - (1+r)\tilde{T}_R\alpha\lambda)$ to infer the fleet size and the fleet size buffer that corresponds to the 90% service level. For completeness, we report the fleet size and number of chargers that correspond to 90% service level

Table 3 Fleet Size and Number of Chargers corresponding to the 90% Service Level.

λ	Series A		Series B		Series C		Series D	
	n	m	n	m	n	m	n	m
5	124	320	130	208	133	144	141	96
10	228	640	234	400	245	256	254	168
20	427	1280	436	752	451	456	470	288
40	806	2560	824	1416	851	808	885	488
80	1532	5120	1557	2656	1600	1448	1653	856
160	2958	10248	3003	5008	3072	2600	3188	1496
320	5769	20504	5841	9416	5956	4672	6123	2640

for different values of β in Table 3. The empirical $1 - \gamma$ correspond to the slope of the linear regression line between $\log(\lambda)$ and $\log(n - (1 + r)\tilde{T}_R\alpha\lambda)$. Similarly, the empirical β correspond to the slope of the linear regression line between $\log(\lambda)$ and $\log(n - r\tilde{T}_R\alpha\lambda)$. Note that, we recalculate the value of β as \tilde{T}_R is now known exactly. This recalculation slightly changes the value of β . For example, Series B now corresponds to $\beta = 0.906$ rather than the originally used $\beta = 0.9$.

Appendix F: Varying Arrival Rate

Recall that $\bar{\alpha}_{\text{eff}}^\pi$ is the long run fraction of trip requests met, given by

$$\bar{\alpha}_{\text{eff}}^\pi = \frac{1}{\lambda_{\text{avg}}} \limsup_{T \rightarrow \infty} \frac{1}{T} \int_0^T \lambda_{\text{eff}}^\pi(t) dt.$$

In addition, we define $\bar{\alpha}_1^\pi$ and $\bar{\alpha}_2^\pi$ as the the long run fraction of trips met during the valleys and peaks respectively. Mathematically, we have

$$\bar{\alpha}_1^\pi = \frac{T_1 + T_2}{T_1} \limsup_{T \rightarrow \infty} \frac{1}{T} \sum_{i=0}^{\lfloor \frac{T-T_1}{T_1+T_2} \rfloor - 1} \int_{i(T_1+T_2)}^{(i+1)T_1+iT_2} \lambda_{\text{eff}}^\pi(t) dt \quad (42a)$$

$$\bar{\alpha}_2^\pi = \frac{T_1 + T_2}{T_2} \limsup_{T \rightarrow \infty} \frac{1}{T} \sum_{i=0}^{\lfloor \frac{T}{T_1+T_2} \rfloor - 1} \int_{(i+1)T_1+iT_2}^{(i+1)(T_1+T_2)} \lambda_{\text{eff}}^\pi(t) dt. \quad (42b)$$

We first present a lemma that relates the service level with the fleet size and number of chargers under an arbitrary policy π . Such a result is analogous to analyzing the ODE (5) for the constant arrival rate setting.

LEMMA 3. *For any arbitrary policy π , the following relations holds true.*

$$\bar{\alpha}_{\text{eff}}^\pi \lambda_{\text{avg}} = \frac{\bar{\alpha}_1^\pi \lambda T_1 + \bar{\alpha}_2^\pi c \lambda T_2}{T_1 + T_2} \quad (43a)$$

$$n \geq \bar{\alpha}_2^\pi c \lambda T_R \quad (43b)$$

$$n \geq (1 + r) \bar{\alpha}_{\text{eff}}^\pi \lambda_{\text{avg}} T_R, \quad m \geq r \bar{\alpha}_{\text{eff}}^\pi \lambda_{\text{avg}} T_R \quad (43c)$$

$$r_d \bar{\alpha}_{\text{eff}}^\pi \lambda_{\text{avg}} T_R \leq \frac{T_1 r_c}{T_1 + T_2} \min \left\{ m, n - T_R \lambda \bar{\alpha}_1^\pi + \frac{T_R^2 \lambda}{T_1} \right\} + \frac{T_2 r_c}{T_1 + T_2} \min \left\{ m, n - T_R c \lambda \bar{\alpha}_2^\pi + \frac{T_R^2 \lambda}{T_2} \right\} \quad (43d)$$

We defer the proof of Lemma 3 to the end of the section. First, we present the proof of Theorem 3 below.

Proof of Theorem 3 Case I: The first case of the theorem follows directly from (43c) in Lemma 3.

Case II: We prove the contrapositive. In particular, we show that if for all $c_\alpha \in \left[0, \alpha - \frac{T_1 + T_2 - c T_R (1 + T_2/T_1)}{T_1 + c T_2}\right]$,

we have

$$n < (1 + r) \alpha \lambda_{\text{avg}} T_R + \frac{T_1}{T_2} \left(\alpha - \frac{T_1 + T_2}{T_1 + c T_2} - c_\alpha \right) \lambda_{\text{avg}} T_R - \frac{c T_R^2 \lambda}{T_2}, \quad \text{OR} \quad m < r \alpha \lambda_{\text{avg}} T_R + c_\alpha \lambda_{\text{avg}} T_R, \quad (44)$$

then $\bar{\alpha}_{\text{eff}}^\pi < \alpha$. First, consider the case when the former holds for all c_α in (44). Then, we have $n < (1+r)\alpha\lambda_{\text{avg}}T_R$. Thus, by (43c), we get $\bar{\alpha}_{\text{eff}}^\pi < \alpha$. Now, consider the case when the latter holds for all c_α in (44). Then, we have $m < r\alpha\lambda_{\text{avg}}T_R$. Thus, by (43c), we get $\bar{\alpha}_{\text{eff}}^\pi < \alpha$. Lastly, consider the case when there exists non-zero subset of $\left[0, \alpha - \frac{T_1+T_2}{T_1+cT_2}\right]$ for which the former holds in (44). Let $c_\alpha^{(1)}$ be the supremum of such constants. Similarly, a non-zero subset for which the later holds and let $c_\alpha^{(2)}$ be the infimum of such constants. To ensure that (44) holds for all $c_\alpha \in \left[0, \alpha - \frac{T_1+T_2}{T_1+cT_2}\right]$, we must have $c_\alpha^{(1)} \geq c_\alpha^{(2)}$. In addition, either the supremum or the infimum is attained. Thus, there exists a $c_\alpha \in [c_\alpha^{(2)}, c_\alpha^{(1)}]$ such that

$$n \leq (1+r)\alpha\lambda_{\text{avg}}T_R + \frac{T_1}{T_2} \left(\alpha - \frac{T_1+T_2}{T_1+cT_2} - c_\alpha \right) \lambda_{\text{avg}}T_R - \frac{cT_R^2}{T_2}, \quad m < r\alpha\lambda_{\text{avg}}T_R + c_\alpha\lambda_{\text{avg}}T_R, \quad (45)$$

or

$$n < (1+r)\alpha\lambda_{\text{avg}}T_R + \frac{T_1}{T_2} \left(\alpha - \frac{T_1+T_2}{T_1+cT_2} - c_\alpha \right) \lambda_{\text{avg}}T_R - \frac{cT_R^2\lambda}{T_2}, \quad m \leq r\alpha\lambda_{\text{avg}}T_R + c_\alpha\lambda_{\text{avg}}T_R. \quad (46)$$

Now, if (45) is satisfied, and $\bar{\alpha}_{\text{eff}}^\pi \geq \alpha$, then, we obtain a contradiction. By (43d), we have

$$\begin{aligned} n &\geq r\bar{\alpha}_{\text{eff}}^\pi\lambda_{\text{avg}}T_R \left(1 + \frac{T_1}{T_2} \right) - \frac{mT_1}{T_2} + T_R c \lambda \bar{\alpha}_2^\pi - \frac{cT_R^2\lambda}{T_2} \\ &\stackrel{(a)}{>} r\bar{\alpha}_{\text{eff}}^\pi\lambda_{\text{avg}}T_R \left(1 + \frac{T_1}{T_2} \right) - \frac{T_1}{T_2} (r\alpha\lambda_{\text{avg}}T_R + c_\alpha\lambda_{\text{avg}}T_R) + T_R c \lambda \bar{\alpha}_2^\pi - \frac{cT_R^2\lambda}{T_2} \\ &\stackrel{(b)}{\geq} r\bar{\alpha}_{\text{eff}}^\pi\lambda_{\text{avg}}T_R \left(1 + \frac{T_1}{T_2} \right) - \frac{T_1}{T_2} (r\alpha\lambda_{\text{avg}}T_R + c_\alpha\lambda_{\text{avg}}T_R) + T_R c \lambda \left(\bar{\alpha}_{\text{eff}}^\pi \left(1 + \frac{T_1}{cT_2} \right) - \frac{T_1}{cT_2} \right) - \frac{cT_R^2\lambda}{T_2} \\ &\stackrel{(c)}{\geq} r\alpha\lambda_{\text{avg}}T_R - \frac{T_1}{T_2} c_\alpha\lambda_{\text{avg}}T_R + T_R c \lambda_{\text{avg}} \frac{T_1+T_2}{T_1+cT_2} \left(\alpha \left(1 + \frac{T_1}{cT_2} \right) - \frac{T_1}{cT_2} \right) - \frac{cT_R^2\lambda}{T_2} \\ &= (1+r)\alpha\lambda_{\text{avg}}T_R + \frac{T_1}{T_2} \left(\alpha - \frac{T_1+T_2}{T_1+cT_2} - c_\alpha \right) \lambda_{\text{avg}}T_R - \frac{cT_R^2\lambda}{T_2}, \end{aligned} \quad (47)$$

where (a) follows by using the upper bound on m given by (45). Next, (b) follows by substituting $\bar{\alpha}_1^\pi$ in (43a) to obtain an upper bound on $\bar{\alpha}_2^\pi$. Lastly, (c) follows as we assume $\bar{\alpha}_{\text{eff}}^\pi \geq \alpha$. Note that the last equation contradicts (45). Similarly, we can obtain a contradiction if instead, (46) were satisfied. This completes the proof of Case II.

Case III: Similarly to the previous case, we prove the contrapositive for this case as well. In particular, we show that if for all $c_\alpha \in \left[0, \frac{\alpha r T_2}{T_1} - \frac{cT_R(1+T_2/T_1)}{T_1+cT_2}\right]$, we have

$$n < (1+r)\alpha\lambda_{\text{avg}}T_R + \frac{T_1}{T_2} \left(\alpha - \frac{T_1+T_2}{T_1+cT_2} - c_\alpha \right) \lambda_{\text{avg}}T_R - \frac{cT_R^2\lambda}{T_2}, \quad \text{OR} \quad m < r\alpha\lambda_{\text{avg}}T_R + c_\alpha\lambda_{\text{avg}}T_R, \quad (48)$$

then, $\bar{\alpha}_{\text{eff}}^\pi < \alpha$. First, consider the case when the former in (48) holds for all c_α . Then, we have

$$n < \alpha\lambda_{\text{avg}}T_R + \frac{T_1}{T_2} \left(\alpha - \frac{T_1+T_2}{T_1+cT_2} \right) \lambda_{\text{avg}}T_R.$$

In addition, by (43b) and (43a), we get

$$n \geq \bar{\alpha}_2^\pi c \lambda T_R \geq c \lambda T_R \left(\bar{\alpha}_{\text{eff}}^\pi \left(1 + \frac{T_1}{c T_2} \right) - \frac{T_1}{c T_2} \right) = \bar{\alpha}_{\text{eff}}^\pi \lambda_{\text{avg}} T_R + \frac{T_1}{T_2} \left(\bar{\alpha}_{\text{eff}}^\pi - \frac{T_1 + T_2}{T_1 + c T_2} \right) \lambda_{\text{avg}} T_R.$$

Thus, the lower and upper bounds on n implies that $\bar{\alpha}_{\text{eff}}^\pi < \alpha$.

Now, consider the case when the latter in (48) holds for all c_α . Then, we have $m < r \alpha \lambda_{\text{avg}} T_R$. Thus, (43c) implies $\bar{\alpha}_{\text{eff}}^\pi < \alpha$. Lastly, consider the case when there exists some c_α for which the former in (48) holds and some c_α for which the latter holds. Thus, similar to Case II, there exists $c_\alpha \in \left[0, \frac{\alpha r T_2}{T_1} - \frac{c T_R (1 + T_2 / T_1)}{T_1 + c T_2} \right]$, such that either

$$n \leq (1 + r) \alpha \lambda_{\text{avg}} T_R + \frac{T_1}{T_2} \left(\alpha - \frac{T_1 + T_2}{T_1 + c T_2} - c_\alpha \right) \lambda_{\text{avg}} T_R - \frac{c T_R^2 \lambda}{T_2}, \quad m < r \alpha \lambda_{\text{avg}} T_R + c_\alpha \lambda_{\text{avg}} T_R, \quad (49)$$

or

$$n < (1 + r) \alpha \lambda_{\text{avg}} T_R + \frac{T_1}{T_2} \left(\alpha - \frac{T_1 + T_2}{T_1 + c T_2} - c_\alpha \right) \lambda_{\text{avg}} T_R - \frac{c T_R^2 \lambda}{T_2}, \quad m \leq r \alpha \lambda_{\text{avg}} T_R + c_\alpha \lambda_{\text{avg}} T_R. \quad (50)$$

As α is large enough for this case, we can verify that $\left[0, \frac{\alpha r T_2}{T_1} \right] \subseteq \left[0, \alpha - \frac{T_1 + T_2}{T_1 + c T_2} \right]$. Thus, by (47), we conclude that (49) implies $\bar{\alpha}_{\text{eff}}^\pi < \alpha$. Similarly, (50) also implies $\bar{\alpha}_{\text{eff}}^\pi < \alpha$. This completes the proof of Case III. \square

Proof of Lemma 3 We start by proving the first equation. By the definition of $\bar{\alpha}_{\text{eff}}^\pi$, we get

$$\begin{aligned} \lambda_{\text{avg}} \bar{\alpha}_{\text{eff}}^\pi &= \limsup_{T \rightarrow \infty} \frac{1}{T} \int_0^T \lambda_{\text{eff}}^\pi(t) dt \\ &= \limsup_{T \rightarrow \infty} \frac{1}{T} \sum_{i=0}^{\left\lfloor \frac{T-T_1}{T_1+T_2} \right\rfloor} \int_{i(T_1+T_2)}^{(i+1)(T_1+T_2)} \lambda_{\text{eff}}^\pi(t) dt + \limsup_{T \rightarrow \infty} \frac{1}{T} \sum_{i=0}^{\left\lfloor \frac{T}{T_1+T_2} \right\rfloor - 1} \int_{(i+1)(T_1+T_2)}^{(i+1)(T_1+T_2)} \lambda_{\text{eff}}^\pi(t) dt \\ &= \lambda \limsup_{T \rightarrow \infty} \frac{1}{T} \sum_{i=0}^{\left\lfloor \frac{T-T_1}{T_1+T_2} \right\rfloor} \int_{i(T_1+T_2)}^{(i+1)(T_1+T_2)} \alpha(t) dt + c \lambda \limsup_{T \rightarrow \infty} \frac{1}{T} \sum_{i=0}^{\left\lfloor \frac{T}{T_1+T_2} \right\rfloor - 1} \int_{(i+1)(T_1+T_2)}^{(i+1)(T_1+T_2)} \alpha(t) dt \\ &= \frac{\bar{\alpha}_1^\pi \lambda T_1 + \bar{\alpha}_2^\pi c \lambda T_2}{T_1 + T_2}. \end{aligned}$$

Note that, for the second equality, we divide the integral into two parts, corresponding to the peaks and valleys. Next, we use the fact that $\bar{\lambda}_{\text{eff}}^\pi(t) = \lambda \alpha(t)$ for the valleys and $\bar{\lambda}_{\text{eff}}^\pi(t) = c \lambda \alpha(t)$ for the peaks. Now, the last equality follows by the definition of $\bar{\alpha}_1^\pi$ and $\bar{\alpha}_2^\pi$ given by (42). Next, we prove (43b) below.

$$\begin{aligned} n &\geq q(T + T_R) \stackrel{(a)}{\geq} c \lambda \int_T^{T+T_R} \alpha(t) dt \quad \forall T : \frac{T}{T_1 + T_2} - \left\lfloor \frac{T}{T_1 + T_2} \right\rfloor \in \left[\frac{T_1}{T_1 + T_2}, 1 - \frac{T_R}{T_1 + T_2} \right] \\ &\stackrel{(b)}{\geq} c \lambda \frac{T_R}{T_2} \int_{(i+1)T_1 + iT_2}^{(i+1)(T_1+T_2)} \alpha(t) dt \quad \forall i \in \mathbb{Z}_+ \\ &\stackrel{(c)}{\geq} c \lambda \frac{T_R}{k T_2} \sum_{i=0}^{k-1} \int_{(i+1)T_1 + iT_2}^{(i+1)(T_1+T_2)} \alpha(t) dt \quad \forall k \in \mathbb{Z}_+ \\ &\geq \bar{\alpha}_2^\pi c \lambda T_R, \end{aligned}$$

where, (a) follows as each admitted customer stays in the system for at least T_R amount of time. Next, (b) follows by taking the average of the previous expression for $T \in \{(i+1)T_1 + iT_2 + kT_R : k \in [T_2/T_R]\}$ and using the fact that T_2 is divisible by T_R . Similarly, (c) follows by taking the average over the first k peaks in the arrival rate. Now, the last inequality follows by first taking the limit supremum as $k \rightarrow \infty$, and then, using the definition of $\bar{\alpha}_2^\pi$. Lastly, to prove (43d), we use (7c), to get

$$\bar{c}_C r_c = (n - \bar{c}_C - \bar{c}_I) r_d \geq \bar{q} r_d \quad (51)$$

To further simplify the above equation, we start by lower bounding the long run average number of customers in the system (\bar{q}). We have

$$\begin{aligned} \bar{q} &= \limsup_{T \rightarrow \infty} \frac{1}{T} \int_0^T q(t) dt \stackrel{(a)}{\geq} \limsup_{T \rightarrow \infty} \frac{1}{T} \int_0^T \int_{\max\{t-T_R, 0\}}^t \bar{\lambda}_{\text{eff}}^\pi(s) ds dt \\ &\stackrel{(b)}{=} \limsup_{T \rightarrow \infty} \frac{1}{T} \int_0^T \int_s^{\min\{s+T_R, T\}} \bar{\lambda}_{\text{eff}}^\pi(s) dt ds \\ &= \limsup_{T \rightarrow \infty} \frac{1}{T} \int_0^T \min\{T_R, T-s\} \bar{\lambda}_{\text{eff}}^\pi(s) ds \\ &\geq T_R \limsup_{T \rightarrow \infty} \frac{1}{T} \int_0^{T-T_R} \bar{\lambda}_{\text{eff}}^\pi(s) ds \\ &\stackrel{(c)}{=} T_R \limsup_{T \rightarrow \infty} \frac{1}{T} \int_0^T \bar{\lambda}_{\text{eff}}^\pi(s) ds \\ &\stackrel{(42)}{=} \frac{\lambda T_R}{T_1 + T_2} (T_1 \bar{\alpha}_1^\pi + c T_2 \bar{\alpha}_2^\pi), \end{aligned}$$

where (a) follows as each admitted customer stays in the system for at least T_R amount of time. Next, (b) follows by interchanging the order of the integrals. Lastly, (c) follows by noting that $0 \leq \int_{T-T_R}^T \bar{\lambda}_{\text{eff}}^\pi(s) ds / T \leq T_R c \lambda / T \rightarrow 0$ as $T \rightarrow \infty$. Now, we upper bound the long run average number of EVs charging in the system.

$$\bar{c}_C = \limsup_{T \rightarrow \infty} \frac{1}{T} \int_0^T \min\{m, n - q(t)\} \leq \min\{m, n - \bar{q}\},$$

where the inequality follows using Jensen's inequality as min is a concave function. Now, by using (51), we immediately get

$$m \geq r\bar{q} \geq r\alpha \lambda_{\text{avg}} T_R, \quad n \geq (1+r)\bar{q} \geq (1+r)\alpha \lambda_{\text{avg}} T_R.$$

Lastly, to prove (43d), we obtain a more fine tuned bound on \bar{c}_C by dividing the integral over t into peaks and valleys as follows:

$$\bar{c}_C = \limsup_{T \rightarrow \infty} \frac{1}{T} \int_0^T \min\{m, n - q(t)\}$$

$$\begin{aligned}
&\leq \limsup_{T \rightarrow \infty} \frac{1}{T} \int_0^T \min \left\{ m, n - \int_{\max\{t-T_R, 0\}}^t \bar{\lambda}_{\text{eff}}^\pi(s) ds \right\} dt \\
&= \limsup_{T \rightarrow \infty} \frac{1}{T} \sum_{i=0}^{\lfloor \frac{T-T_1}{T_1+T_2} \rfloor} \int_{i(T_1+T_2)}^{(i+1)T_1+iT_2} \min \left\{ m, n - \int_{\max\{t-T_R, 0\}}^t \bar{\lambda}_{\text{eff}}^\pi(s) ds \right\} dt \\
&\quad + \limsup_{T \rightarrow \infty} \frac{1}{T} \sum_{i=0}^{\lfloor \frac{T}{T_1+T_2} \rfloor - 1} \int_{(i+1)T_1+iT_2}^{(i+1)(T_1+T_2)} \min \left\{ m, n - \int_{\max\{t-T_R, 0\}}^t \bar{\lambda}_{\text{eff}}^\pi(s) ds \right\} dt
\end{aligned}$$

Now, we simplify each of the above integrals separately. For the valleys, we have

$$\begin{aligned}
&\limsup_{T \rightarrow \infty} \frac{1}{T} \sum_{i=0}^{\lfloor \frac{T-T_1}{T_1+T_2} \rfloor} \int_{i(T_1+T_2)}^{(i+1)T_1+iT_2} \min \left\{ m, n - \int_{\max\{t-T_R, 0\}}^t \bar{\lambda}_{\text{eff}}^\pi(s) ds \right\} dt \\
&\stackrel{(a)}{\leq} \min \left\{ \frac{mT_1}{T_1+T_2}, \frac{T_1n}{T_1+T_2} - \liminf_{T \rightarrow \infty} \frac{1}{T} \sum_{i=0}^{\lfloor \frac{T-T_1}{T_1+T_2} \rfloor} \int_{i(T_1+T_2)}^{(i+1)T_1+iT_2} \int_{\max\{t-T_R, 0\}}^t \bar{\lambda}_{\text{eff}}^\pi(s) ds dt \right\} \\
&\stackrel{(b)}{=} \min \left\{ \frac{mT_1}{T_1+T_2}, \frac{T_1n}{T_1+T_2} - \liminf_{T \rightarrow \infty} \frac{1}{T} \sum_{i=0}^{\lfloor \frac{T-T_1}{T_1+T_2} \rfloor} \int_{\max\{i(T_1+T_2)-T_R, 0\}}^{(i+1)T_1+iT_2} \int_{\max\{s, i(T_1+T_2)\}}^{\min\{s+T_R, (i+1)T_1+iT_2\}} \bar{\lambda}_{\text{eff}}^\pi(s) dt ds \right\} \\
&\stackrel{(c)}{=} \min \left\{ \frac{mT_1}{T_1+T_2}, \frac{T_1n}{T_1+T_2} - T_R \lambda \bar{\alpha}_1^\pi - \liminf_{T \rightarrow \infty} \frac{1}{T} \sum_{i=0}^{\lfloor \frac{T-T_1}{T_1+T_2} \rfloor} \int_{\max\{i(T_1+T_2)-T_R, 0\}}^{i(T_1+T_2)} (s+T_R-i(T_1+T_2)) \bar{\lambda}_{\text{eff}}^\pi(s) dt ds \right. \\
&\quad \left. + \limsup_{T \rightarrow \infty} \frac{1}{T} \sum_{i=0}^{\lfloor \frac{T-T_1}{T_1+T_2} \rfloor} \int_{(i+1)T_1+iT_2-T_R}^{(i+1)T_1+T_2} (s+T_R-(i+1)T_1-iT_2) \bar{\lambda}_{\text{eff}}^\pi(s) dt ds \right\} \\
&\leq \min \left\{ \frac{mT_1}{T_1+T_2}, \frac{T_1n}{T_1+T_2} - T_R \lambda \bar{\alpha}_1^\pi \frac{T_1}{T_1+T_2} + \frac{T_R^2 \lambda}{T_1+T_2} \right\} = \frac{T_1}{T_1+T_2} \min \left\{ m, n - T_R \lambda \bar{\alpha}_1^\pi + \frac{T_R^2 \lambda}{T_1} \right\}
\end{aligned}$$

where, (a) follows by Jensen's inequality as min is a concave function. Next, (b) follows by the interchange of integrals. Now, (c) follows by splitting the outer integral into three parts - $[i(T_1+T_2)-T_R, i(T_1+T_2)]$, $[i(T_1+T_2), (i+1)T_1+iT_2-T_R]$, and $[(i+1)T_1+iT_2-T_R, (i+1)T_1+iT_2]$. Similarly, we can upper bound the integral corresponding to the peaks to get

$$\bar{c}_C \leq \frac{T_1}{T_1+T_2} \min \left\{ m, n - T_R \lambda \bar{\alpha}_1^\pi + \frac{T_R^2 \lambda}{T_1} \right\} + \frac{T_2}{T_1+T_2} \min \left\{ m, n - T_R \lambda \bar{\alpha}_2^\pi + \frac{T_R^2 \lambda}{T_2} \right\}.$$

Now, by substituting the bounds on \bar{q} and \bar{c}_C in (51), we get (43d). This completes the proof. \square